STRUCTURAL ANALYSIS OF SHEAR AND DILATIONAL FRACTURES AND THEIR IMPLICATIONS FOR THE NEOTECTONICS OF SURGHAR-SHINGHAR RANGE, TRANS-INDUS RANGES, PAKISTAN
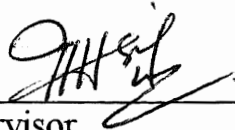
BY

MOHAMMAD SAYAB

A thesis submitted to the National Centre of Excellence in Geology, University of Peshawar in partial fulfillment of the requirements for the M. Phil degree in Structure Geology
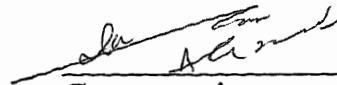
2002

NATIONAL CENTRE OF EXCELLENCE IN GEOLOGY
UNIVERSITY OF PESHAWAR
PESHAWAR, PAKISTAN

APPROVED BY

_____
Supervisor
Prof. Dr. Mohammad Asif Khan (T.I.)
National Centre of Excellence in Geology
University of Peshawar

_____
Co-supervisor
Prof. Dr. Iftikhar Ahmad Abbasi
Department of Geology
University of Peshawar

_____
External Examiner - I
Prof. Dr. Mohammad Niamatullah
Department of Geology
University of Karachi

_____
External Examiner - II
Dr. Mohammad Raza Shah
Deputy Director
Geological Survey of Pakistan
Peshawar

_____
Director
National Centre of Excellence in Geology
University of Peshawar

ABSTRACT

This study entails structural analysis of fractures and fracture-related structures in the southern part of the Surhgar-Shinghar Range between Qabul Khel in the south and Thatti Nasrati in the north, Trans-Indus Ranges. This part of the Surghar-Shinghar Range is oriented north-south, almost at right angle to its segment between Kalabagh in the east and Thatti-Nasrati in the west. Previously, the north-south oriented part of the range was considered as a single structure, i.e., Makarwal anticline. However, we divide this part of the range into two anticlinal structures: Makarwal anticline to the north and Sarkai-Mochi Mar (SMM) dome-shape anticline to the south. These two anticlinal structures are separated by an exceptionally low topographic relief, characterized by a small basin as the Gulapa-Darsola basin.

Mainly shear and dilational fractures have been recognized in the Siwalik sediments of the western exposed flank of the Surghar-Shinghar anticline. The shear fractures have been classified into: 1. bedding or layer-parallel shear fractures, 2. longitudinal or fractures normal to the bedding planes and 3. diagonal or conjugate shear fractures. The bedding or layer-parallel shear fractures and longitudinal or fractures normal to the bedding planes have same strike (NNW/NS/NNE), but dip in opposite directions. The layer-parallel shear fractures (N40°-50°W) are developed mostly along clay ball scoured surfaces, shale horizons and rarely along channel conglomerates. Reverse sense of shear has been interpreted for layer-parallel shear fractures as inferred from rotated and displaced clay balls in the sandstones and displaced pebbles and cobbles in the channel conglomerates. The longitudinal or fractures normal to the bedding planes dip towards the east. They cut the layer-parallel shear fractures and the sedimentary bedding at varying angles ($\geq 90°$). The layer-parallel shear fractures, therefore, appear to have formed prior to the fractures normal to the bedding planes.

Orthogonal to the bedding and longitudinal shear fractures is a set of east-west oriented cross or dilational fractures in the Siwalik strata of Surghar-Shinghar Range. Image interpretation using Landsat TM and SPOT suggest predominance of roughly east-west oriented parallel, sub-parallel drainage pattern across the range, which to a large extent is controlled by the east-west dilational fractures. These east-west oriented extensional fractures appear to be dilated by seasonal drainage, forming steep gorges, especially in the Siwalik sediments. A parallelism between the drainage pattern of the range and the east-west oriented dilational fractures suggest role of the structural control on the geomorphology.

Infrequent and less populated than those of bedding and longitudinal shear fractures are the diagonal or conjugate shear fractures with dextral and sinistral sense of shear. These shear fractures are well developed on the limbs. The orientation of these fracture sets varies according to the local attitude of the beds. The acute angle between the two oblique fracture sets is not more than 75°.

Using different classical stress and strain models, it is suggested that the bedding or layer-parallel shear fractures are induced by flexural-slip folding, whereas, longitudinal or fractures normal to the bedding planes might have initially formed as dilational fractures across the sedimentary bedding, but later, due to the change in stress direction (rotation of beds) formed as shear fractures with reverse sense of slip. The diagonal or conjugate shear fractures on the limbs are geometrically related with the folding of Surghar-Shinghar Anticline. As with the dilational or cross fractures, exposed on the western limb of Surghar-Shinghar Anticline, accommodated north south extension perpendicular to the regional fold axis.

In addition, two joint sets i.e., NS/NNE and EW/WNW are observed at the hinge zone of the Sarkai Mochi-Mar (SMM) dome-shape anticline, where the strike of the strata is about eastwest. Field observations show that NS/NNE oriented joints are compressional and EW/WNW oriented joints are extensional in geometry. Minor folds with fold axes and axial planes parallel to the compressional joints (NS/NNE) are not uncommon.

The area also contains two sets of conjugate strike-slip deformation band shear zones (DBSZs) cut across the sedimentary strata at high angles. The NS steeply oriented DBSZs with dextral sense of movement are characterized by thick and relatively resistant deformation bands that can be traced for long distances. The second set with N50°-60°E deformation bands are attributed to incipient tabular zones with nice geometrical arrangement of Riedel fractures. Sinistral movement has been interpreted from Riedel fracture assemblage within the Principal Shear Zones of N50°-60°E. The two sets form a conjugate geometry. The frequency of these DBSZs is high close to the trace of the Dara Tang fault (Surghar Thrust).

Based on field evidences, two deformational phases have been suggested for the formation of joints and deformation band shear zones at the southern end of SMM dome-shape anticline. The compressional and extensional joints might have initially formed as tensional joints due to the bending of layers, as observed at some places in the north-south oriented part of the SMM dome-shape anticline. However, later, due to change in stress direction (possibly stresses of Dara Tang Fault), the NS/NNE oriented tensional joints induced to compression with a component of folding, whereas, EW/WNW oriented joints accommodated north-south extension. At the same time, two sets of conjugate strike-slip banded shear zones, i.e., NS and N50°-60°E are formed. As the north-south oriented Dara Tang Fault cuts across the sedimentary strata (the fault is characterized by high-angle oblique-reverse slip movement), which is passing at the core of the SMM anticline, the strike-slip deformation band shear zones in the area appear to be dynamically related with this fault.

ACKNOWLEDGEMENT

TABLE OF CONTENTS

Appendix-1
References

LIST OF FIGURES

Chapter 1

INTRODUCTION

A part of the Surghar-Shinghar Range, exposed between Thatti Nasrati in the north and Qabul Khel in the south is subject of this study. Geological mapping of regional structures is followed by a detailed study of fractures, deformation band shear zones and joints in terms of their geometry, kinematics and relationship with regional structures.

The aim of this chapter is to provide the scope and objectives of the present work. Previous investigations, regarding regional and local geology of the area, tectonic setting and economic geology are summarized. A brief account on the geomorphology, accessibility and climatic conditions of the study area is also discussed. Field, laboratory techniques and working plan are considered under the methodology.

1.1. AIMS AND OBJECTIVES

This study involves the structural analysis of the Siwalik Group of the north-south oriented southern Surghar-Shinghar Range (Fig. 1.1). The prime objectives of the present research are as under:

1. *Structural analysis of shear and dilational fractures exposed in the sandstones of the Siwalik Group of Surghar-Shinghar Range with reference to the neotectonics of the area,*

2. *Stress and strain analyses based on field observations, graphical techniques and orientation diagrams,*

3. *Preparation of suitable structural models for the formation of these orderly sets of fractures in terms of regional geodynamics,*

4. *Geometrical and kinematic analyses of conjugate strike-slip deformation band shear zones at the southern most tip of the Surghar-Shinghar Range and to interpret their origin within the sandstone horizons,*

5. *Kinematic and dynamic analysis of joints at the southern end of the Surghar-Shinghar Range and to propose suitable models for their origin.*

1
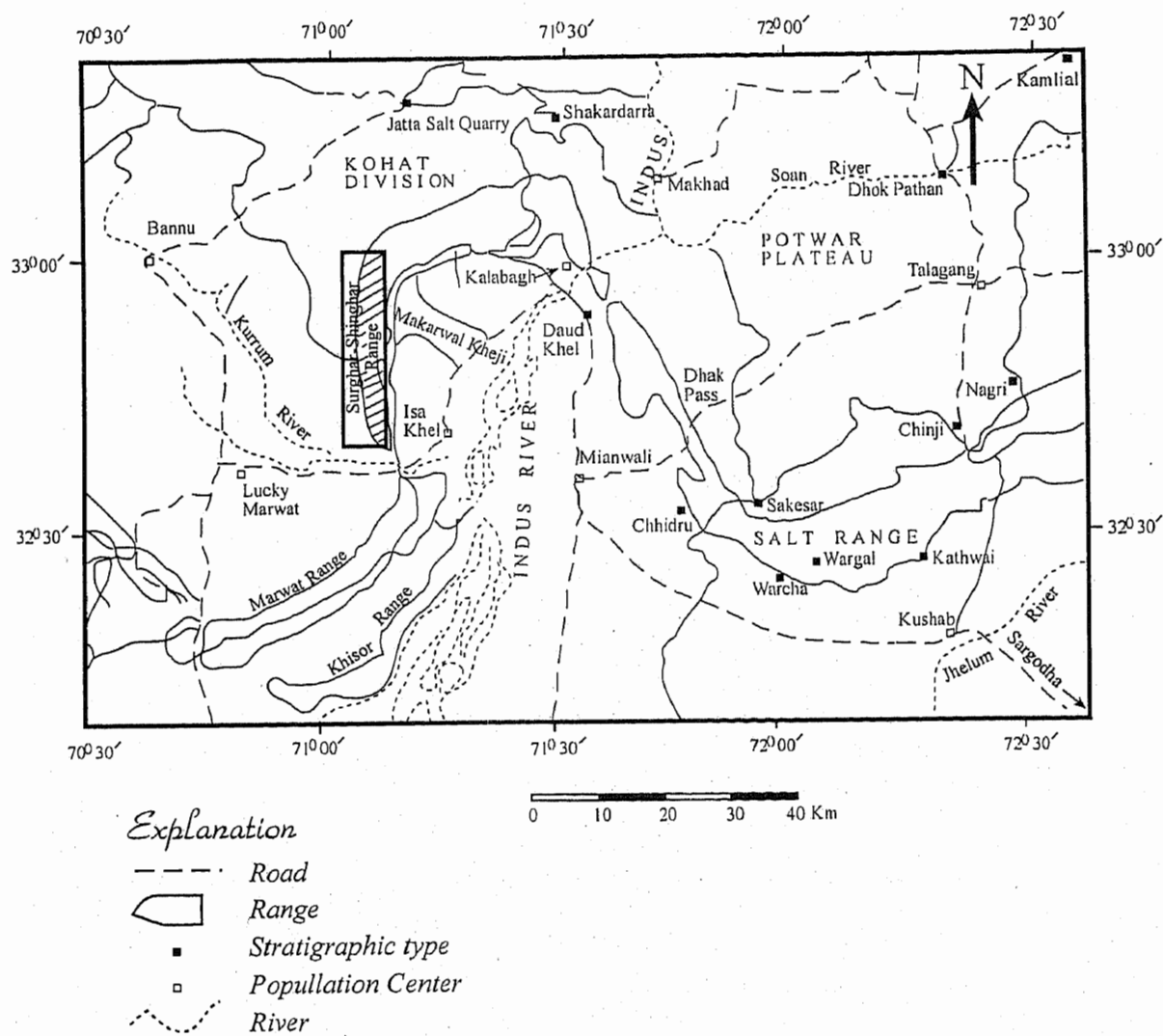
Fig. 1.1. Location of the study area and some cultural features of Trans-Indus mountains, Salt Range, Kohat and Potwar Plateuas (modified from Danilchik and Shah, 1987).

1.2. LOCATION AND ACCESSIBILITY

The Surghar-Shinghar Range is located in the southern parts of North West Frontier Province (N. W. F. P.) of Pakistan and administratively falls under districts Karak, Lucky Marwat and Mianwali (Fig. 1.1). The north-south oriented part of the range is covered by Survey of Pakistan topographic sheet nos. 38 $^P/_1$, 38 $^P/_2$ and 38 $^0/_4$. With reference to Pakistani Himalayas, the range is a part of Trans-Indus Ranges, Sub-Himalayas (Khan, 1991) covering the north-eastern peripheral boundary of the Bannu Basin. The Trans-Indus Ranges are apparently the western continuation of the Salt Range, west of the Indus River (Gee, 1989).

The range is accessible by various fair-weather jeapable metalled and unmetalled roads from both southern and northern sides. From the southern side the range is easily accessible by a partially metalled road, which is connected to the main Mianwali–Bannu road near Darra Tang. From the northern side the range is accessible by an unmetalled dirt road, which is connected to the Indus Highway near Thatti-Nasrati. Travel to the Makarwal coal mines to the western part of the Surghar Range is by metalled Isa-Khel-Kalabagh road to the town of Kamar Mushani, and from there to Makarwal station along another metalled road.

1.3. GEOGRAPHY

1.3.1. Physiography

The Bannu Basin covers an area of about 8,000 km^2 (Bender and Raza, 1995) and is surrounded by Trans-Indus Ranges namely, Surghar-Shinghar, Marwat-Khisor and Pezu-Mazani (Gee, 1989). These ranges forming "Recess" and "Salient" geometries (Macedo and Marshak, 1999) of Himalayan Frontal Fold and Thrust Belt of Pakistan (Gee, 1989). Since, these ranges lie in the Sub-Himalayan sedimentary sequence of Pakistan, their average height is 600-1200 meters. The Surhgar-Shinghar Range is at the north-western periphery of Thal desert, which is the second biggest recognized desert of

3

Pakistan covered with alluvial soils (Khan, 1991). Kurrum River separates the Surghar-Shinghar and Marwat Ranges near Dara Tang village and joins the mighty Indus to the south east of Isa-Khel.

The Surghar Range covers the north-eastern boundary of the Bannu Basin and consists of low altitude sandy mountains. The range comprises friable to moderately hard and slippery sandstone and shale horizons of Upper Miocene-Pliocene age. Care should be taken during travel and activity in these mountains, especially during the rainy season.

1.3.2. Drainage

Landsat TM and SPOT images are used for the recognition of drainage patterns. Kurrum is the major river in the Bannu Basin flowing in the north-west to the south east direction and ultimately joins the Indus to the east. Therefore, the regional flow direction is towards southeast. However, small streams originating from the mountainous terrains have *sub-parallel* flow patterns. Flow direction of streams emanating from the western side of Surghar Range is south-west, while those originating from Marwat have roughly north-north-west flow direction. Birgi, Gulapa, Samandi, Abbasa, Shanawah and Thatti Nasrati are the major east-west oriented streams of the Surghar-Shinghar Range, which generally drain during the rainy seasons.

1.3.3. Climate

The area experience semi-arid (steppe) climate with warm summer (21°-32°) and cool winter (0°-10°) (Khan, 1991). However, some days in June and July experience temperature as high as 45°C. The humidity is low during winters, while it becomes high during Monsoon season. The rainy season during the winters is from the Western Depression and occasionally in the summers from the Monsoon (Khan, 1991). Geological fieldwork is most feasible from October to April.

1.4. PREVIOUS WORK

Wynne (1878, 1880) presented the earliest published work on the Salt and Trans-Indus Ranges. He carried out pioneer survey of the Salt Range and

briefly described the lithological units of the area. Simpson (1904) studied and pointed out the major coal localities between Makarwal and Kalabagh and referred to them as "the Maidan Range Coal Field". A detailed and comprehensive study, regarding stratigraphy and structure of the Salt Range and adjoining geological related areas is presented by Gee (1945, 1989).

Chaudhry (1970) studied the petrography of Siwalik formations of Pakistani Himalayas. He studied the provenance and proposed criteria for correlating the Siwaliks based on heavy minerals. Shah (1977) discussed detail stratigraphic setup of Pakistan. He described lithological characteristics, contact relationships, type localities, age and correlation of Siwalik Group in detail. Akhtar (1983) reported Kamlial Formation of Rawalpindi Group in the Surghar Range, which is absent according to some authors (Danilchik and Shah, 1987; Azizullah, 1995). Danilchik and Shah (1987) prepared a fairly detailed report on the stratigraphy, coal resources and economic geology of the Makarwal area of Surghar Range and named as "Makarwal Coal Field". Abid et al., (1983) gave a brief account of the petrography, geochemistry and provenance of the Dhok Pathan Formation from upper part of the Surghar Range. Khan (1983) and Khan and Khan and Opdyke (1987) have studied magnetostratigraphy of the Surghar Range and have suggested, based on magnetic polarity data, that the Siwaliks of the Trans-Indus are younger than the Siwaliks of Potwar Plateau.

Yeats et al., (1984), Jaume et al., (1988), McDoughall et al., (1990, 1991) and Pivnik et al., (1993) discussed structural studies related with the fold and thrust belt of Kohat-Potwar plateaus. Yeats et al., (1984) first described the Kalabagh Fault. However, this fault appears on the map of active faults (Kazmi, 1979a) on tectonic map of Pakistan (Kazmi et al., 1979b) and in a satellite scene described by De Jong (1986).

Bajwa (1987), Bajwa et al., (1987) and Bajwa and Shams (1986) studied the petrology and geochemistry of Siwalik of Potwar area. They concluded that the Siwalik of different areas have been derived from different source regions,

however, in the case of Potwar plateau they have suggested that these rocks have been derived from the south eastern part of the Himalayas.

Wang et al., (1989, 1995), Moghal (1974a, 1974b) Moghal et al., 1997 and Azizullah (1995) have studied the sandstone type uranium deposits in the Siwaliks of Pakistan. They have reported strong radioactive anomalies at several places in the Dhok Pathan formation of the Siwalik Group. Baghal Chur has been developed as a producing mine (Moghal, 1974b). From Qubul Khel, at the southern tip of Surghar Range, uranium is being mined by in situ leaching (ISL) process (Wang et al., 1989, 1995), while Shanawah-Godi Khel has good uranium reserves (Azizullah, unpublished reports). According to Moghal et al., (1997) the main source of uranium are the interstratified beds, which contain uranium-bearing feldspar. Azizullah (1995) discussed petrography, petrotectonics and stratigraphy of Siwalik group in detail of Shanawah-Godi Khel and Thatti Nasrati area.

1.5. ECONOMIC SIGNIFICANCE

The Surghar-Shinghar Range has an important economic value as for as the fuel and minerals are concerned. The unconventional mining of Makarwal coal was started as early as 1903 (Ball and Simpson, 1913). Uranium is being mined from Qabul Khel since 1990 (Wang et al., 1995). In addition, glass sand, iron and limestones have been exploited for mineral industry for years (Danilchik and Shah, 1987).

1.5.1. Uranium Geology

The upper part of the Dhok Pathan Formation of the Siwalik Group of Surghar-Shinghar Range hosts potential uranium prospects. However, three important locations, which contain potential uranium mineralization, are the Qabul Khel (ISL Project), Shanawah-Gadi Khel and Thatti-Nasrati. From the Qabul Khel (ISL Project), located at the southern tip of Surghar-Shinghar Range, uranium is being mined and the calculated reserves are larger than those found in the Baghal Chur located in the Dera Ghazi Khan District (Director

6

ISL Project, personal communications, 2000). In Situ Leaching (ISL) process is adopted for the extraction of uranium from the Upper part of the Dhok Pathan Formation in the Qabul Khel Project. The Shanawah-Gadi Khel exploration area, some 20 km north of the Qabul Khel Project is recently proved as the largest uranium deposit of Pakistan hosting some more than 2000 tons of uranium (Azizullah, unpublished reports). This deposit is marked in the middle- and upper part of the Dhok Pathan Formation both in the oxidized and reduced zones (above and below the water table) of Surghar-Shinghar Range (Azizullah, unpublished reports). The third important location, as for as the uranium mineralization is concerned, the Thatti-Nasrati bend, hosts some good uranium prospects.

1.5.2. Coal

The coal in the Markarwal Coal field occurs at the base of the Hangu Formation or from the Makarwal coal bed (Danilchik and Shah, 1987). The coal is locally regarded as "Lignite", however, the analysis of the coal show that the fixed carbon of moisture- and ash-free coal is about 50% (Danilchik and Shah, 1987). The total reserve of coal in the Makarwal coal field is about 16,600,000 tons (Danilchik and Shah, 1987).

1.6. METHODOLOGY

1. Edge-enhanced LandSat TM (1:65,000) and SPOT (1:50,000) images were utilized for preliminary mapping of lithological units, structures and lineaments using GIS software ER Mapper Ver. 5.5.

2. For the generalization of sedimentological and structural behavior of the rocks, reconnaissance traverses along various streams were made in the Surghar-Shinghar Range,

3. Geological mapping of Shava-Shanawah-Puki area and the southern part of the Shinghar Range was carried out on 1:50,000, using Survey of Pakistan topographic sheet nos. $38^P/_1$ and $38^P/_2$ as base maps,

4. Special emphasis was given to structural analysis, regarding preparation of orientation and frequency diagrams, stereographic projections, fracture pattern within a fold system, and stress and strain models,

5. Theodolite mapping (Grid) on 1:5000 scale was carried out in the Mochi Mar and part of the Qabul Khel area, located at the southern tip of Surghar-Shinghar Range for detail statistical and structural analysis of joints and shear zones,

6. Generalized stratigraphic cross-sections were made in the area for studing vertical and horizontal variations and correlations of the Siwalik strata,

7. Silva Ranger 15TDCL was used for measurements in the field; important features were photographed for illustrations,

8. Computer softwares i.e., Corel Draw 9.0 and Freehand 9.0 were used for graphics and drafting. Georient Ver. 8.0 has been utilized for the preparation of frequency diagrams.

Chapter 2

REGIONAL GEOLOGY & TECTONICS

2.1. INTRODUCTION

This chapter summarizes the geodynamic setting of the Indian plate with respect to regional tectonics and chronologcial history dating back to 130 million years (m.y.). Himalayan thrust system, major syntaxes and sub-divisions of the Pakistani Himalayas are briefly discussed under Himalayan Thrust Tectonics. Structure of Surghar-Shinghar, Marwat and Khisor Ranges, neotectonics and their geometry are discussed under the Tectonics of Trans-Indus Ranges. At the end of the chapter, stratigraphy of the Siwalik Group of Surghar-Shinghar Range is described regarding lithological characteristics, contact relationships, fossil contents, thickness and age of the formations.

2.2. GEODYNAMICS

The Indo-Pakistan sub-continent is surrounded by the Indian Ocean to the south and the Himalayas to the north. Sea-floor spreading, continental drift, and collision tectonics are responsible for the formation of Himalayas and accretion of Indo-Pakistan sub-continent with Eurasia. The sub-continent was separated from the Gondwanaland about 130 m.y. ago (Johnson et al., 1976). It is estimated, on the basis of magnetic anomalies that between 130 m.y. and 80 m.y. Indo Pak sub-continent moved northward at a rate of about 3 to 5 cm/year (Johnson et al., 1976). From 80 m.y. India moved at an average rate of 15-25cm/year relative to Australia and Antarctica (Powell, 1979; Patriat and Achache, 1984). During this period the movement was facilitated by extensive sea-floor spreading along Mid Indian Ocean Ridge and transform faulting in the Proto-Owen fracture zone (Kazmi and Jan, 1997). Between 60-65 m.y. the northward drift of India was accompanied by extensive extrusion of Decan Trap Basalts (Duncan and Pyle., 1988).

The opening of Indian Ocean in the south and squeezing of Tethys Ocean in the north started at 130 m.y. ago when India started its northward drift

(Johnson et al., 1976). Intra-oceanic volcanic island arcs were formed (Kohistan-Ladakh, Nuristan, Kandhar) by the Intra-oceanic subduction within the Neotethys during the Cretaceous times forming back-arc ocean at the southern margin of Eurasia (Searle, 1991). By closing of the back-arc basins, the Kohistan-Ladakh island arc collided with Eurasia along the southern margin of the Karakoram plate, and once accreted formed an Andean-type continental margin (Petterson and Windley, 1985). The youngest marine sediments deposited in the back-arc basin, between the Kohistan and Karakoram, are Early to Middle Cretaceous carbonates and volcanics, i.e., the Yasin Group and Chalt Formation (Searle, 1991).

To the south, the subsequent drift and northward subduction of the Indian plate resulted in complete consumption of the leading oceanic edge of the Indian plate and its eventual collision with the Kohistan-Ladakh arc. The abrupt slowing down of India's northward movement between 55 and 50 m. y. ago is attributed to this collision (Powell, 1979). At the time of 50 m. y. the northward drift of India was slowed down due to collision with Eurasia and the closure of Neo-Tetheys in Tebet and Karakorum (Patriat and Achache, 1984). Paleomagnetic data, however, shows that the slowing down of India from 19 cm/year to 4 cm/year occurred at 55 m. y. (Klootwijik et al., 1992). After crossing the equator, the initial contact between northwestern India and Asia was established at about 65 m.y (Klootwijik et al., 1992).

Subsequently, the directions of relative motion of Indian, Australian and Antarctican plates changed significantly, resulting in the formation of ridge sediments, transform faults and other sea-floor features (Mckenzie and Sclater, 1976). India has steadily rotated counterclockwise (Fig. 2.1) coupled with the separation of Arabian plate from Africa about 20 m. y. ago. This rotation caused closure of the Katawaz and Seistan basins, collision of various crustal blocks in Iran-Afghanistan region, convergence in Balochistan and formation of the Balochistan fold-and-thrust belt (Powell, 1979).

The product of India-Eurasia collision yields the Great Himalayas along some 2500 km long Indo-Pakistan plate margin (Le Fort, 1975). The collision

zones are marked by the extensive emplacement of ophiolites along the Indus-Tsango Suture Zone, Waziristan, Zhob Valley and Lasbela area (Gansser, 1964; Le Fort, 1975). Along Suture zone Lower-Middle Eocene marine sediments are the youngest. Siwaliks are the product of Himalayan uplift, which directly overly the Eocene limestones and contains debris of both Eurasian and Indian terrains (Le Fort, 1975).

2.3. HIMALAYAN THRUST SYSTEM

Continental collision of India with Eurasia formed vast mountain range with a thick pile of intensely deformed and thrusted Phanerozoic sediments and Proterozoic basement, affected by various metamorphic events and intruded by a series of magmatic rocks. The present-day Pakistani Himalayan Thrust System from north to south, (Fig. 2.2; 2.3) comprises of Main Karakoram Thrust (MKT) (Gansser, 1980; Coward and Butler, 1985; Coward et al., 1986; Rex et al., 1988; Searle, 1988, 1991), Main Mantle Thrust (MMT) (Tahirkheli and Jan, 1979; Kazmi et al., 1986), Main Boundary Thrust (MBT) (Wadia, 1931; Calkins et al., 1975; Sarwer and DeJong., 1979; Yeats and Lawrence., 1984; Bossart et al., 1984; Treloar et al., 1989; Greco, 1991), Main Central Thrust (MCT) (Auden, 1937; Heim and Gansser, 1939; Le Fort, 1975; Valdiya, 1980; Tahirkheli, 1989, 1992; Chaudhry and Ghazanfar, 1990) and Salt Range Thrust (Gee, 1945, 1989; Yeats et al., 1984; Lillie et al., 1987) or Main Frontal Thrust (MFT) (Nakata, 1972, 1989). This thrust system is the natural basis for the sub-division of Himalayas in Pakistan from hinterland to the north and foreland to the south (Gansser, 1964). General characteristics of each thrust and their respective blocks in Pakistan are briefly discussed below.

The MKT or Shyok Suture Zone is located to the south of Karakoram batholith along the meta-sedimentary belt. The southern meta-sedimentary belt of the Karakoram terrane is thrust over the Kohistan-Ladakh sequence along this suture zone. This structural horizon is characterized by grey to green slates, interbeded clastic sediments and blocks and exotic clasts of greenstone,

11

limestone, red shale and minor ultramafics and is considered an olistostromal (Pudsey, 1986) or a melange (Searle, 1991).

The MMT zone terminates the Tethyan Himalayan on the north and marks the boundary between the Indian crustal plate and the Kohistan Island Arc (Tahirkheli and Jan, 1979). In Pakistan, the Indus Suture is comprised of a complex sequence of imbricated melanges, which are composed of tectonic blocks of ophiolites, blueschists, greenschists, metavolcanics and metasediments in a matrix of shear meta-sediments and or serpentinite (Tahirkheli and Jan, 1979, 1982; Jan, 1980; Kazmi et al., 1984, 1986). The Indus Suture Zone or MMT and Shyok Suture zone or MKT bound the Kohistan-Ladakh island arc to its south and north, respectively. The MMT also bordered a structural conspicuous feature called as the Nanga Parbat Syntaxis interrupt the regional trend of the Himalayas (Coward, 1985; Zeitler, 1985). Gravity data modeling indicates that the MMT and MKT dip northward at 35° to 50° (Malinconico, 1989). Seismological data suggests that the arc is underlain by the Indian crustal plate (Seeber and Armbuster, 1979; Fineti et al., 1979) and the thickness of the Kohistan terrain is about 8 to 10km, based on gravity modeling data (Malinconico, 1989).

The Main Central Thrust (MCT) was first recognized by Heim and Gansser (1939) as a tectonic contact between the low grade Lesser Himalayan sedimentary sequence and the overlying High Himalayan crystalline complex. It is extended from Nepal up to the Kashmir (Gansser, 1964). However, its western extension in Pakistan across the Hazara-Kashmir Syntaxis has been in great controversy and doubt because of its scanty mapping and complex geology in the northwestern region (Kazmi and Jan, 1997).

The rocks of the Lesser Himalayas are thrust southward over the sub-Himalayan sequence of Neogene Siwalik molasse along the Main Boundary Thrust zone (MBT). The MBT zone is comprised of a series of parallel or en echelon thrust faults dividing the NW Himalayan sequence into a deformed southern zone or foreland zone, and a deformed and metamorphosed northern zone or the hinterland zone (DiPietro et al., 1996; Pivinik and Wells, 1996).

From NE to SW, the MBT is located in the Hazara-Kashmir Syntaxis, northern Potwar and Kohat plateau of Pakistani Himalayas.

The Himalayan Frontal Fault or the Salt Range Thrust (SRT) is the southern most thrust zone along the foothills of Salt and Trans-Indus Himalayan Ranges (Nakata et al., 1989; Gee, 1945; 1989; Yeats et al., 1984). This thrust is largely covered by alluvium and fanglomerates (Kazmi and Jan; 1997). However, at places the thrust is exposed and shows the Paleozoic rocks overlying the Neogene or Quaternary deposits of the Jhelum Plain (Gee, 1945, 1989; Yeats et al., 1984). Along the SRT there is a southward transport of the Salt Range and Potwar Plateau in the form of a large slab over the Jhelum Plain. Thus the SRT is the surface expression of the leading edge of a decollement thrust (Lillie et al., 1987).

2.4. SALT RANGE AND KOHAT-POTWAR FOLD BELT

The east-west trending fold-belt comprises the low altitude hills and valleys of the uplifted Kohat-Potwar Plateau, the Salt Range and Trans-Indus mountain Ranges (Fig. 2.4). This sedimentary fold belt is bounded in the north by the Main Boundary Thrust (Sarwar and DeJong., 1979; Yeats et al., 1984; Coward et al., 1986). Southward the Salt Range Thrust and the Surghar Thrust form its southern boundary (Gee, 1989; Yeats and Lawrence, 1984). West and eastward it is terminated by the N-S oriented Kurram Thrust and Jhelum Fault respectively (Kazmi and Rana, 1982).

2.4.1. Salt Range

The Salt Range is a complex anticlinorium structure with a series of salt anticlines (Gee, 1945, 1989). The structure along its northern slop is comprised of broad, simple and shallow folds followed by a gentle monocline (Gee, 1945, 1989). Along the southern scarp the structures are more complicated and comprise east-west trending faults and tight overfolds (Gee, 1945, 1989). The Pre-Cambrian Salt Range Formation is exposed along these overfolded and faulted anticlines. The general trend of the folds is east-west in the Central Salt Range, a few north-north-east and north-north-west trending and northward

plunging anticlines forming "nose" type structures (Kazmi and Jan, 1997). Eastward the Salt Range bifurcates into two narrow northeast trending ridges, the Diljabba and the Chambal-Jogi Tilla, both are folded and thrusted (Gee, 1989). Westward the Kalabagh Fault separates the Salt Range from the Trans-Indus Ranges (Yeats and Lawrence., 1984; McDougall and Khan, 1990).

2.4.2. Salt Range Thrust

The Salt Range Thrust forming the southern margin of the Salt Range, apparently continues westward along the southeastern margins of the Surghar-Shinghar and Khisor-Marwat Ranges (Gee, 1989). The thrust is largely covered by recent fanglomerates (Gee, 1989). However, near Jalapur and Kalabagh, the thrust is exposed and shows the Paleozoic rocks overlying the Neogene or Quaternary deposits of the Jhelum Plain (Gee, 1945, 1989; Yeats and Lawrence., 1984). Along the Salt Range Thrust, effective decoupling of sediments from the basement along the Salt layer has led to southward transport of the Salt Range and Potwar Plateau in the form of a large slab over the Jhelum Plain (Lillie et al., 1987).

A few teleseismic events are located along the southern margin of the central and eastern Salt Range (Kazmi, 1979). According to Allen (1976) there is good evidence for ongoing thrust faulting at the base of the Khisor Range. The teleseismic data from Tarbela-Chashma network shows that the Salt Range, particularly the Trans-Indus Ranges is an active structure (Seeber et al., 1980).

2.4.3. Potwar Plateau

The Potwar Plateau is bounded by the Kalachitta-Margalla Hill Ranges to the north and the Salt Range to the south, Indus River to the west and the Jhelum River to the east (Fig. 2.4). Its northern part known as the North Potwar Deformed Zone (NPDZ) is more intensely deformed. It is characterized by east-west tight folds, overturned to the south and sheared by steep-angle faults, pop-up and triangle zones (Kazmi and Rana 1982, Bannert, 1986). NPDZ is followed to the south by, wide and broad asymmetrical Soan syncline, with a gentle northward dipping southern flank along the Salt Range and a steeply

dipping northern limb along NPDZ (Khan et al., 1986; Bannert 1986). In its eastern part the strike abruptly changes to the northeast and the structures comprise tightly folded anticlines and broad synclines (Khan et al., 1986). Faulting of the anticlines is rare (Pennock et al., 1989). In the western part this basin is comprised of several east-west, broad and gentle folds. This east to west difference in the structural style has been attributed to the reduced thickness of evaporites and lesser basement slope in the eastern part of the Potwar and Salt Range.

Geophysical data and surface geology of the area shows that the Salt Range and Potwar are underlain by a gentle northward-dipping basement, with an upward convexity, and traversed by north-dipping normal faults (Lillie, 1987). Above the basement there is a decollement zone in Pre-Cambrian evaporites, which have been an effective zone of decoupling allowing thrusting without involving the basement (Lillie et al., 1987). The Salt Range is the topographic expression of this great thrust sheet. Beneath NPDZ the Phanerozoic sedimentary wedge thickens to 9 km and forms a north dipping stack of thrust faults, some of which reach the surface while others terminate at depth as blind thrust (Lillie et al, 1987).

2.4.4. Kohat Plateau

The Kohat plateau is located to the west of Potwar, and comprised of east-west trending, gentle to steeply dipping, doubly plunging, overturned folds tens of kilometer long. Likewise in the Potwar the Kohat plateau is divided into northern and southern parts. Tight, commonly overturned folds, out-of-syncline faults and several thrust faults, characterize the northern region. Some of the low angle thrust faults have folded and form klippen. They constitute a distinct thrust belt, the Kir Khweli Sar Thrust Belt (MKSTB). According to Pivnik and Sercombe (1993) it is compression related thin skinned thrust belt.

In the southern part of the Kohat Plateau east-west trending folds and north-and south-dipping dipping reverse faults are common. Fault propagation folds are common in the southern part. The Bahadur Khel Salt is exposed in anticlinal cores, where Jatta Gypsum is commonly imbricated and folded with

slivers of Panoba Shale. In this region, the lower Eocene rocks have been thrusted over the Miocene molasse at several places (Pivnik and Sercombe, 1993).

Based on field surveys and seismic profiles across the Kohat Plateau, Pivnik and Sercombe, (1993) demonstrated the absence of duplexes, passive roof thrusts, antiformal stacks in this region. They invoked that the Kohat basement is traversed by high angle conjugate reverse faults and this shows a significant degree of wrench faulting and positive flower structures (Fig. 2.5). Thus, the geometries of structures in Kohat Plateau are the product of both compressional and transpressional tectonics (Pvinik and Sercombe, 1993).

2.5. STRUCTURE OF THE TRANS-INDUS RANGES

Trans-Indus Mountains include the Surghar-Shinghar, Marwat and Khisor Ranges flanking the north-eastern and south-eastern margins of the Bannu Basin, respectively (Danilchik and Shah, 1987), whereas, Pezu, Manzai and Bhittani Ranges form the southern margin of the Bannu Basin (Gee, 1989). These ranges are a part of Himalayan Frontal Fold and Thrust belt of Pakistan lying west of the Indus River (Gee, 1989; Danilchik and Shah, 1987). These ranges are apparently the western extension of the Salt Range displaced by an active Kalabagh Fault (Yeats and Lawrence, 1984; Kazmi, 1979). Hemphill and Kidwai (1973) mentioned two parallel NE trending faults, west of Bhittani Range, parallel to the Bhittani Syncline, the Mandanna Kach and Sora Rogha Faults.

2.5.1. Kalabagh Fault

The Surghar-Shinghar Range is separated from the Salt Range by an active dextral strike-slip called as the Kalabagh Fault (Yeast and Lawrence., 1984; Kazmi, 1979). This NNW oriented fault has a long southward continuation as indicated by lineaments on Landsat images and buried dextral wrench fault inferred from seismic data (Seeber and Armbuster, 1979; Seeber et al., 1980; Kazmi, 1979, Kazmi and Rana, 1982). Southward the Kalabagh Fault apparently displaces the Salt Range Thrust and splays out into two

additional subparallel faults, the Dinghot and Ainwan Faults (McDougall and Khan, 1990). At its northern end the Kalabagh Fault bends westward and branches out into a number of smaller, north-dipping thrust faults. According to McDougall and Khan (1990), the Kalabagh Fault system forms a lateral ramp extending to the base of Salt Range-Potwar Plateau allochthon. They interpret the residual gravity anomalies in this region in terms of NNW-trending discontinuous basement ridge (Fig. 2.6). According to their model the Kalabagh Fault over-rides this ridge.

2.5.2. Surghar-Shinghar Range

The Surghar and Shinghar are north-south oriented parallel ranges covering the north-eastern margin of the Bannu Basin. The Surghar Range is characterized by Pre-Siwalik sediments, escarpment ridges facing the Indus River towards the east and the Shinghar Range mostly comprises Siwalik sediments facing the Bannu Basin towards west (Danilchik and Shah, 1987). Thus, the term Surghar-Shinghar Range is applied for the same range (Danilchik and Shah, 1987; Gee, 1989). According to Gee (1989) the range forms asymmetrical, overfolded anticlinal structure plunging to the south near the Kurram River (Akhtar, 1983), with Permian strata exposed in the core, overlain by Mesozoic and Paleogene rocks. The western limb of the range is well exposed, while its eastern limb is deeply eroded exposing older formations (Gee, 1989). The Surghar Thrust corresponding to the Salt Range Thrust is expected to continue along the axis of the Surghar Anticline bringing Punjab foreland alluvium in contact with Permian and Mesozoic rocks in the north and Neogene rocks in the south (Gee, 1989).

The earliest tectonic phase of Surghar-Shinghar Range is characterized by the formation of north-south oriented Makarwal anticline. This is followed by normal and thrust faulting on the flank of Surghar Range (Danilchik and Shah, 1987). Compressive forces produced the structure in the area also produced strike slip Miranwal fault (Danilchik and Shah, 1987). After uplift of the area, headward erosion of streams produced the steep cliffs and rugged topography of the Surghar-Shinghar Range and the material eroded from these

mountains is being deposited on the adjacent Bannu and Indus Plains (Danilchik and Shah, 1987).

2.6. STRATIGRAPHY

Sedimentary rocks of marine and non-marine origin ranging in age from Permian to Pleistocene constitute most of the stratigraphic sequence in the Surghar-Shinghar Range. Danilchik and Shah (1987) established the stratigraphy of the Makarwal and adjacent areas of the Surghar-Shinghar Range (Table-2.1) and prepared a comprehensive map on 1:50,000 scale, whereas, Azizullah (1995) carried out the sedimentological studies of the Siwalik Group of the same area. However, the southern part of the Surghar-Shinghar Range remained unmapped. Therefore, a generalized geological map on 1:50,000 scale is prepared (see chapter-3, section-II for detail) using Survey of Pakistan topographic sheet no. $38^P/_2$ and Landsat TM image (1:50,000) as base maps. Since, the area is the southern extend of the Makarwal anticline, therefore, for the identification and mapping of lithological units, stratigraphic codes used by Danilchik and Shah (1987) were used. Five lithological units have been recognized to the south of the Makarwal anticline i.e., from top to bottom:

5. Soan Formation
4. Dhok Pathan Formation
3. Nagri Formation
2. Chinji Formation
1. Mitha–Khattak Formation

2.6.1. Mitha Khattak Formation

The Mitha Khattak Formation (Danilchik and Shah, 1987) underlies the rocks of the Siwalik Group with a transitional contact in the Surghar-Shinghar Range. However, at some places it is faulted. The type locality of the Mitha Khattak Formation is along the mouth of the gorge northeast of the village of Mitha Khattak (Danilchik and Shah, 1987).

Above a basal conglomerate, thick beds of moderate-yellowish-brown, fine-grained, pebbly sandstone with rounded to subrounded grains are

18

interbedded with very thick beds of moderate-reddish-brown, clayey siltstone that is increasingly abundant towards the top of the Mitha Khattak Formation. The basal conglomerate ranges from 1.7m to 8m in thickness. It is yellowish brown and consists predominantly of well-sorted cobbles and pebbles of limestone and rarely, of chert derived from the underlying Sakesar Limestone. The matrix of the conglomerate and the overlying beds of sandstone are mostly yellowish brown, fine to coarse grained, and consists of rounded to subrounded polished quartz grains. Cement is calcareous (Danilchik and Shah, 1987).

A sequence of red siltstone overlies the topmost sandstone bed of the Mitha Khattak Formation. These beds are not included in the Mitha Khattak because the rocks are also similar to the brick-red siltstone and claystone of the Chinji Formation marks a transitional contact (Danilchik and Shah, 1987).

The age of the Mitha Khattak Formation is not known. The formation may be equivalent to the "Red claybeds" of Eocene age that crop out in the western Salt Range near Daud Khel or the Bhadrar beds also of Eocene age, or they may be equivalent to part of the Murrees (Danilchik and Shah, 1987).

2.6.2. Chinji Formation

The Chinji was named by Pilgrim (1913) after the village of Chinji on the Potwar Plateau. In the Surghar Range the formation consists of maroon to brownish red colored shales and subordinate greenish gray colored sandstones (Azizullah, 1995). However, according to Danilchik and Shah the Chinji Formation in the area predominantly consists of very thick beds of reddish-brown to reddish-gray sandstone. The sandstone is fine- to medium-grained and occasionally gritty. Grit, clay balls and pebbles are present along the cross-bedding of paleostream channels (Azizullah, 1995). Lithofacies of the formation exhibit the presence of scouring surfaces (Sc), trough cross-bedding (St), low angle bedding (Sl), planar-tabular cross-bedding (Sp), horizontal bedding (Sh) and ripple marks (Sr). Sedimentary structures like parallel, horizontal, lenticular, wavy and graded bedding within the shale horizons are present. Some shale horizons show relatively mature paleosols with concretions, animal burrows and mud cracks. Sand/Shale ratio within this

formation is 1:0.82 along Garang Nala section and 1:1.5 along Zhira Nala section. Thickness of the formation varies from 1160m to 1400m (Azizullah 1995). The Chinji Formation unconformably overlies the Sakesar Limestone and the Mitha Khattak Formation in the Surghar Range. The upper contact with the Nagri Formation is transitional (Danilchik and Shah). The age of the formation is 10 m.y. in the area (Khan, 1983; Khan and Opdyke, 1987).

2.6.3. Nagri Formation

The Nagri Formation (Pilgrim, 1913; Lewis, 1937) consists of thick massive sandstones without any shale or mudstone (Azizullah 1995). However, in the study area, minor shale horizons have been recognized. Sandstones are mainly medium grained, but fine as well as coarse-grained sandstones are also present. Sandbodies can be differentiated by the erosional or truncated paleochannel surfaces. Occasional pebbles are also present within sandbodies. The pebbles are rounded and consist of chert, quartzite, milky quartz, granite, diorite and rarely rhyolite (Danilchik and Shah, 1987). The color of the sandstone varies from greenish gray to light gray and dark grey. In general the sandstones are immature and poorly to moderately sorted. Sandbodies are mainly composed of different storeyed stacked both vertically and laterally. Common lithofacies are massive gravel (Gm), trough gravel (Gt), scouring surfaces (Sc), trough cross sand (St), planner sand (Sp) and horizontal sand (Sh) (Azizullah 1997). Maximum thickness of the formation along the Garang Nala section is 2075m in Shinghar Range (Azizullah, 1995). Its upper contact with the Dhok Pathan Formation is transitional (Azizullah, 1995). Age of the Nagri Formation in the Shinghar Range is from 7.5 m.y. to 2.4 m. y. (Khan, 1983; Khan and Opdyke, 1987).

2.6.4. Dhok Pathan Formation

The Dhok Pathan Formation (Pilgrim, 1913; Lewis, 1937) shows excellent cyclic deposition of shales and sandstones (Azizullah, 1995). The color of sandstones varies from light gray to ash gray and gleaming white. Grain sizes are generally fine to medium grained, but within the paleochannel, coarse-grained gritty sandstone is also present. At some places, small brownish

red colored clay balls are embedded along cross-sets. Sandbodies are generally multi-storeyed. Cross-sets thickness varies from half to two meters. Lithofacies vary from scouring surfaces (Ss), trough cross-bedding (St) to horizontal bedding (Sh), massive gravel (Gm) and trough gravel (Gt) facies (Azizullah, 1995).

Shales are generally light reddish brown to grayish colored. Intercalations of very fine sand and silt are present within shale beds. Sedimentary structures like graded bedding, parting lineation and slickensides are present. Deformation and compressional features like bioturbation/disruption are also present. The thickness of the formation varies from 950 to 1200m (Azizullah, 1995). Age of the Dhok Pathan Formation in the area ranges from 2.4 m. y. to 0.85 m. y. (Khan, 1983; Khan and Opdyke, 1987).

2.6.5. *Soan Formation*

Soan Formation (Kravtchenko, 1964) in the Shinghar Range consists of massive conglomerates, sandstone and siltstone/mudstone (Azizullah, 1995). At the base of the formation, sandstone and siltstone are dominant, while in the upper part conglomerates predominate. The color of sandstone is light gray, silstone/mudstone are pale pinkish to earthy buff color. Sandstone are medium to coarse grained and friable. Small pebble, grit and clay balls occur along the cross-sets. Sandstone and siltstone intercalations are common. The conglomerates are composed of clasts of limestone, quartzite, andesite, rhyrolite, agglomerate, granite, chert, glauconitic sandstone, graywacke, vein quartz, diorite-tonalite and amphibolite. Size of the clasts varies from few centimeters to twenty centimeters. Lithofacies like massive gravel (Gm), trough cross-bedded (Gt), planner gravel (Gp), scouring surfaces (Ss), trough cross sand (St) and horizontal sand (Sh) are present (Azizullah, 1995).

The thickness of the formation is more than 1000m (Azizullah, 1995). Lower contact with the Dhok Pathan Formation is gradational. Age of the formation ranges from 0.8- 0.5 m. y. (Khan, 1983, Khan and Opdyke, 1987).

21

Table 2.1. Stratigraphy of the Trans-Indus Mountains (Danilchik and Shah, 1987).

System			Surghar-Shinghar Range	Marwat-Khisor Range
Tertiary/ Quaternary	Siwalik	Group	Dhok Pathan Formation Nagri Formation Chinji Formation	Malagan Formation Dhok Pathan Formation Nagri Formation Chinji Formation
Tertiary			Mitha Khattak Formation Sakessar Limestone Nammal Marl Patala Shale Lockhart Limestone Hangu Formation (includes Makarwal coal beds)	?
Cretaceous			Lumshiwal Formation Chichali Formation	Chichali Formation
Jurassic			Samana Suk Limestone Shinawari Formation Datta Formation	Samana Suk Limestone Shinawari Formation Datta Formation
Triassic	Tredian Formation		Kingriali Dolomite Khatkiara Sandstone Member Landa Member	Kingriali Dolomite Tredian Formation
	Mianwali Formation		Narmia Member Mittiwali Member Kathwai Member	Mianwali Formation
Permian	Zaluch	Group	Chidhru Formation Wargal Formation	Chidhru Formation Wargal Formation Amb Formation
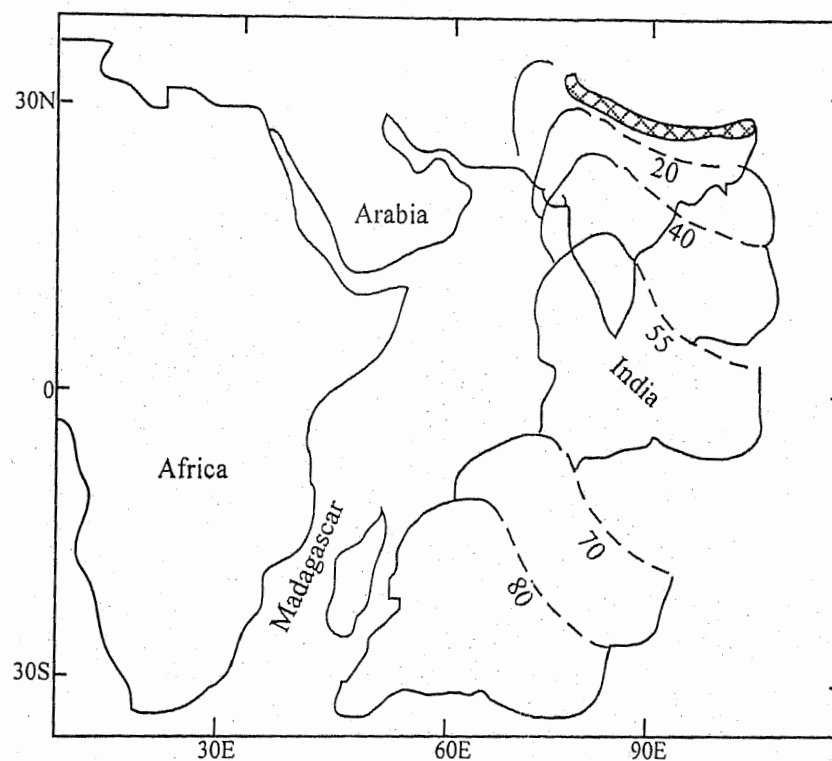
Fig. 2. 1. Reletive motion of Indian subcontinent to the Africa and Madagascar since 80 m. y. (from Powell, 1979).
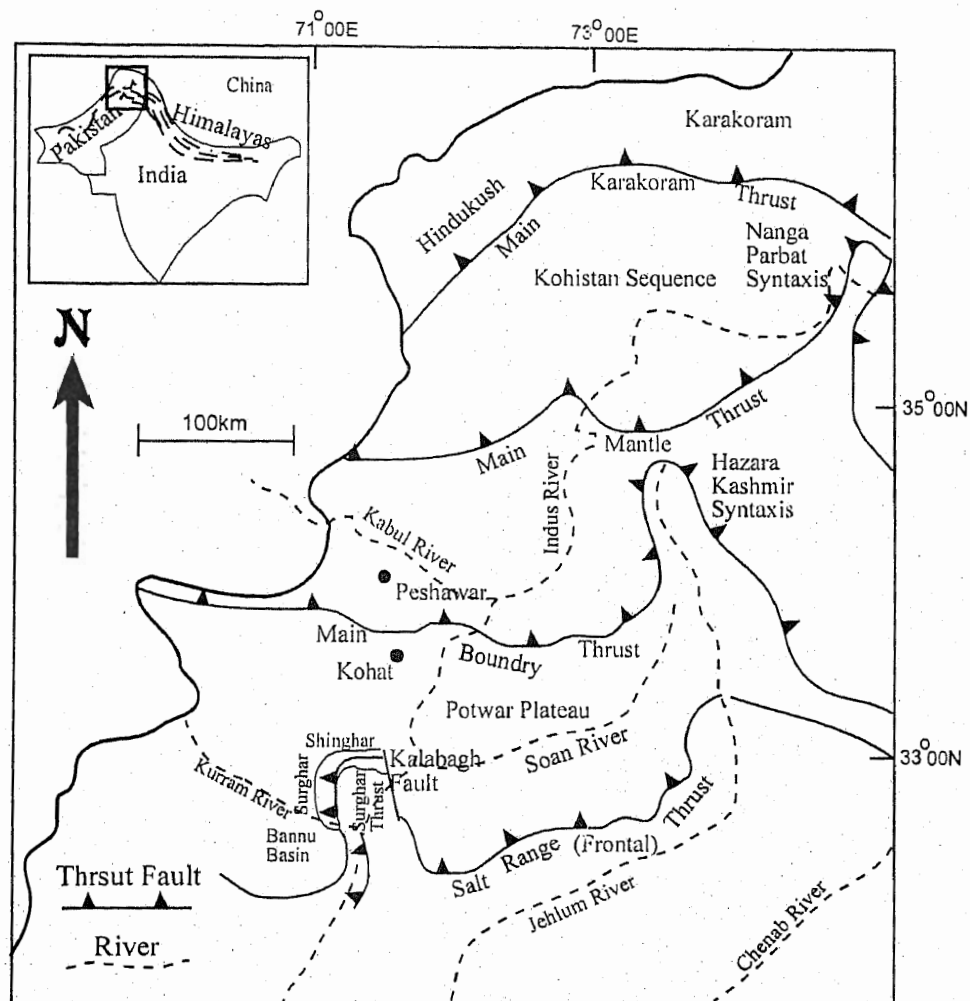
Fig.2.2. Outline structural map of northern Pakistan.

NNW

Kohistan   Mansehra   Abbottabad   Hazara Hills   Rawalpindi   Potwar   Eastern
                                                                    Plateau   Salt Range

MMT : Main Mantle Thrust
MT   : Mansehra Thrust
AT   : Abbottabad Thrust
NGT : Nathia Gali Thrust

0 ▭▭▭▭ 25Km

▭ Siwaliks
▭ Murrees
▭ Perm-Eoce. L.st.
▭ Lwr. Palaeozoic
▭ Hazara Slates
▭ Granitic Basement
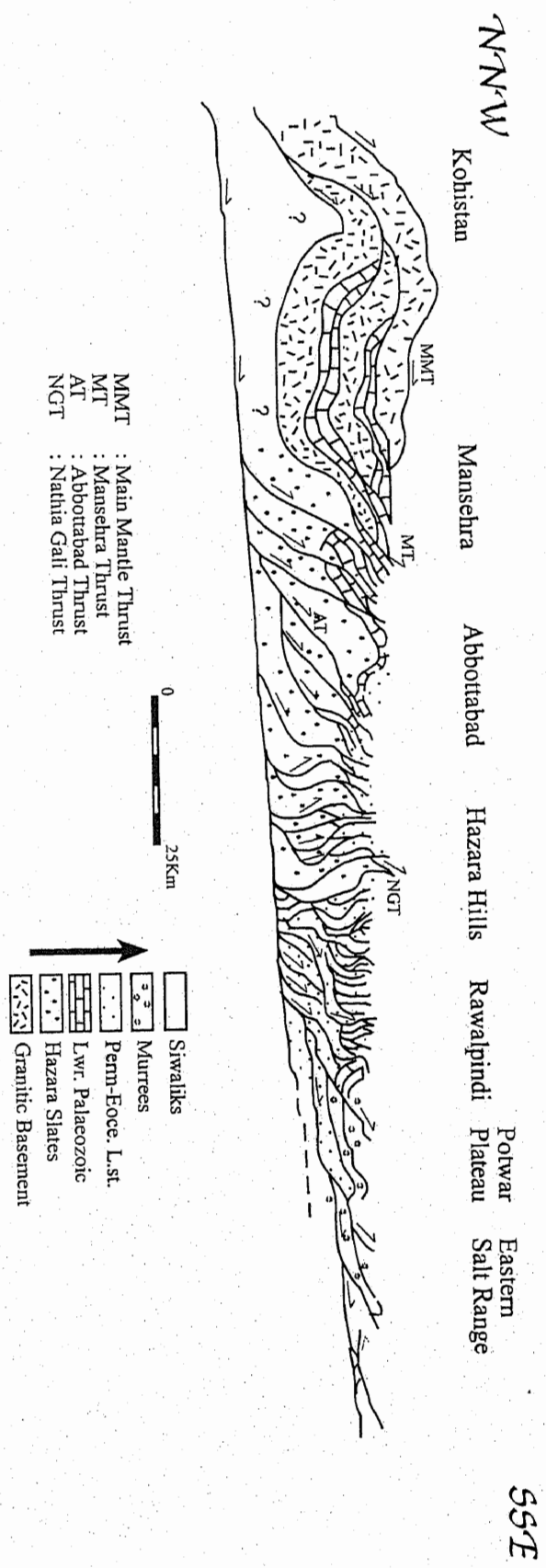
Fig. 2.3. Simplified balanced cross-section through Pakistan Himalayas, from Main Mantle Thrust (MMT) to foreland (after Coward and Butler, 1985).
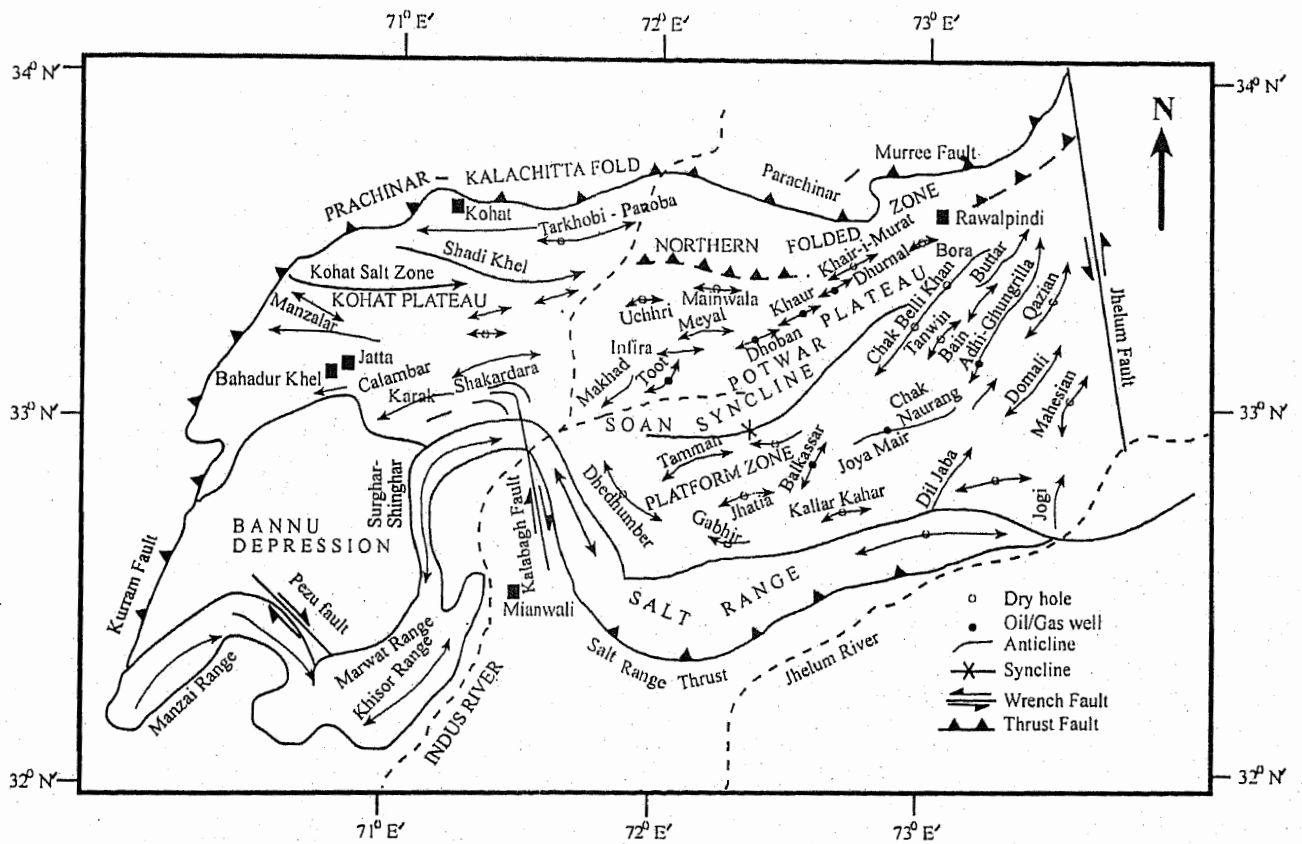
Fig. 2.4. Simplified structural and oil-geological map of the Kohat-Potwar Plateau (after Khan, et al., 1986)
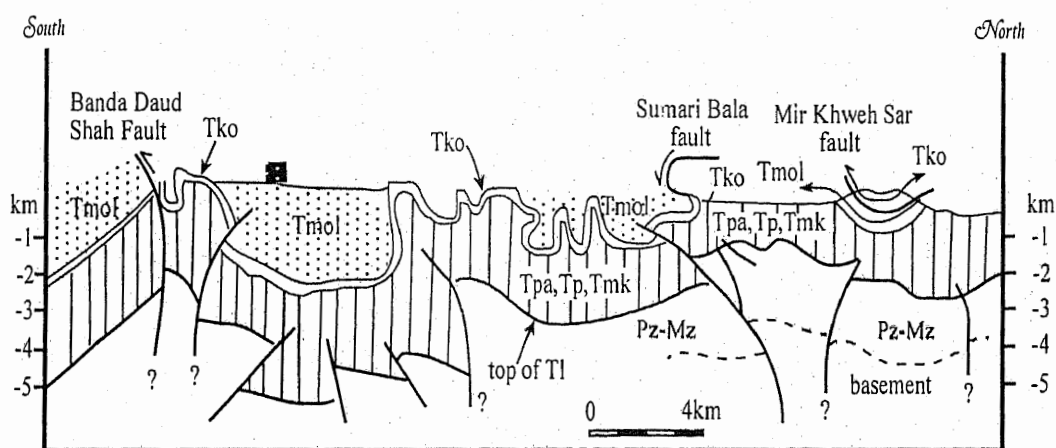
Fig. 2.5. Geological cross-section across the Kohat Plateau (from Pivnik et al., 1993).

Tmol, *Rawalpindi & Siwalik* Gr; Tko *Kohat Fm*; Tmk, *Mamikhel Fm*; Tp, *Panoba sh*; Tps, *Patala Fm*; Tl *Lochart Fm*; Pz-Mz, *Paleozoic to Mesozoic*.

Key

(dotted)	Siwalik Molasse
(dark shaded)	Paleozoic-Late Tertiary Strata
(dashed)	Eo-cambrian Salt Range Formation
(cross-hatched)	Basement
(line)	Fault, with teeth on upper plate
(dashed line)	Subsurface Projection
(arrow)	Surface structure

VISOR FAULT

SURGHAR RANGE

Kalabagh

5 km

σ₁
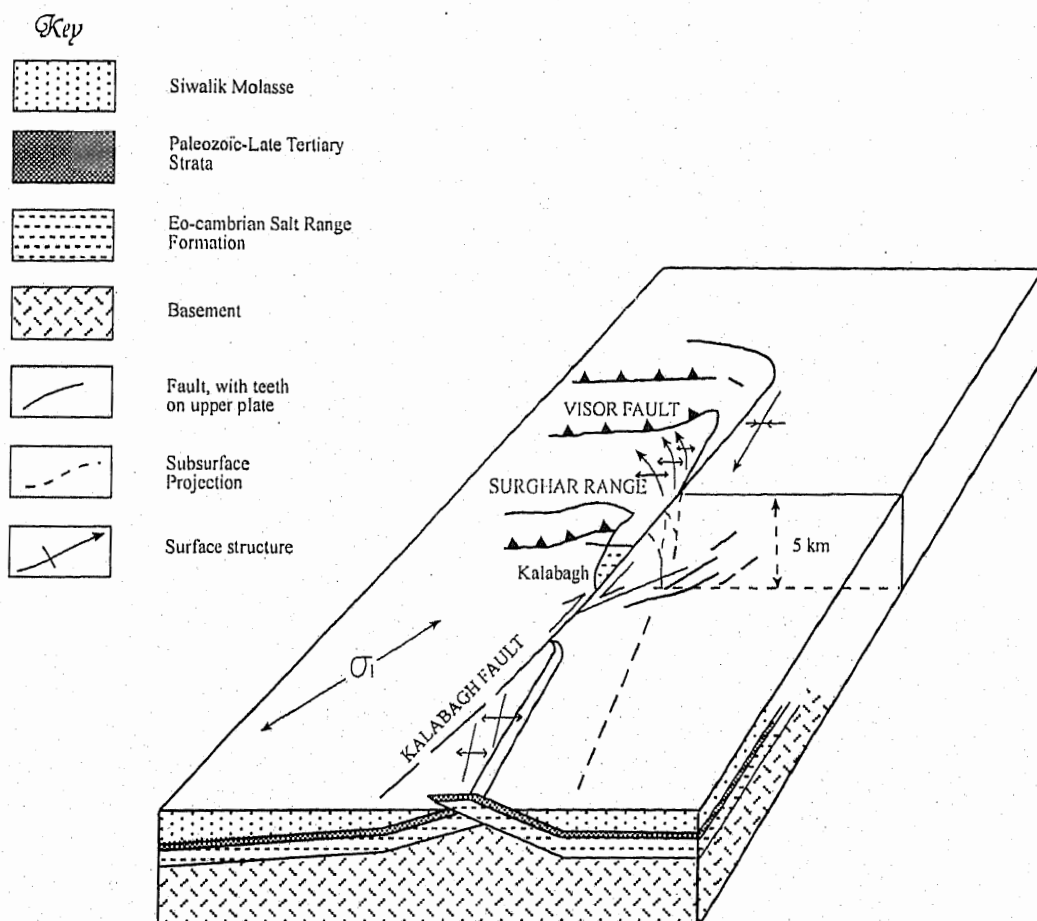
KALABAGH FAULT

Fig. 2.6. Block diagram of the Kalabagh fault lateral ramp. The basement ridge extends north to the Kalabagh area where it dies out, as suggestrd by reduction of the residual gravity anomaly (after, McDougall & Khan, 1990).

Chapter 3

DESCRIPTIVE ANALYSIS

3.1. INTRODUCTION

Descriptive analysis concerned with recognizing and describing structures and measuring their locations, geometries and orientations (Davis and Reynolds, 1996). Orthographic and stereographic projections are used in the descriptive analysis for proper orientation of data collected in the field. Therefore, this chapter is divided into two sections; in the first section various standard methods are described according to which data is recorded in the field. Then various graphical techniques have been adopted for detailed descriptive analysis. The second section deals with the detailed description of geological field observations. Macroscopic (regional scale) and mesoscopic (outcrop scale) structures are observed, photographed and described.

SECTION I

3.2. METHODS

3.2.1. Image interpretation

Edge enhanced Landsat TM (1:65,000) and SPOT (1:50,000) images are used for preliminary mapping of lithological units and structures in the Surghar-Shinghar Range. The images are especially enhanced by using directional filters for structural interpretations, whereas, tonal enhancements are carried out for the identification of lithological units. A computerized tracing of major geological features is prepared from these images, which was, later, used as a base-map for geological mapping on 1:50,000 scale.

3.2.2. Geological mapping

A geological map of Shava-Shanawah-Puki area has been prepared on 1: 50,000 scale using Survey of Pakistan topographic sheet no. $38^P/_1$. The map covers the lithogical units and main structures of the area. For the identification and mapping of lithological units of the Siwalik Group in the area, stratigraphic

29

codes i.e., color, lithological differences, contact relationships, etc., used by Danilchik and Shah (1987) were utilized. However, SPOT image on 1: 50,000 scale have also been used in the field for the identification of lithological units.

3.2.3. Mapping of fractures

Field data has been collected from seven different sites around the Shinghar Range i.e., from south to north, Qabul Khel, Gulapa, Samandi, Abbasa, Shanawah, Thatti-Nasrati and Seraj Khel areas. Circle inventory (Davis, 1984) and traverse (Marshak and Mitra, 1988) methods have been adopted for fracture analysis. A Grid map of Mochi-Mar and Qabul Khel areas have been prepared for lithological and structural mapping of shear zones.

3.2.4. Circle inventory method (Davis, 1984; Davis and Reynolds, 1996)

This method allows a systematic collection of orientation data in a limited area to be used for statistical analysis and frequency diagrams. A circle of known diameter is predetermined on a bedrock surface (Fig. 3.1), where maximum numbers of fractures are exposed. Then, the orientation and trace length of each fracture within the circle are measured. The measure of fracture density is *"the summed length of all the fractures within an inventory circle, divided by the area of the circle"*,

$$pf = \frac{L}{\pi r^2}$$

where, pf = fracture density
L = cumulative length of all fractures
r = radius of inventory circle

Total twenty two inventory stations have been located mostly on the western side of the Shinghar Range. Four in Gulapa (Appendix-1, Table-3.1), four at Samandi (Appendix-1, Table-3.2), four at Abbasa (Appendix-1, Table-3.3), four at Shanawah (Appendix-1, Table-3.4), three at Thatti Nasrati (Appendix-1, Table 3.5) and three at Seraj Khel (Appendix-1, Table-3.6). Fracture density is calculated for each station and their averages have been re-calculated.

3.2.5. Traverse method (Marshak and Mitra, 1988)

Reconnaissance and detailed field traverses have been made in the Qabul Khel, Gulapa, Samandi, Abbasa, Shanawah, Shava, Thatti-Nasrati and Seraj Khel *nalas*. These streams perpendicularly cut the strike of the range i.e., east-west oriented. Shanawah *nala* has been selected for detail fracture analysis; as it is located in the middle of the range and nicely exposes the fracture patterns. A detailed structural and generalized sedimentological cross-section of Shanawah-Godi Khel *nala* on 1:5000 scale is prepared covering some 8 Km. Most of the prominent fracture sets are mapped along the section line (structural cross section, in pocket). It is worth noting that the general characteristics and attitudes of the fracture sets in all the above mentioned streams are similar. Therefore, the Shanawah *nala* has been selected as a representative section.

3.2.6. Grid mapping

A grid map of Qabul Khel and Mochi Mar areas has been prepared for detailed structural analysis of deformation band shear zones on 1:5000 scale. This area was selected for grid mapping for its nice exposures of both the joints and shear fractures. Theodolite was used for the preparation of grids in the area for locating and mapping structures (Fig. 3.2).

3.2.7. Rose diagrams

Rose diagrams provide an immediate visual estimate regarding any orientation data. A standard rose diagram is constructed on a grid composed of concentric circles superimposed on a set of radial lines (Marshak and Mitra, 1988). The orientation data collected from the inventory circles is organized into class intervals of 10° with respect to geographical coordinates. Data is then plotted according to the scale by number of fracture readings occupy each class interval. Representative frequency diagrams have been shown in figures 3.4 – 3.9.

3.2.8. Stereographic Projections

Equal-area stereographic projections have been used for plotting the strike/dip data, their respective poles and for the determination of the angle between two fracture planes.

No. 44 – C

2002

SECTION II

3.3. MACROSCOPIC STRUCTURES

For the recognition and interpretation of macroscopic structures, Landsat TM (1: 65,000) and SPOT (1: 50,000) images were used for preliminary geological investigations. Field observations were made for detailed structural studies.

The Surghar-Shinghar Range at the eastern margin of the Bannu Basin forms an anticlinal structure. Its outer flank (convex side) is nicely exposed, whereas its inner flank (concave side) is deeply eroded, exposing core formations (Gee, 1989). Regional strike of the range from Qabul Khel to Thatti-Nasrati is north-south, north-northwest dipping towards west with an angle of about 35°-45° at the outer limbs of the anticline and 45°-55°, occasionally 55°-65° near the core (Fig. 3.3). Previously, the north-south oriented part of the range was considered as a single structure, i.e., Makarwal anticline (Danilchik and Shah, 1987). However, based on satellite image interpretation and field observations, it is interpreted that the southern part of the Surghar-Shinghar Range forms a dome-basin pattern (Fig. 22.15, Type-1 of Ramsay and Huber, 1987), that is, Makarwal anticline (Danilchik and Shah, 1987) to the north and Sarkai-Mochi Mar (SMM) dome-shape anticline to the south (Fig. 3.10, 3.11). The Sarkai is the only population center located on the eastern margin of the anticline, whereas the Mochi Mar *nala* is one of the accessible streams to the main structure. These two anticlinal structures are separated by an exceptionally low topographic relief, characterized by a small basin structure, where the Gulapa-Darsola *nala* flows from west to east. We name this structure as the Gulapa-Darsola basin in this study (Fig. 3.11).

The Makarwal anticline plunges towards the south, where the strike of the beds gradually changes and forms a loop. The SMM anticline forms a dome-shape (semi-circular) structure predominantly composed of Siwalik sediments with a patch of Mitha-Khattak Limestone, which is the oldest rock unit observed at the core of the anticline. Mainly Chinji, Nagri and Dhok Pathan formations of the Siwalik Group have been recognized. As the SMM

32

dome-shape anticline is the southern continuation of the Makarwal anticline, therefore, for the recognition and mapping of lithological units, stratigraphic codes used by Danilchik and Shah (1987) were adopted.

The Surghar Thrust in the Makarwal anticline is characterized by steep scarps and cliffs, overturned/overfolded rocks (Gee, 1989) and tectonic uplift in the area (Khan, 1987; Danilchik and Shah, 1987). The thrust appears on the geological maps of north Pakistan (Searle and Khan, 1996) and on the seismo-tectonic maps of Kazmi (1979). Overall, the thrust runs along the eastern margin of the Surghar Anticline bringing Punjab foreland alluvium in contact with upper Permian and Mesozoic rocks in the northern (Makarwal anticline), and Neogene rocks in the southern (SMM dome-shape anticline) parts of the fault trace.

To the south of the Mitha Khattak village, the Surghar Thrust (ST) is passing at the core of SMM dome-shape anticline and appears to split into number of faults into adjacent sandstone horizons of the Siwalik Group in the form of deformation bands. In Sarkai area major movement along the ST is reverse, however, at places it is oblique slip e.g., in Sarkai *nala* one of the major thrust splays marks by an high-angle oblique-reverse slip movement between the Mitha Khattak Limestone and Chinji Formation (Fig. 3.12). The sense of movement along this fault is inferred from slickenlines and minor asymmetric folds. However, southwards it gradually changes to strike-slip fault, offsetting the Kurrum River near Dara Tang, before it dies out at the northern tip of the Marwat Range. We name this prominent structural feature as the Dara Tang Fault. This fault is a very prominent structural feature on the SPOT and TM images (Fig. 3.11).

Thus, it is concluded that the southern part of the Surghar-Shinghar Range at the eastern margin of the Bannu Basin structurally form a basin-dome pattern, consisting of Makarwal anticline to the north and SMM dome-shape anticline to the south separated by a narrow Gulapa-Darsola basin in the hanging-wall of the Surghar Thrust (Main Frontal Thrust or Salt Range Thrust).

3.4. MESOSCOPIC STRUCTURES

Field observations are made and structural data has been collected along various streams around the Surghar-Shinghar Range, however, we select the north-south oriented part of the Range from Qabul Khel to Thatti-Nasrati to represent the area under particular structural case for fracture analysis. As the strike of the beds changes from north-south to east-northeast near Thatti-Nasrati, the orientation of fracture pattern changes as well, but the geometrical characteristics remains the same as observed in the north-south oriented part of the range. *cf.* Table 3.1-3.6 (Appendex-1) and figures 3.4-3.9.

3.5. DESCRIPTIVE ANALYSIS OF FRACTURES

The Siwalik Group of the Surghar-Shinghar Range, especially the Nagri and Dhok Pathan formations are bisected by various sets of fractures, whereas the southern end of the Sarkai-Mochi Mar dome-shape anticline i.e., the Qabul Khel and Mochi-Mar areas expose incipient deformation band shear zones, tensional and compressional joints.

Genetically there are three types of fractures, namely, 1. dilation fractures, 2. shear fractures (Griggs and Handin, 1960), and 3. hybride or shear-dilation fractures. (Price and Cosgrove, 1990). We will use this classification and other relative terms (bedding or layer-parallel shear fractures, cross, longitudinal and diagonal fractures; Han Closs, 1922; Ramsay and Huber, 1987) in our study.

The age of the Dhok Pathan Formation is not more than 0.85 m.y. (Khan, 1983, 1987). The age of the Surghar-Shinghar Anticline and associated structures is constrained by the sediments involved in the deformation. The involvement of these sediments together with recent Soan conglomerates in the deformation suggest role of neotectonics in the origin of the Surghar-Shinghar Range.

Generally, sandstones of the Siwalik Group are thick-bedded with channels and clay ball scoured surfaces and varying proportions of shale horizons. The clay ball scoured surfaces are more frequent than the shale

horizons particularly in the Dhok Pathan and Nagri formations of the Siwalik strata. Hence, shale and clay ball scoured surfaces are the major weak planes to accommodate stresses during folding rather than thick sandstone horizons.

3.5.1. Shear fractures

3.5.1.1. Bedding or layer-parallel shear fractures:

Bedding or layer-parallel shear fractures (Ramsay and Huber, 1987) are in the form of reverse faults along the sedimentary bedding. These fractures are the most conspicuous structural feature of the range concordant with the regional strike and dip of the Siwalik strata. (NNW/NS/NNE/ 40°-50°W; Table 3.1-3.6 see Appendix-1; Fig 3.4-3.9) (cross section, in pocket). These fractures are preferentially concentrated along the clay ball scoured surfaces (Fig. 3.13) and infrequently along shale horizons and in the sandstone bodies. The clay balls along these fractures are rotated and displaced, and are used as indicators of sense of movement in this study. Mainly reverse sense has been interpreted from the clay ball kinematic geometry. Other than sheared clay ball scoured surfaces, the layer-parallel shear fractures have also been observed within the sandstone bodies forming dark gray, very fine-grained gouge matrix (Fig. 3.14).

3.5.1.2. Descriptive analysis of strained clay balls

The clay ball scoured surfaces are frequently exposed within the thick sandstone bodies of the Siwalik Group of Surghar-Shinghar Range providing weak planes for deformation (Fig. 3.13). The deformed clay balls observed along sheared scoured surfaces range in size from few millimeters to tens of centimeters, grounded and displaced within the sandstone matrix (Fig 3.13 – 3.23). The color of the clay ball varies from one unit to the other within the Siwalik Group. The clay balls observed in the Dhok Pathan Formation are light-yellowish brown to dark brown; while those found in the Nagri Formation are dark-gray and occasionally greenish gray-yellowish brown in color. Greenish gray, maroon to light brown clay balls are observed in the Chinji Formation. To understand the geometry of rotated and displaced clay balls with respect to their internal fabric, we can deal them separately.

3.5.1.3. *Displaced clay balls*

Clay balls, which are moderately hard due to calcification or may be due to black, very fine carbonaceous material, are totally displaced along shear planes. Their displacement clearly shows the reverse sense of shear and amount of displacement (Fig. 3.15 - 3.17). It appears that their hardness is responsible for their displacement along the shear planes. Some of the displaced clay balls form internal fabric in the form of Riedel fractures (Fig. 3.15). Two sets i.e., synthetic R_1 and antithetic R_2 conjugate Riedel patterns have been recognized within the strained clay balls.

3.5.1.4. *Rotated clay balls*

Most of the rotated clay balls observed along shear zones form asymmetric tails (Fig. 3.18-3.20) just like the asymmetric tailed porphyroclasts formed in metamorphic shear zones. The sense of asymmetry of the tails is used as the sense of shear in the deformed rocks (Passchier and Simpson, 1986). The leading and trailing edges, which are common in most of the rotated clay balls observed along shear zones, are considered as the shear sense indicators in this study. Most of the rotated clay balls are very similar in shape with those of sigma (σ) porphyroclasts. Other rotated clay balls along the scoured surfaces are rotated with no tail edges. Within this category two types are recognized regarding their internal structure. Rotated clay balls with no tail edges, fairly rounded with rotated internal structure to a greater extent in some cases and to lesser extent in all cases, indicating shear sense (Fig. 3.21). The second type forms discrete fractures, clearly indicating reverse shear sense with oxidized boundaries of yellowish brown to dark brown color (Fig. 3.22, 3.23).

Reverse incipient movements, concordant to the bedding, have also been observed within the channel conglomerates of the Siwalik Group (Fig. 3.24). Pebble-size gravels are displaced with antithetic R_2 Riedel fractures showing reverse sense of movement along the channel scoured surfaces.

3.5.1.5. *Longitudinal or fractures normal to the bedding planes*

North-south oriented longitudinal or fractures normal to the bedding planes (Ramsay and Huber, 1987; Price and Cosgrove, 1990) generally cut across the layer-parallel shear fractures, are not uncommon within the sandstone horizons (Fig. 3.25, 3.14) (cross section, in pocket; Fig. 4.2). These fracture sets dip towards east with varying degree of angles (Fig. 3.26, 3.27, 3.28) displacing the bedding fractures forming net of fracture sets (Fig. 3.29). The angular relationship of bedding and longitudinal fractures is almost perpendicular ($\geq 90°$). At places it is worth noted that most of the longitudinal fractures form two distinct fracture sets at slightly different angles (Fig. 3. 30). Reverse sense of movement has been interpreted for these longitudinal fractures as they displaced the first phase of layer-parallel shear fractures (Fig. 3.25). Most of these fracture sets are gouge filled, however some are calcified with whitish gray, gray and light brownish gray color (Fig. 3.30).

3.5.2. Dilational fractures

Orthogonal to the bedding and longitudinal fracture sets, there are east-west oriented dilational (Price, 1966) or cross fractures (Ramsay and Huber, 1987) in the Siwalik strata of Surghar-Shinghar Range (Fig. 3.31; Table 3.1-3.6 see Appendix-1; Fig 3.4-3.9). The scale of these fractures ranges from meso- to macroscopic. These extensional fractures are well exposed on the hard sandstone bands of the Chinji, Nagri and Dhok Pathan formations.

Image interpretations using Landsat TM and SPOT suggest predominance of roughly east-west oriented parallel, sub-parallel drainage pattern across the range. A parallelism between the drainage pattern of the range and the east-west oriented extensional fractures suggests role of the structural control on the geomorphology. These east-west oriented extensional fractures are dilated by seasonal drainage, forming steep gorges, especially in the Siwalik sediments (Fig. 3.32). The dilational fractures in these lithologies facilitate drainage along these lines, thereby controlling the geomorphic processes (Fig. 3.33).

3.5.3. Conjugate shear fractures

Infrequent and less populated than those of bedding, longitudinal and dilational fractures are the oblique-slip or conjugate shear fractures (Price. 1966; Price and Cosgrove, 1990) with dextral and sinistral sense of shear. The orientation of these fracture sets varies according to the local attitude of the beds (*cf.* Table 3.1-3.6 see Appendix-1; Fig 3.4-3.9). These fractures are nicely exposed on the hard sandstone bands of Chinji and Nagri formations in general and Dhok Pathan Formation in particular of the Shinghar Range (Fig. 3.34, 3.1). Generally, the acute angle between these two fracture sets is not more than 75°.

3.6. SHEAR ZONES

3.6.1. General Characteristics

Geometry of shear zones and their deformational mechanism largely depend upon syn-shearing breakage style and P/T conditions (Fig. 3.35) and classified as cataclastic, transitional and mylonitic types (Sibson, 1977). Generally, a shear zone is defined as "a long, narrow, broadly tabular zone of concentrated inhomogeneous deformation across which one block of rock is displaced with respect to second one" (Mawer, 1992). Shear zones can develop at any scale from lithospheric plates to that of single grain. Micro- to macro-structures may developed at shear zone boundaries and within the shear zones, which are asymmetric with respect to the internal fabric are considered to have their asymmetry directly related to the direction and sense of displacement and are referred to as "Kinematic indicators" (e.g., Berthe et al., 1979; Lister and Snoke, 1984; Passcheir and Simpson, 1986; White et al., 1986; Cobbold et al., 1987; Mawer, 1992; Mawer and White, 1987).

Cataclastic deformation is characterized by fractured rocks, which may be either incohesive/brittle (gouge, breccia) or cohesive (cataclasites) (Sibson, 1977). However, the incohesive cataclastic shear zones show grain rolling, reduction in grain size and comminution by brittle fracturing (Sibson, 1977; McKlay, 1997; Mawer, 1992).

The southern part of the SMM dome-shape anticline is deformed by a system of conjugate strike-slip deformation band shear zones (DBSZs) (Aydin, 1978; Davis et al., 2000) with Riedel fracture sets. This study examines the geometry of outcrop-scale Riedel shear zones composed of deformation bands marked by grain-scale cataclasis and compaction of sandstone of the Nagri and Dhok Pathan formations. The physical and geometrical characteristics of the DBSZs are unique in many ways. The shear is accomplished through a mechanism that involves stress-induced collapse of porosity, grain-scale fracturing, grain-size reduction and cataclastic flow (Aydin, 1978; Aydin and Johnson, 1978; Antonellini et al., 1994).

3.6.2. Field observations and shear zone geometries

The southern part of the Sirkai-Mochi Mar dome-shape anticline exposes strike-slip DBSZs. Since, these are developed in poorly to moderately cemented sandstones, therefore by virtue of loss of porosity and volume during shearing and calcification by solution action, are strongly resistant to erosion and thus stand out like ribs or fins in the outcrops (Fig. 3.36) or form wall like structures (Fig. 3.37). Differential resistance to erosion displayed by the shear zones relative to the normal porous sandstones in between the shear bands, creates magnificent inside views of Riedel deformation band architecture (Fig 3.38). Thus, these shear zones are formed through a combination of shear and volume reduction in the younger sedimentary sequence of the Shinghar Range.

The Principal Shear Zones (PSZs) occur in two conjugate sets: right-handed set striking NS and a left-handed set striking N50°-60°E. The NS oriented DBSZs are dominant in the Mochi Mar and Qabul Khel area, close to the Dara Tang fault. These DBSZs are relatively thick (5-20cm), massive, continuous with dextral sense of movement. The sense of shear is interpreted from the displacement in the hard sandstone bands (Fig. 3.39, 3.40). Offset on map-scale PSZs is strike-slip and ranges from tens of centimeters to few meters or more.

The second set of DBSZs is broad and tabular with N50°–60°E orientation, showing strike-slip sinistral shearing. The sense of shear in this

39

type is interpreted from incipient Riedel fractures developed within the N50°–60°E oriented Principal Shear Zones (PSZs). The Riedel fracture (Riedel, 1929) sets are very useful kinematic indicators in cataclastic/brittle shear zones because direction and sense of movement can be deduced from these patterns (Mawer, 1992; Ahlgren, 2001). The ideal situation is represented by their fullest development of complete set i.e., R_1, R_2, P, Y, T and X shear fractures (Fig. 3.41). Geometrically, the idealized Riedel pattern is defined by "a series of fractures oriented at specific angles to the trend of Principal Shear Zone (PSZ)" (Ahlgren, 2001). In natural systems, the most widely accepted model for Riedel shear zone development is that the low-angle R_1 and P shears generally pre-date higher-angle R_2 shear fractures (Ahlgren, 2001). Most workers agree that R_1 shear fracture are the first or one of the first shear to form (Morgenstern and Tchalenko, 1967; Barlett et al., 1981), although P shear fracture may also form first, especially in dilational systems (Moore and Byerlee, 1992) (Fig. 3.42).

Mainly R_1, R_2, P and Y Riedel fractures have been observed within the N50°–60°E oriented PSZs (Fig. 3.43, 3.44, 3.45). Normal slip has been observed along R_2 Riedel fabric in some of the tabular shear zones (Fig. 3.44).

Displacement along the NS oriented DBSZs is greater than those of tabular N50°–60°E oriented DBSZs, as inferred from the relatively greater amount of strain in the former. The interaction of these incipient shear zones makes a strike-slip conjugate relationship at an angle of about 50° to 60°. The N50°–60°E oriented tabular DBSZs cut sinisterly the main fabric of NS oriented shear zones and are, thus interpreted to be relatively younger. Since, the age of the Dhok Pathan Formation in the area is 2.4-m.y. to 0.8-m.y. (Khan, 1983), therefore the incipient structure styles in the form of conjugate shear zones reflect neotectonics activities in the Shinghar Range.

4.7. JOINTS

Joints are fractures along which there has been little or no displacement (Badgley, 1965), that are reasonably continuous and through-

going planar fractures commonly on the scale of centimeters to tens or hundreds of meters in length (Davis and Reynolds, 1996). Systematic joints (Hodgson, 1961) display preferred orientation and symmetry. Irregular sets with random orientations are generally categorized as non-systematic (Hodgson, 1961; Ramsay and Huber, 1987).

Two sets of joints are observed i.e., NS/NNE and EW/WNW (Fig. 3.46). These joints are well developed in the hard sandstone bands of the Nagri and Dhok Pathan formations in particular at the southern part of the SMM dome-shape anticline, where the strike of the beds is eastwest (Fig. 3.11). The mutual orthogonal relationship/interaction of these joints form rectangular blocks (~15×6cm) of equal dimensions. Field evidences show that both the sets (NS/NNE and EW/WNW) are initially formed as tensional joints in the Mochi-Mar area and part of Qabul Khel area as noted in the north-south oriented part of SMM dome-shape anticlinal structure, where a system of tensional joints (tension in all four sides) have been observed (Fig. 3.47), but they are not as frequent as observed in the southern end of the anticlinal structure.

The NS/NNE oriented joints show east-west compression with a component of folding at places (Fig. 3.48). The fold axes and axial planes are parallel to the NS/NNE oriented joints. The EW/WNW oriented joints show north-south extension (Fig. 3.46, 3.48), which are symmetrical and perpendicular to the compressional joints. A maximum 2.5-3cm of joint space or dilation has been noted. The frequency of these joints is high at the hinge zone of SMM dome-shape anticline.
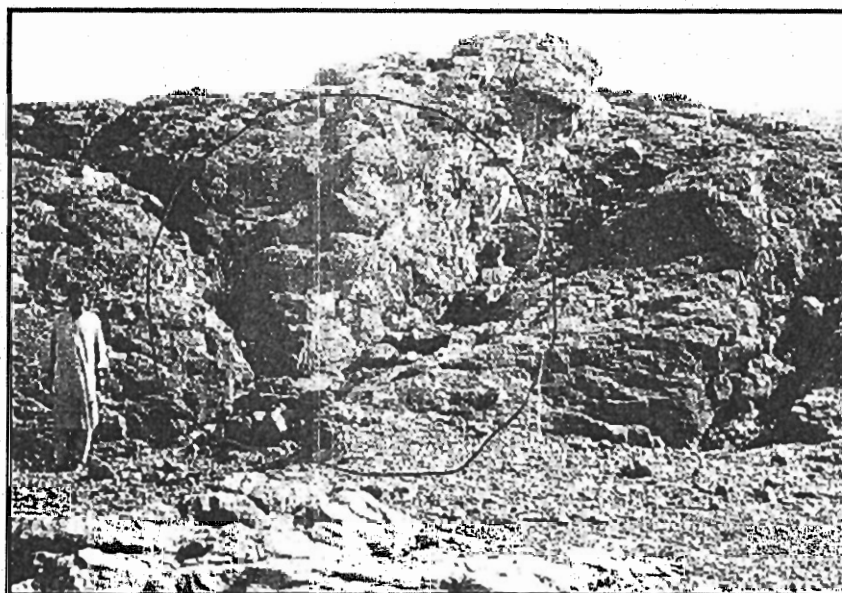
Fig. 3.1. Circle-inventory method (*dia: ~2m*) for recording fractures in the field.
Note: the inventory circle encompassing both conjugate shear and
extensional fracture sets; Dhok Pathan Formation, Shanawah-Godi Khel area.

Fig. 3.2. Grid map of Mochi-Mar and part of Qabul Khel area, depicting geometry of conjugate deformation band shear zones.

1:5000
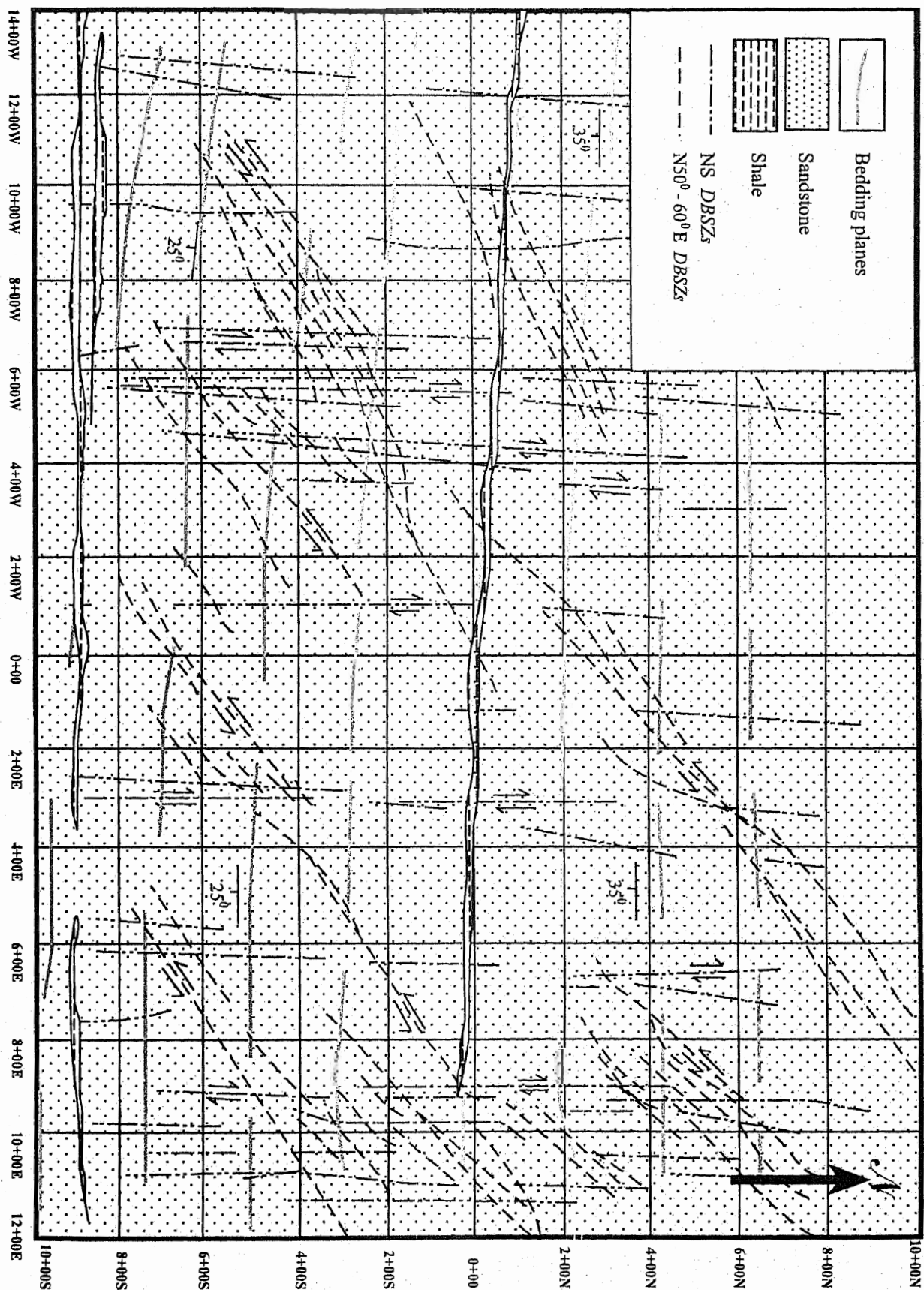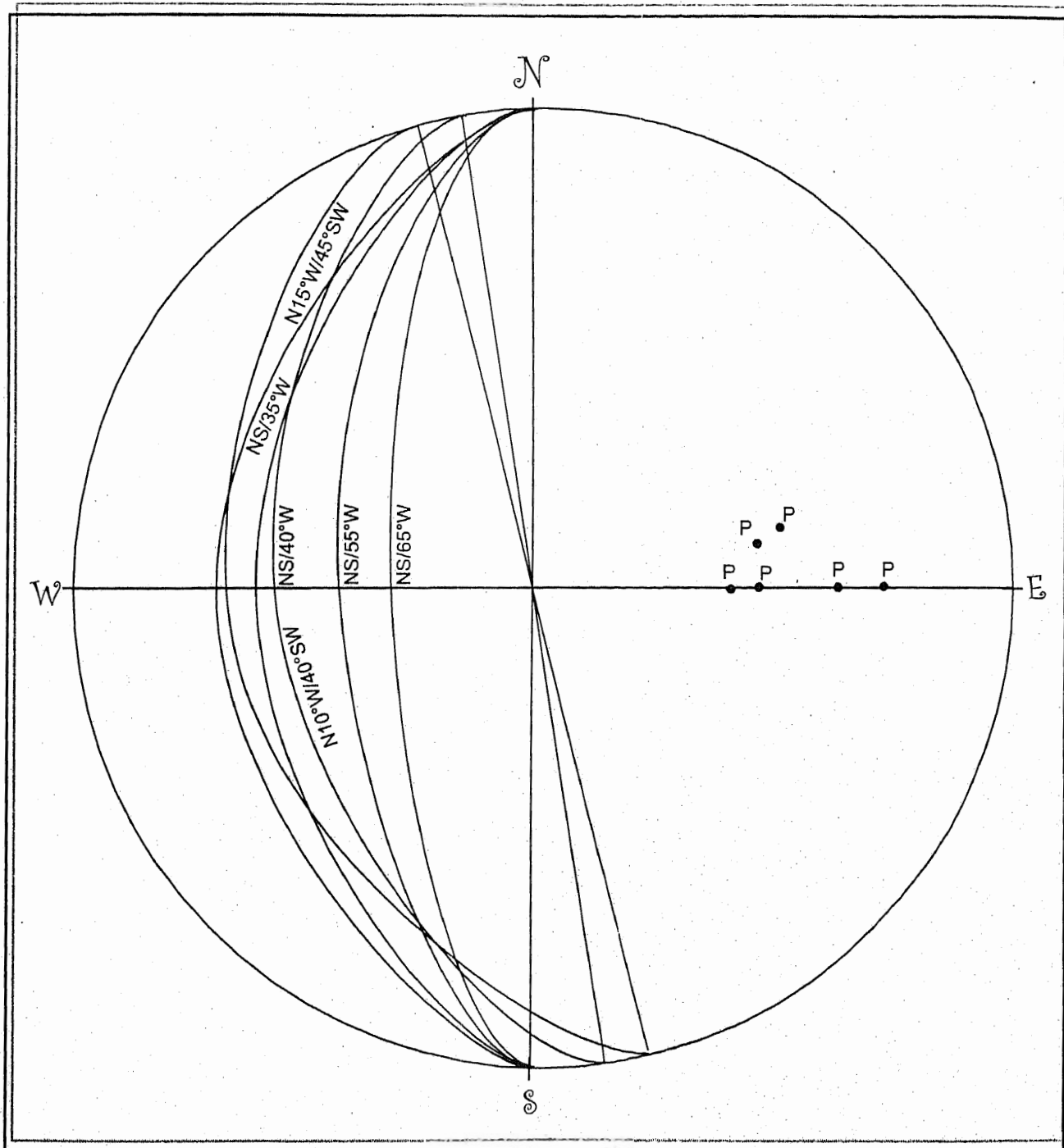
Fig. 3.3. Equal-area stereographic representation of regional strike and dip of the Siwalik strata of the Surghar-Shinghar Range.

Fig. 3.4. Frequency and geographic distribution of fractures recorded in the Gulapa area.
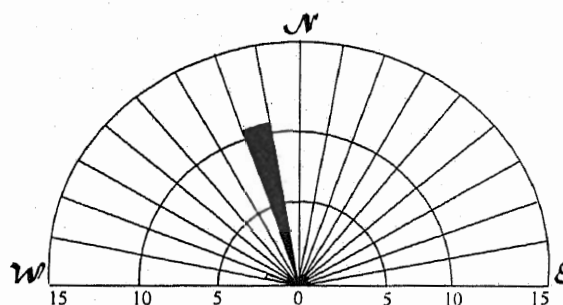
Fig. 3.4.1. Gulapa
(Total: 12 fractures)

▮ *Compressional fractures*

▧ *Conjugate fractures set II*

Fig. 3.4.2. Gulapa
(Total: 6 fractures)

▮ *Compressional fractures*

Fig. 3.4.3. Gulapa
(Total: 11 fractures)

▤ *Dilational fractures*

▨ *Conjugate fractures set I*

▧ *Conjugate fractures set II*

Fig. 3.4.4. Gulapa
(Total: 16 fractures)

▤ *Dilational fractures*

▨ *Conjugate fractures set I*

▧ *Conjugate fractures set II*

45

Fig. 3.5. Frequency and geographic distribution of fractures recorded in the Samandi area.

Fig. 3.5.1. Samandi
(Total: 7 fractures)

■ *Compressional fractures*

Fig. 3.5.2. Samandi
(Total: 9 fractures)

■ *Compressional fractures*
■ *Conjugate fractures set I*
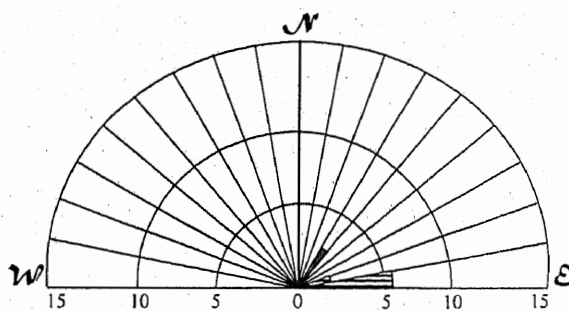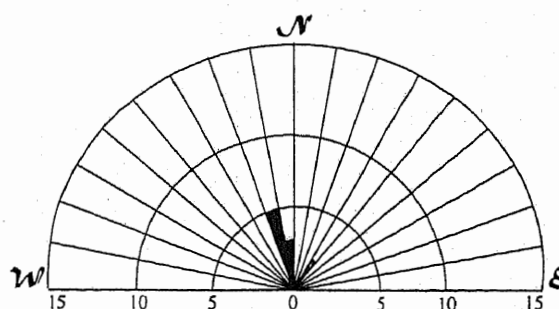
Fig. 3.5.3. Samandi
(Total: 8 fractures)

▤ *Extensional fractures*
▦ *Conjugate fractures set I*

Fig. 3.5.4. Samandi
(Total: 11 fractures)

▤ *Dilational fractures*
■ *Conjugate fractures set I*
▦ *Conjugate fractures set II*
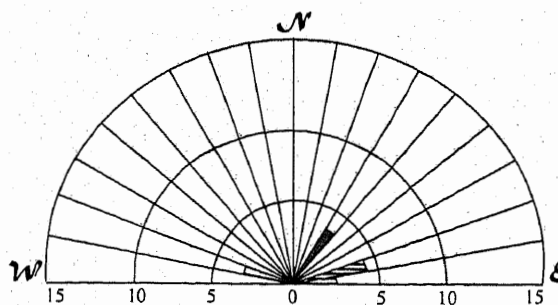
Fig. 3.6. Frequency and geographic distribution of fractures recorded in the Abbasa area.
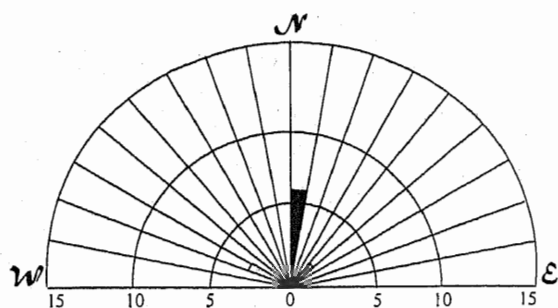
Fig. 3.6.1. Abbasa
(Total: 9 fractures)

- Compressional fractures
- Conjugate fractures set I
- Conjugate fractures set II
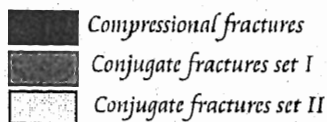
Fig. 3.6.2. Abbasa
(Total: 7 fractures)
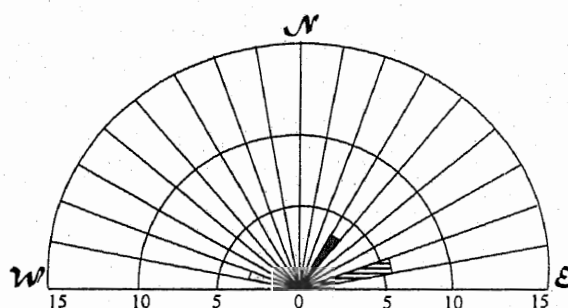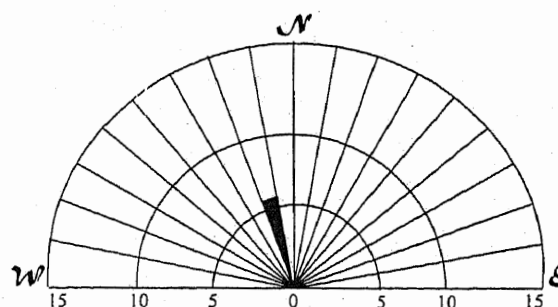
- Compressional fractures
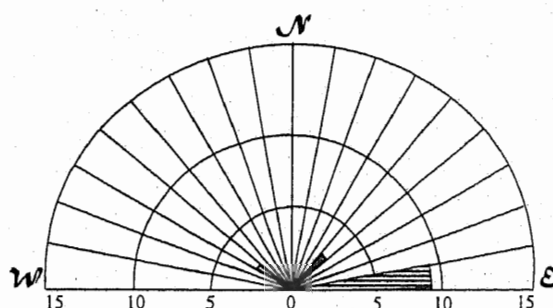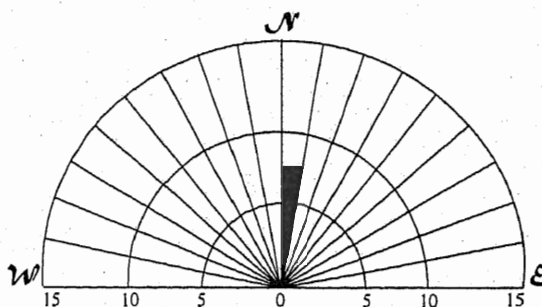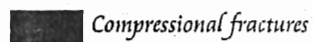
Fig. 3.6.3. Abbasa
(Total: 12 fractures)

- Dilational fractures
- Conjugate fractures ser I
- Conjugate fractures ser II
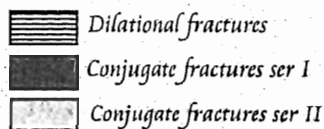
Fig. 3.6.4. Abbasa
(Total: 15 fractures)

- Dilational fractures
- Conjugate fractures set I
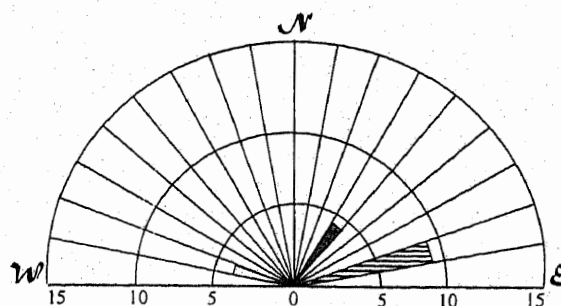- Conjugate fractures set II

47
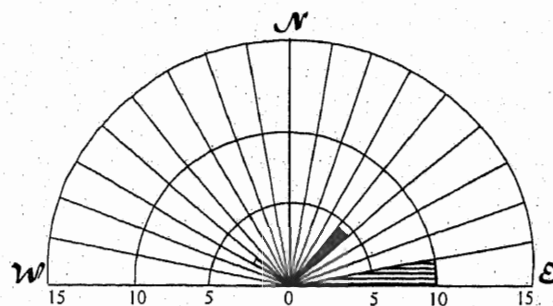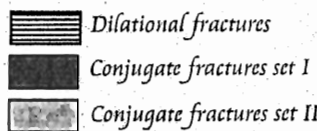
Fig. 3.7. Frequency and geographic distribution of fractures recorded in the Shanawah-Godi Khel area.
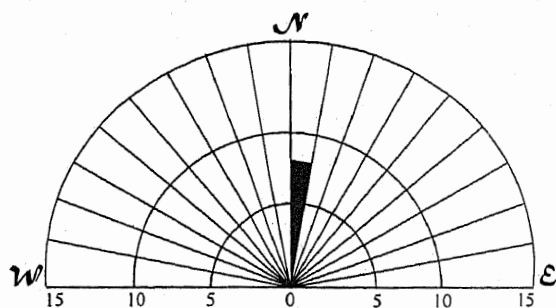
Fig. 3.7.1. Shanawah-Godi Khel
(Total: 7 fractures)

▮ *Compressional fractures*

Fig. 3.7.2. Shanawah-Godi Khel
(Total: 9 fractures)

▮ *Compressional fractures*
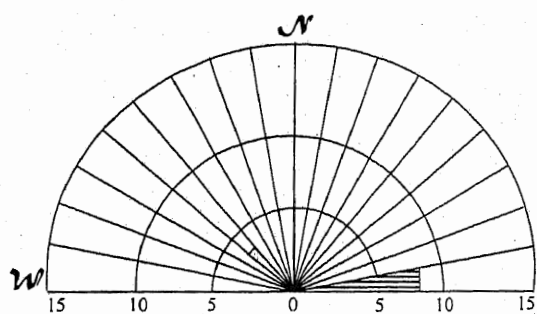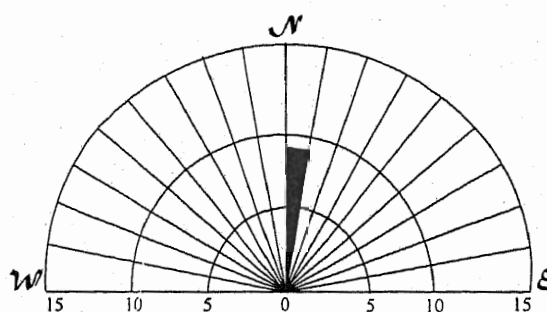
Fig. 3.7.3. Shanawah-Godi Khel
(Total: 10 fractures)

▤ *Dilational fractures*
▦ *Conjugate fractures set II*

Fig. 3.7.4. Shanawah-Godi Khel
(Total: 14 fractures)

▤ *Dilational fractures*
▮ *Conjugate fractures set I*
▦ *Conjugate fractures set II*

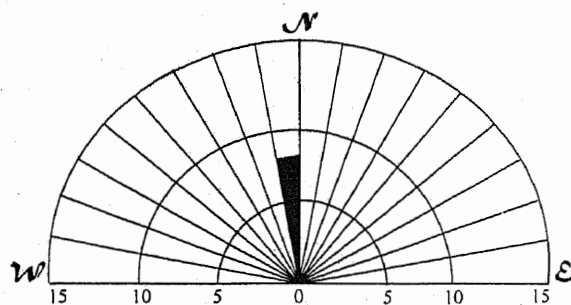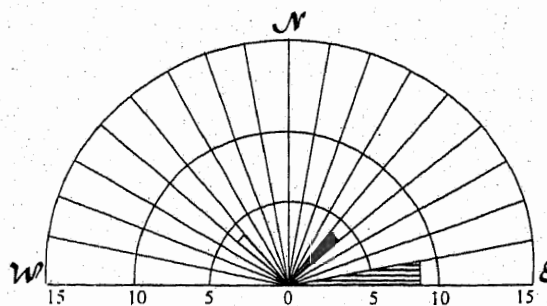Fig. 3.8. Frequency and geographic distribution of fractures recorded in the Thatti-Nasrati area.
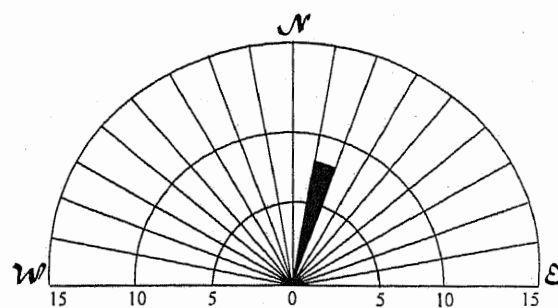
Fig. 3.8.1. Thatti-Nasrati
(Total: 7 fractures)

▮ *Compressional fractures*

Fig. 3.8.2. Thatti-Nasrati
(Total: 11 fractures)

▤ *Dilational fractures*

▨ *Conjugate fractures set I*

▢ *Conjugate fractures set II*
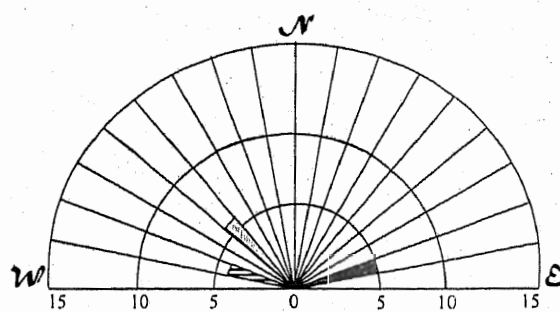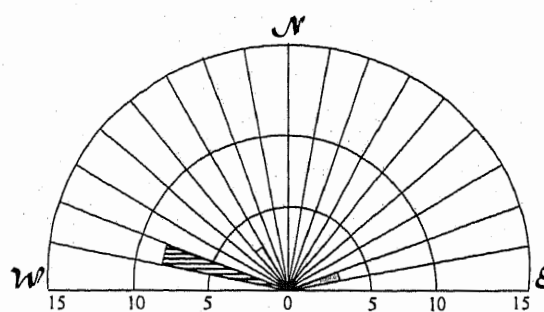
Fig. 3.8.3. Thatti-Nasrati
(Total: 15 fractures)

▤ *Dilational fractures*

▮ *Conjugate fractures set I*

▦ *Conjugate fractures set II*

Fig. 3.9. Frequency and geographic distribution of fractures recorded in the Seraj Khel area.

Fig. 3.9.1. Seraj Khel
(Total: 9 fractures)

◼ *Compressional fractures*

Fig. 3.9.2. Seraj Khel
(Total: 13 fractures)

▤ *Dilational fractures*

◼ *Conjugate fractures set I*

▦ *Conjugate fractures set II*

Fig. 3.9.3. Seraj Khel
(Total: 3 fractures)

◼ *Compressional fractures*
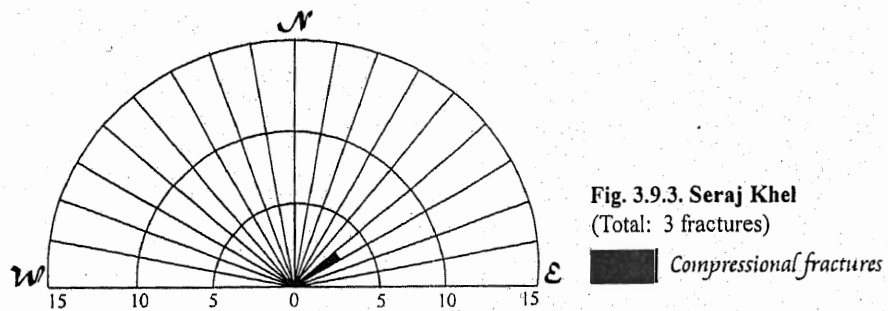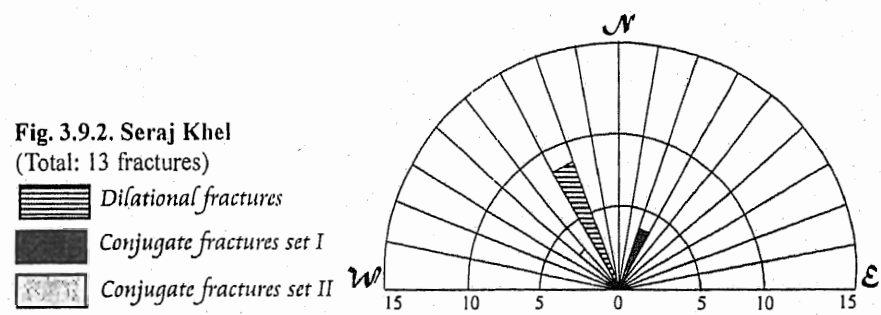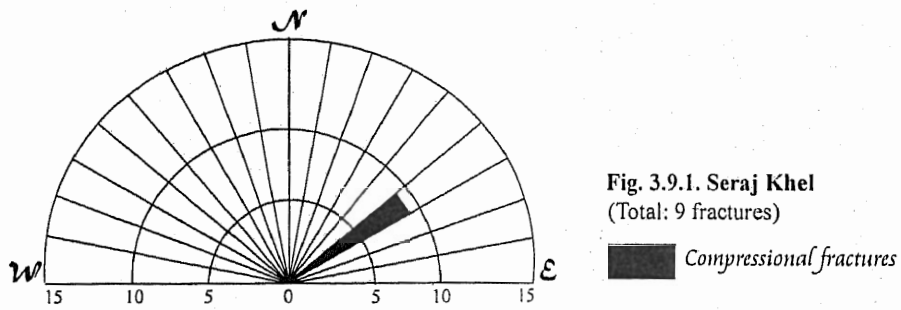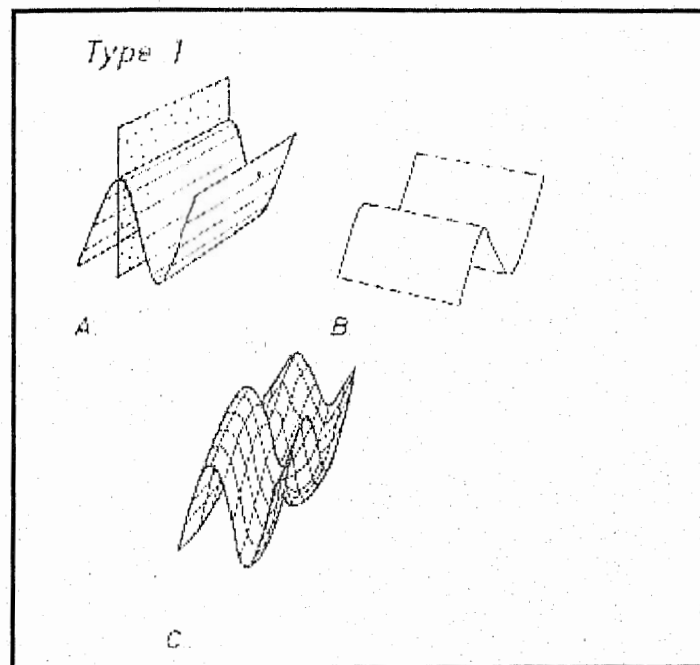
Fig. 3.10. Type-1 dome-basin pattern of Ramsay and Huber, 1987.

Fig. 3.11. Generalized geological map of Surghar-Shinghar Range showing Makarwal anticline, Sarkai-Mochi Mar dome-shape anticline and Dera Tang fault.

1 : 50,000

Explanation

QTsd	Dhok Pathan Formation
QTsn	Nagri Formation
Tsc	Chinji Formation
Tmk	Mitha-Khattak Limestone
↔	Anticline
→	Plunging Anticline
⊤	Dip/Strike
⤵	Contacts
⋰	Pre-Siwalik Sequence
---	River
▮	Village

52

Looking to the north

Mitha Khattak
Limestone
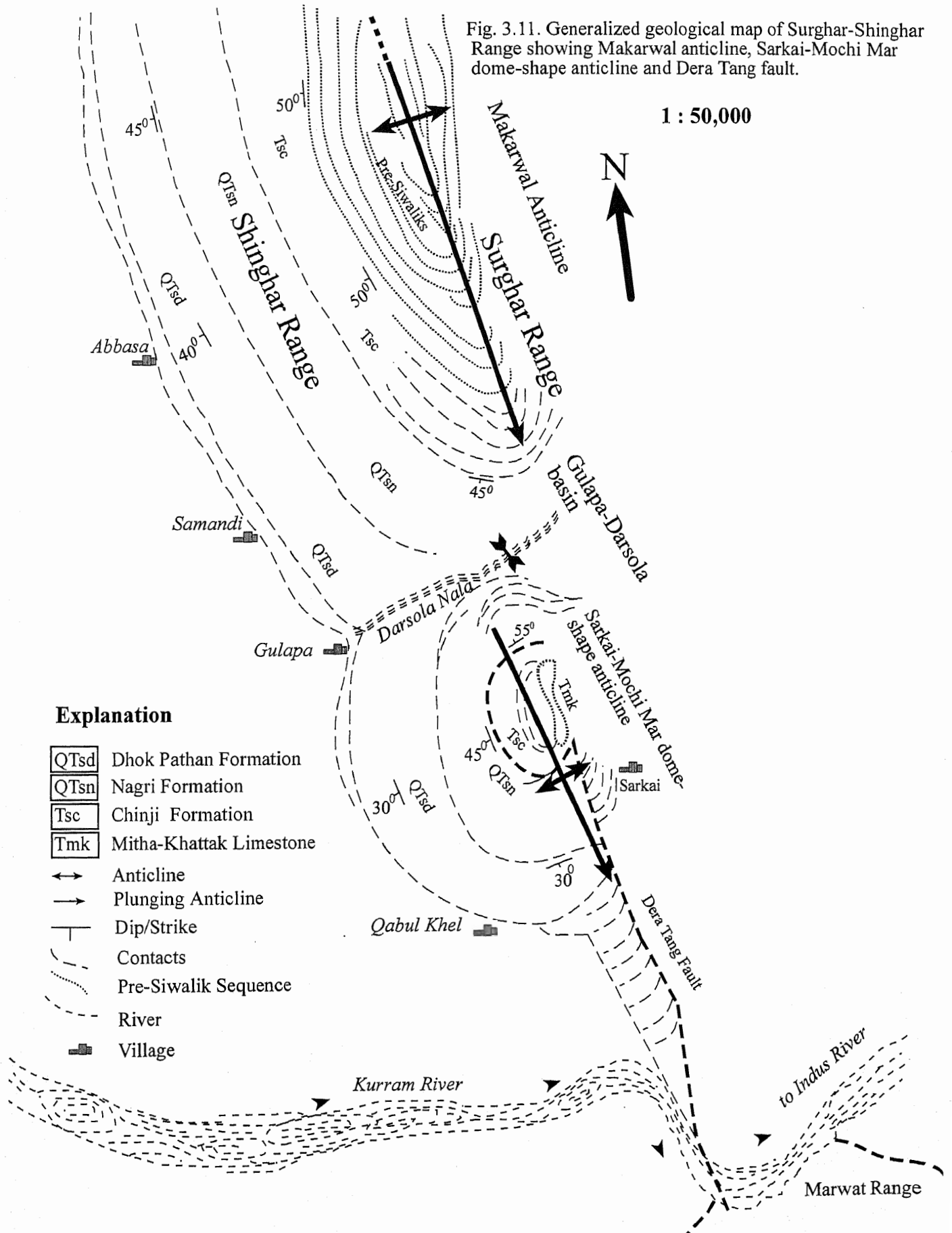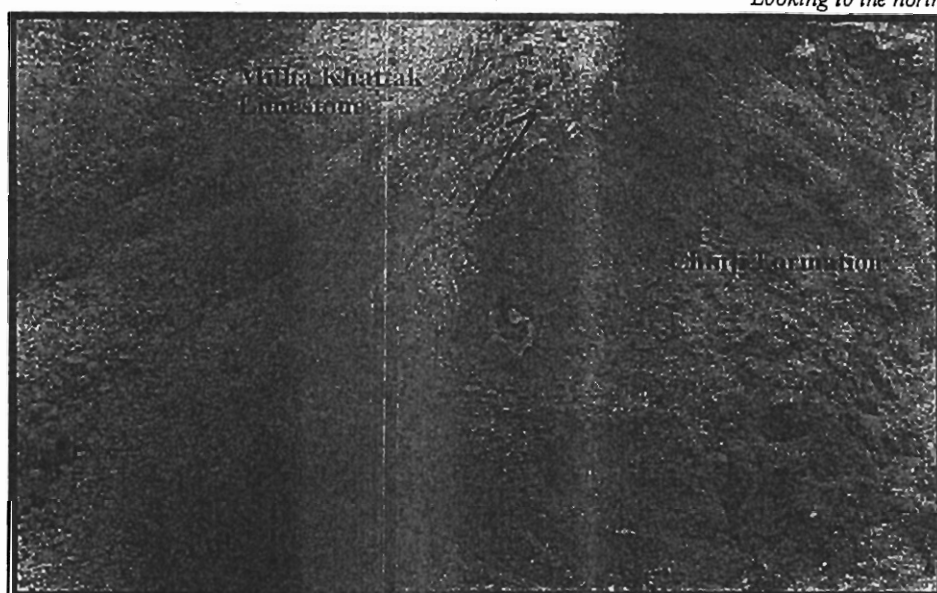
Chinji Formation

Fig. 3.12. Sheared reverse (oblique) slip contact of Mitha Khattak Limestone and
Chinji Formation in the core of Sarkai-Mochi Mar dome-shape anticline.

Looking to the south
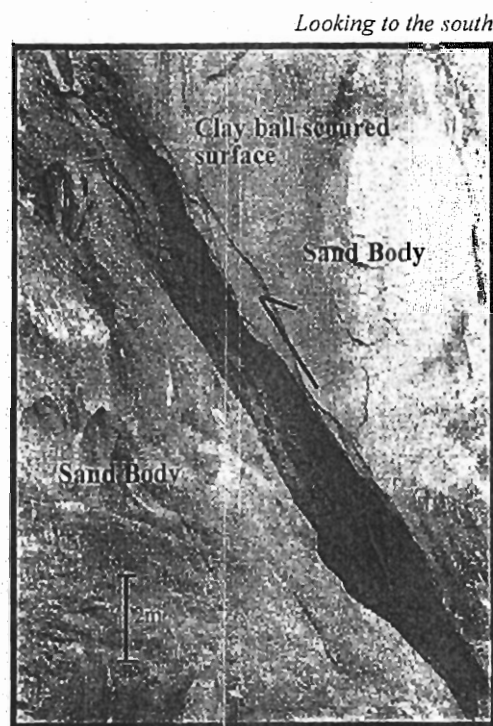
Fig. 3.13. Clay ball scoured surface within the sandstone body of the Siwalik Group provides weak plane for flexural slip.

Looking to the north
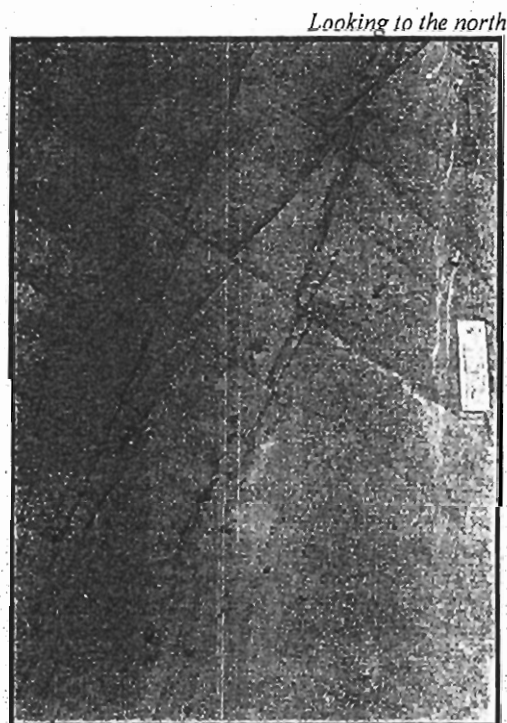
Fig. 3.14. Bedding and longitudinal fracture pattern within the sandstone body. The fractures are filled with gouge matrix.
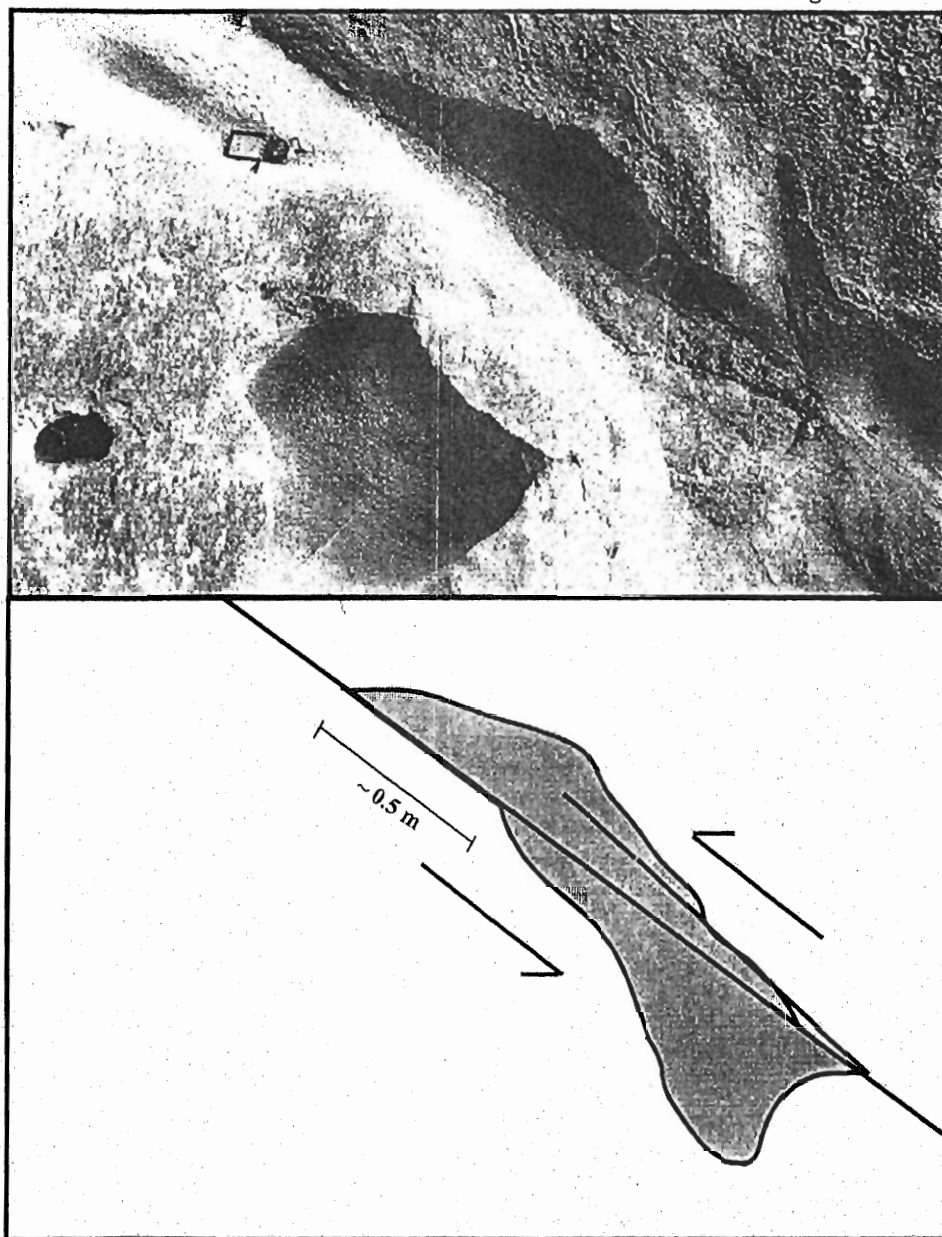
Fig. 3.15. Displaced clay ball with maximum 0.5 meter displacement.
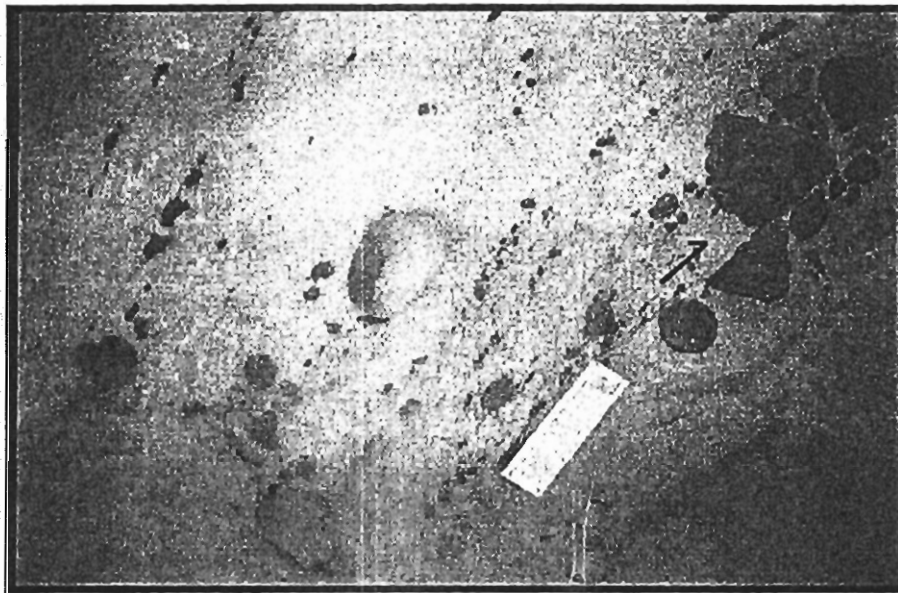
Fig. 3.16. Moderately hard clay ball displaced along the shear plane, showing reverse sense, exposed in the Dhok Pathan Formation.

Looking to the north
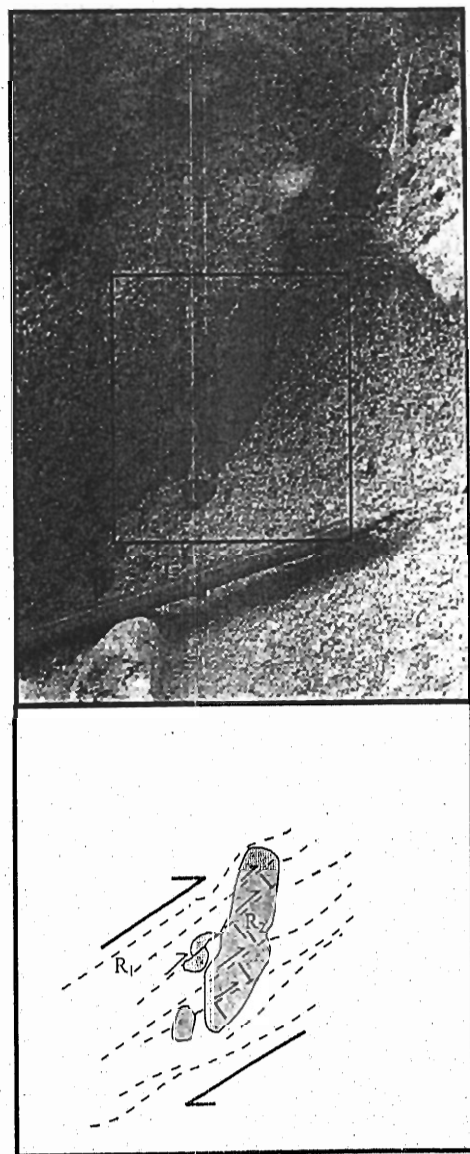
Fig. 3.17. Displaced clay balls with Riedel fractures indicating sense of shear.

57
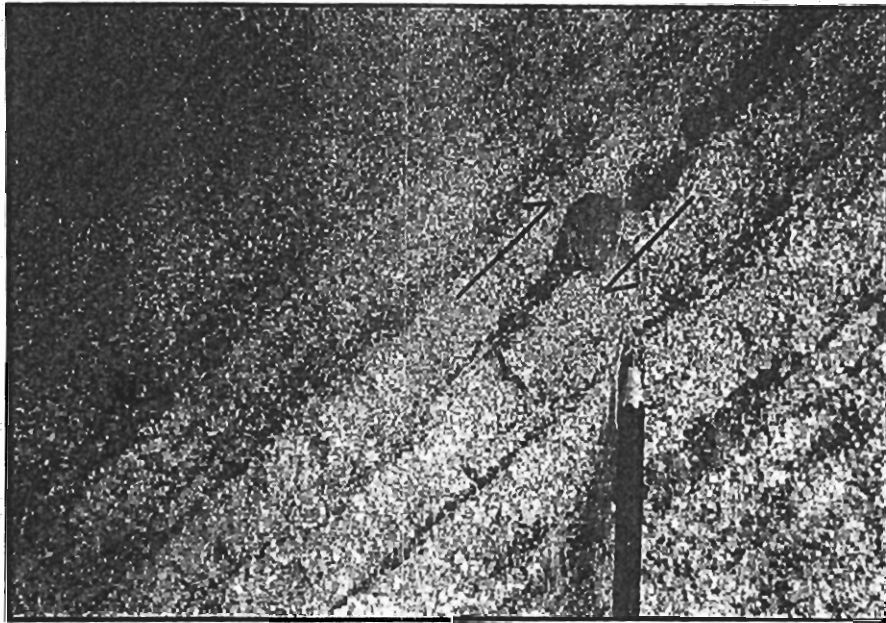
Fig. 3.18. Rotated and displaced clay balls grounded within the sandstone matrix.
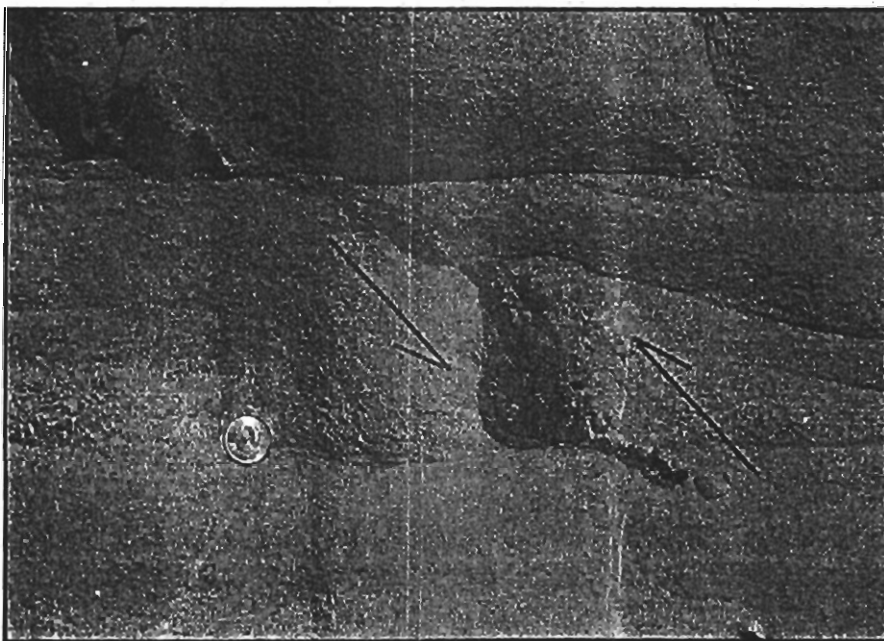
Fig. 3.19. A rotated clay ball along the shear zone with asymmetric tails showing sense of movement.

Fig. 3.20. A rotated clay ball with asymmetric tails, indicating reverse sense.
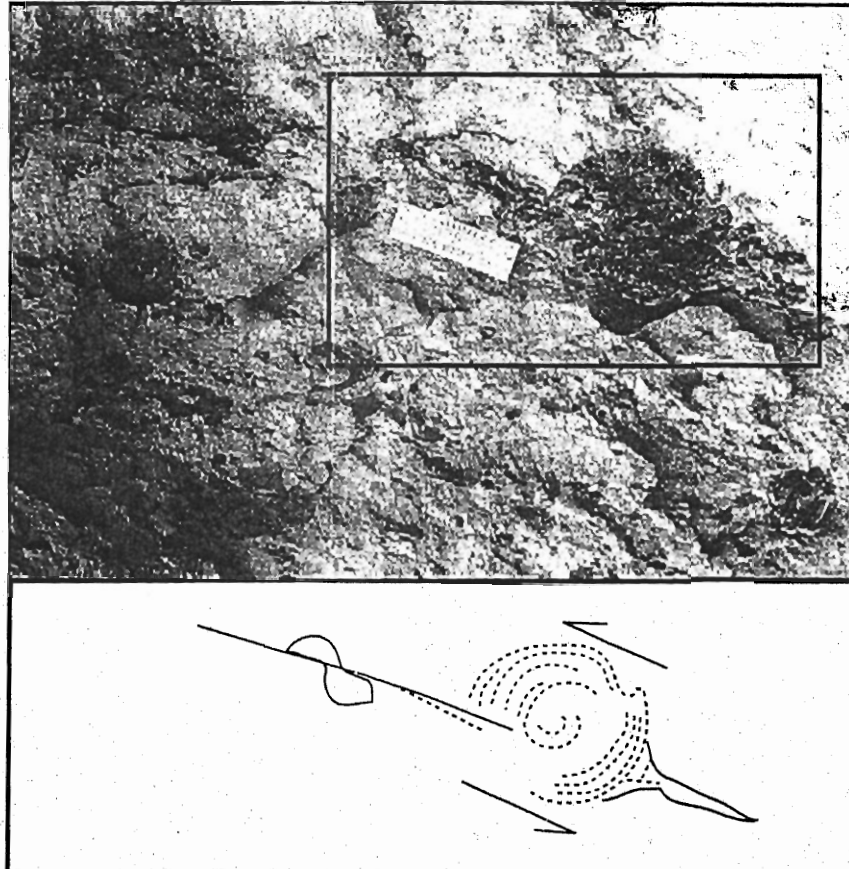
Fig. 3.21. A rotated clay ball with internal fabric, showing reverse sense.
Note: reverse sense of movement along a displaced clay ball in the same shear zone.

Looking to the south
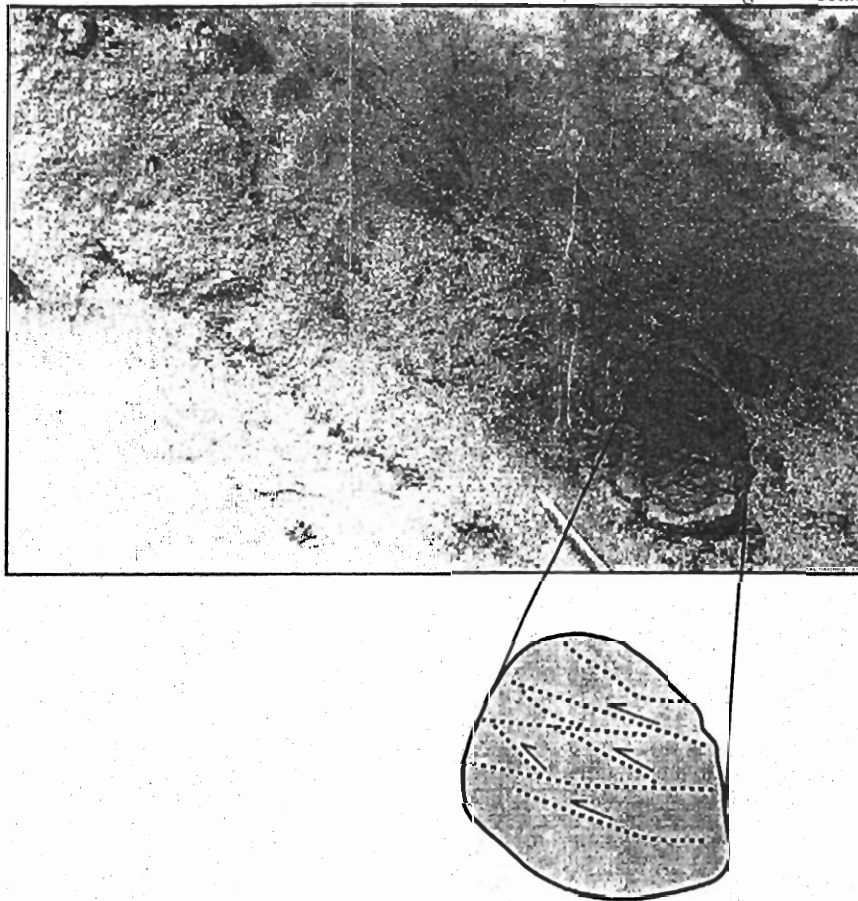
Fig. 3.22. Strained clay ball with discrete fractures showing reverse sense of movement. Note: the outer rim of the clay ball is oxidized.

Looking to the north
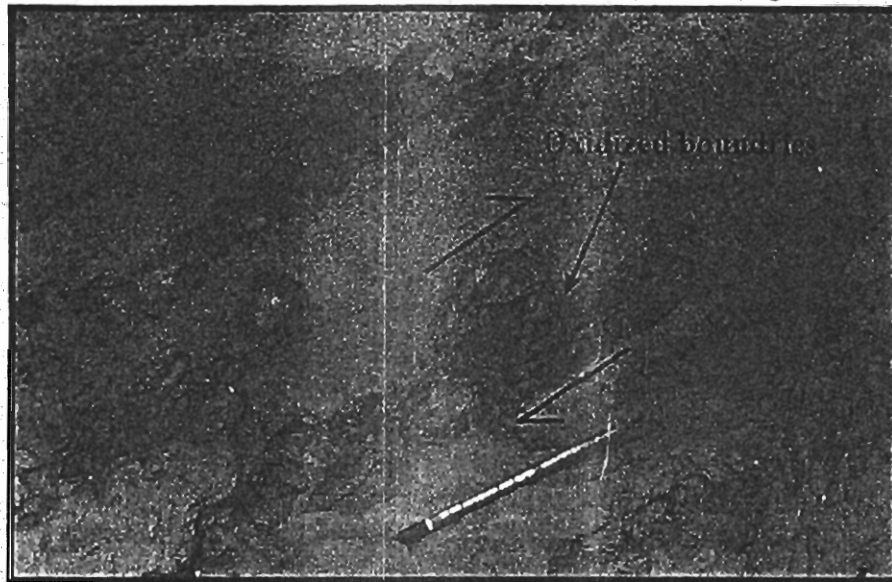
Fig. 3.23. Rotated clay balls with oxidized boundaries and discrete fractures accomodating strain, showing sense of movement.

Looking to the south
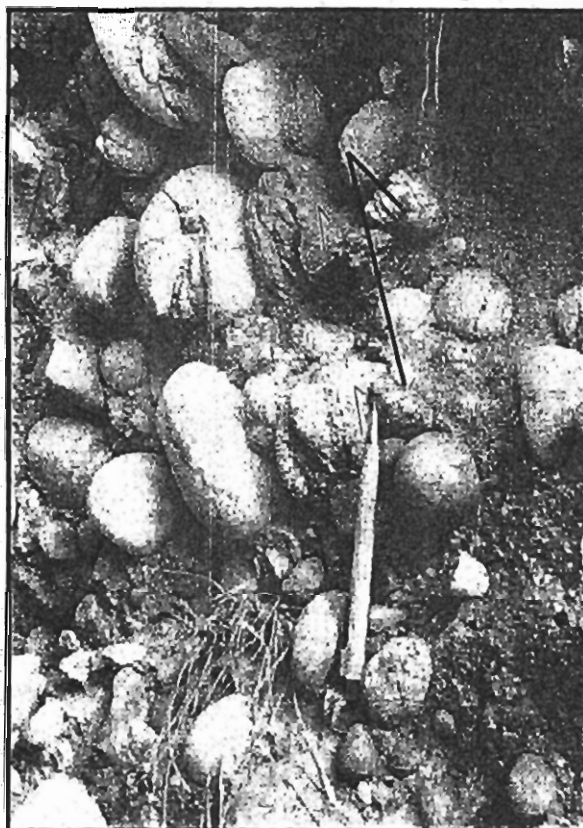
Fig. 3.24. Fractured pebbles in channel conglomerates of Dohk Pathan Formation.
Note the two sets of fractures.

Fig. 3.25. Bedding (solid lines) and longitudinal (dash lines) fractures with shear senses.
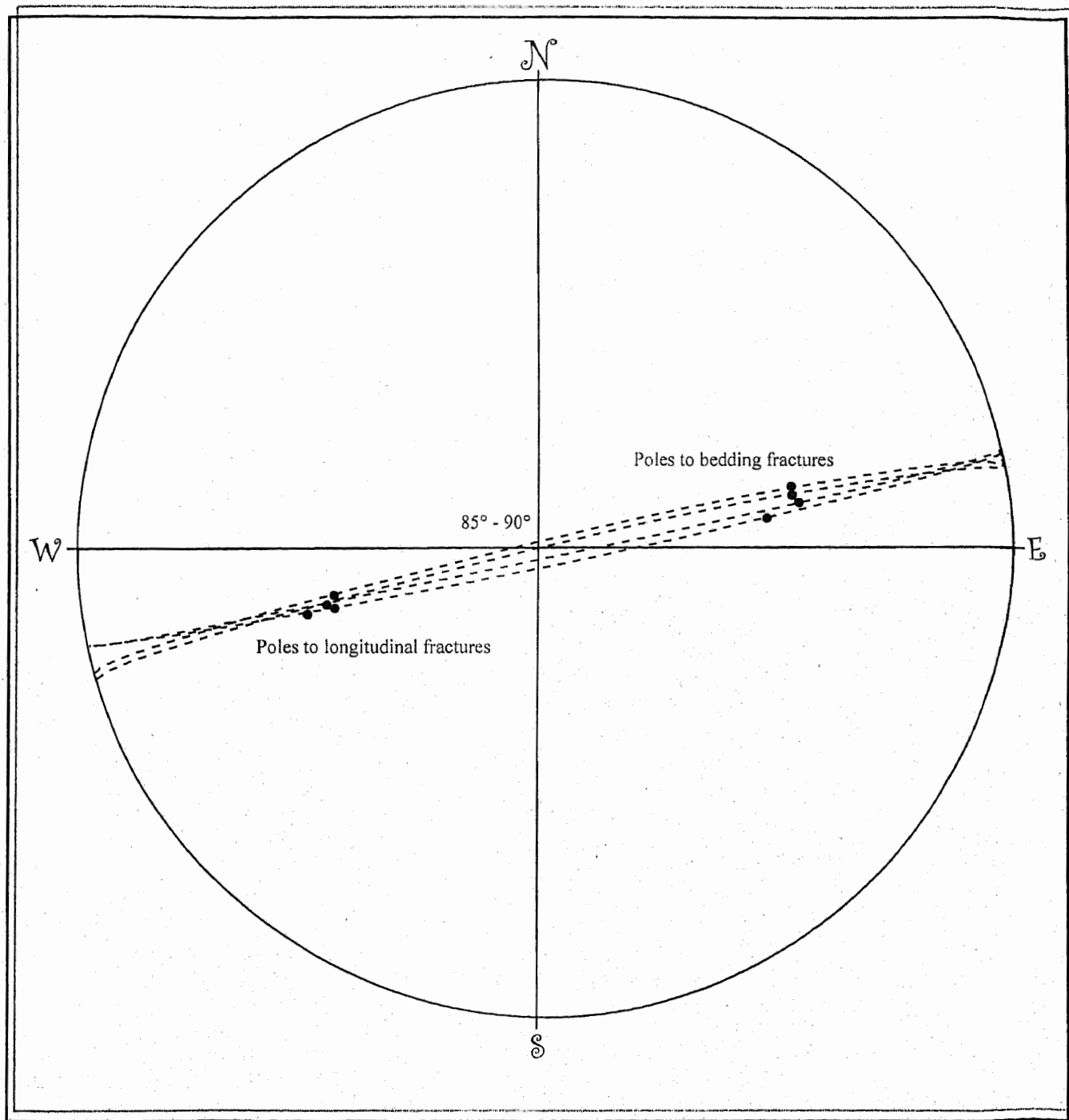
Fig. 3.26. Equal-area stereographic determination of the angles between bedding and longitudinal fractures, Station No. 1, Gulapa area.
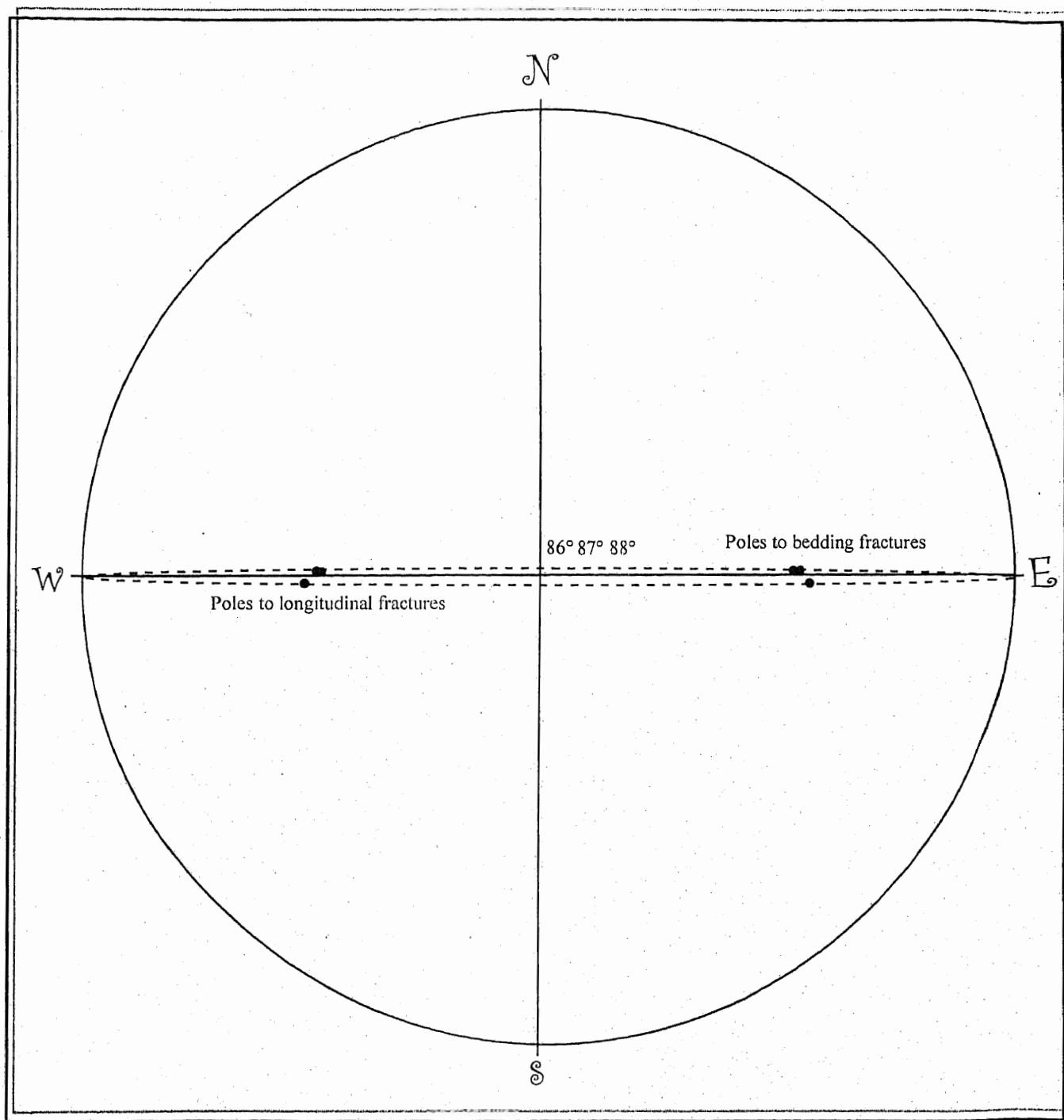
Fig. 3.27. Equal-area stereographic determination of the angles between bedding and longitudinal fractures, Station No. 1, Abbasa area.
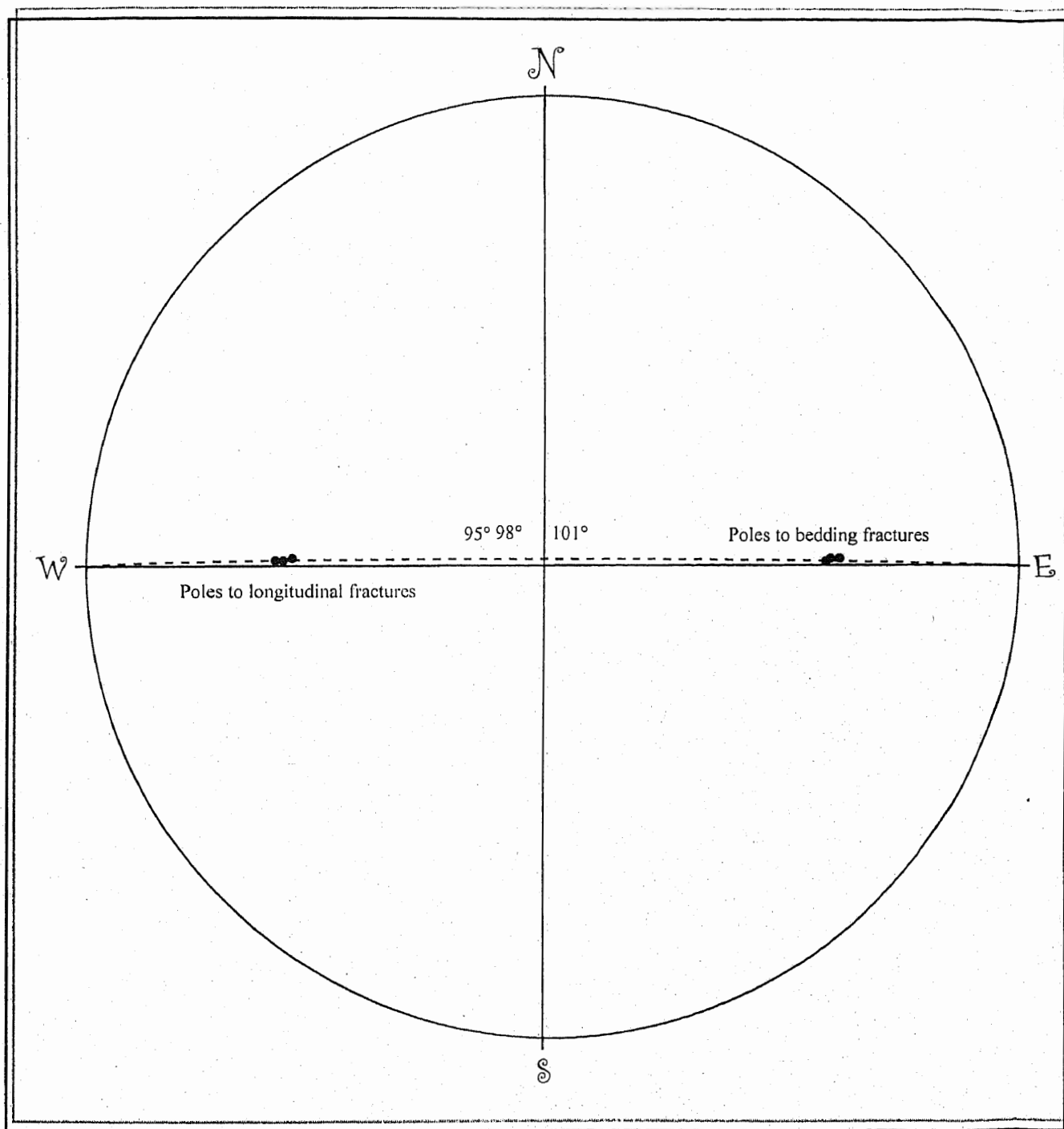
Fig. 3.28. Equal-area stereographic determination of the angles between bedding and longitudinal fractures, Station No. 2, Shanawah-Godi Khel area.
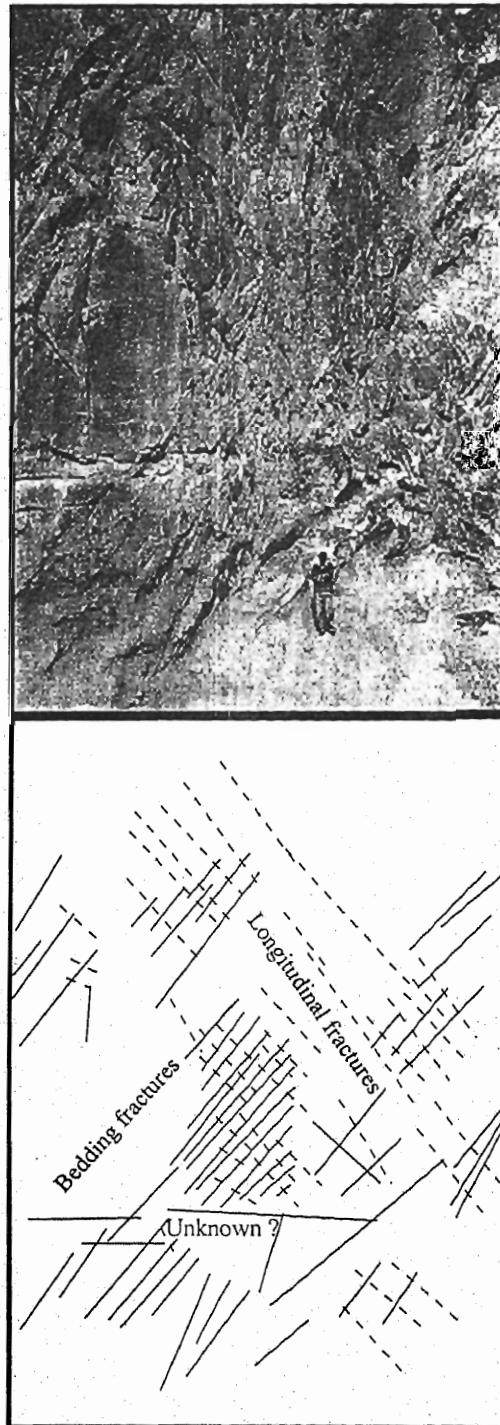
Fig. 3.29. **Bedding** (layer-parallel shear fractures, solid lines) and longitudinal (fractures normal to the bedding planes, dash lines) fractures developed within the Siwalik sandstones.
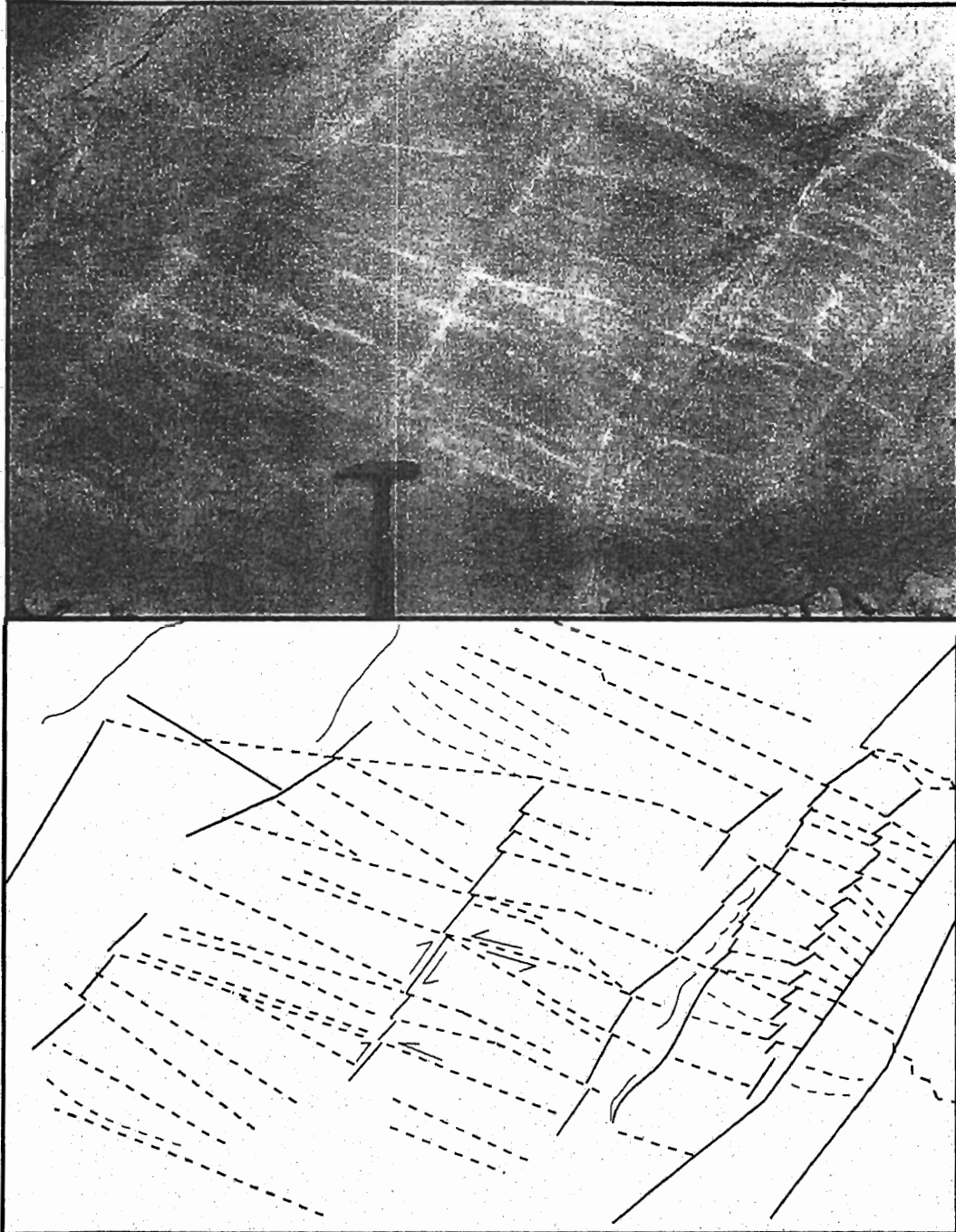
Fig. 3.30. Incipient calcified bedding (solid lines) and longitudinal (dash-lines) fractures making an angle of about 70°-90°. Note two sets of longitudinal fractures.

Looking to the east
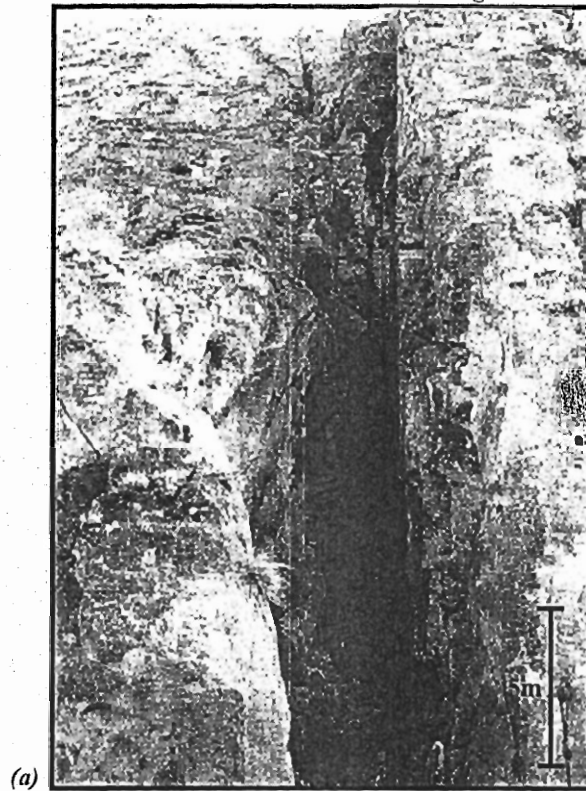
Looking to the east

Fig. 3.31. East-west oriented dilational fractures exposed in the Siwalik Group of Surghar-Shinghar Range (photographs taken at two different scales). Note havey rain pits in the hard sandstone bands in (b).
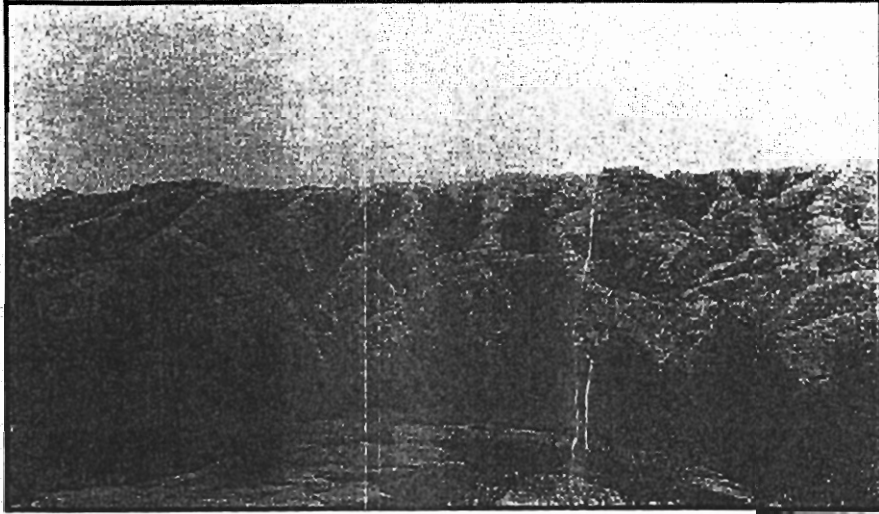
Looking to the east
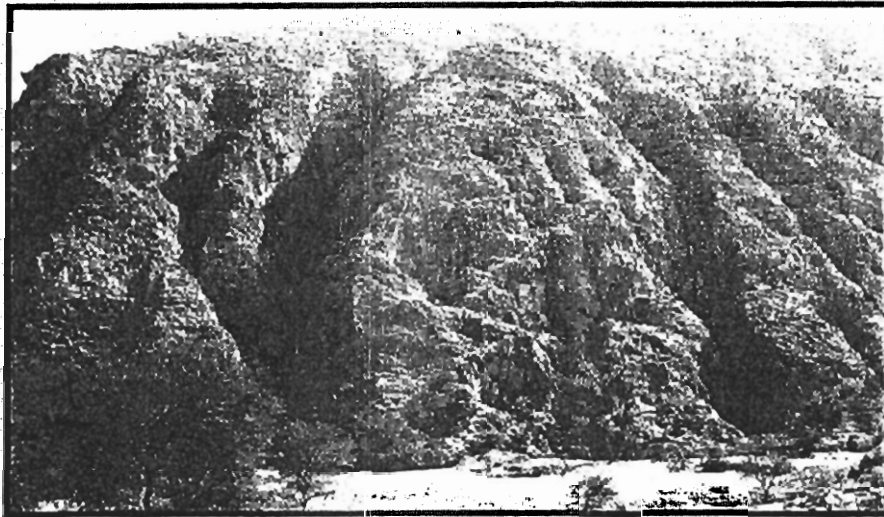
Fig. 3.32. The uplifing and the presence of east-west oriented extensional fractrues in the Siwalik sediments of Shinghar Range facilitate drainage along these fractures, thereby controlling the geomorphic processes.

71
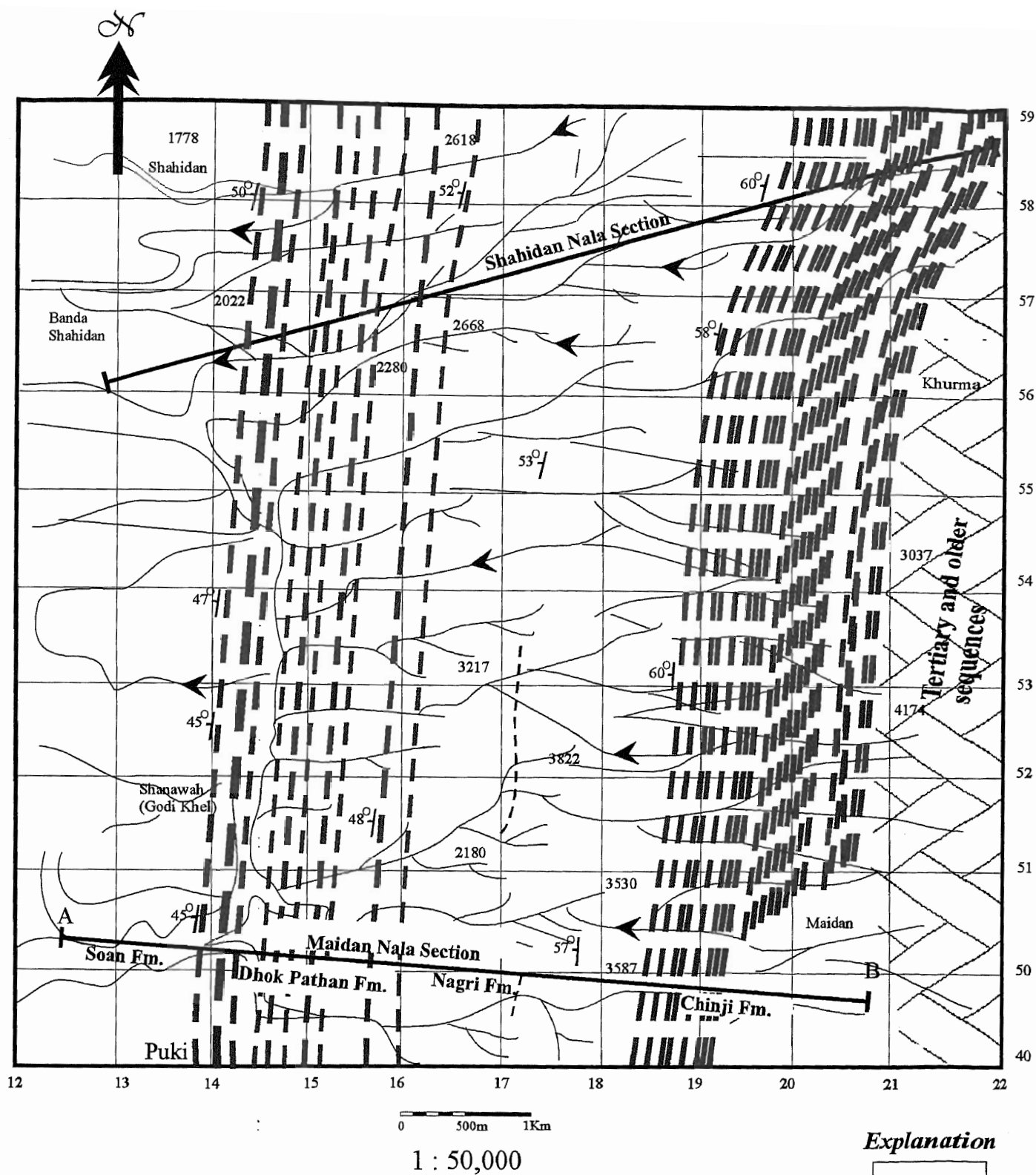
Fig. 3.33. Generalize geological map of Shanawah-Godi Khel area, Surghar-Shinghar Range. Note, sub-parallel drainage pattern across the range has almost east-west orientation. The eastern part of the range has higher altitudes (uplifted) than the western part.

72
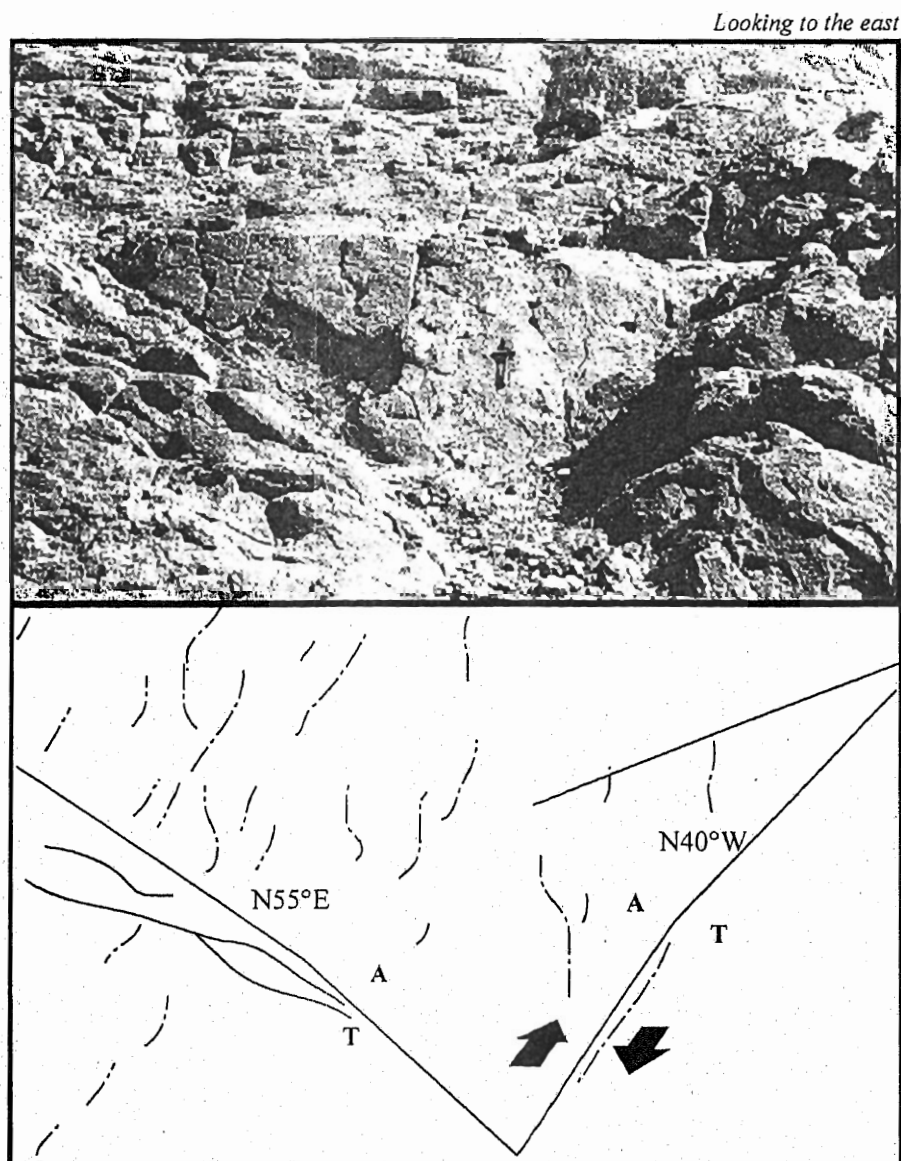
Fig. 3.34. Dextral and sinistral oblique conjugate shear fractures (solid lines) in the hard
sandstone band of Dhok Pathan Formation. Note extension fractures in dash lines.
T: towards
A: Away
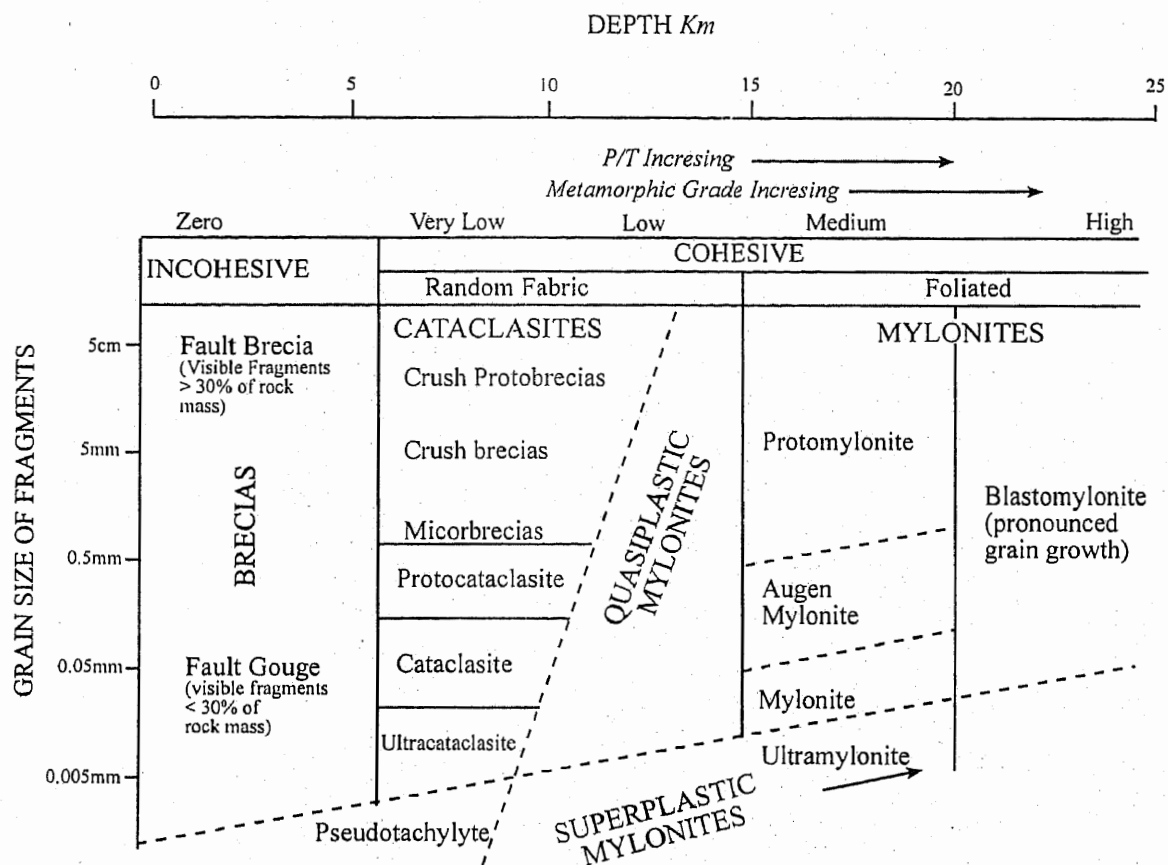
Fig. 3.35. Classification of fault rocks (Sibson, 1977).

Looking to the N60°E
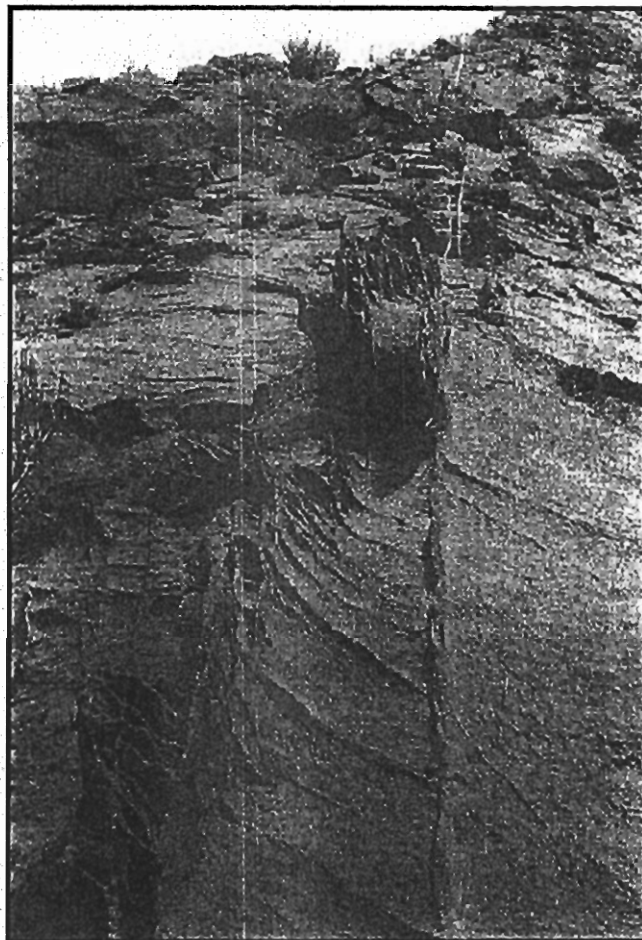
Fig. 3.36. The deformation band(s) in this photograph showing thin and discrete ribs and fins in the outcrop and because of differential weathering forming wall like structures.

Fig. 3. 37. Outcorp expression of calcified deformation bands strongly resistant to weathering relative to the sandstone bed rock forming wall-like structure.

Fig. 3. 38. Differentail weathering between the shear bands and the normal
porous sandstone produced magnificent inside views of Riedel fractures.
Note nice exposures of R2 Riedel fractures.

Fig. 3. 39. NS oriented DBSZs with dextral sense of shear.
Note that the sense of shear in this type is interpreted from the
relative displacement in the hard sandstone band.
T : towards
A : away
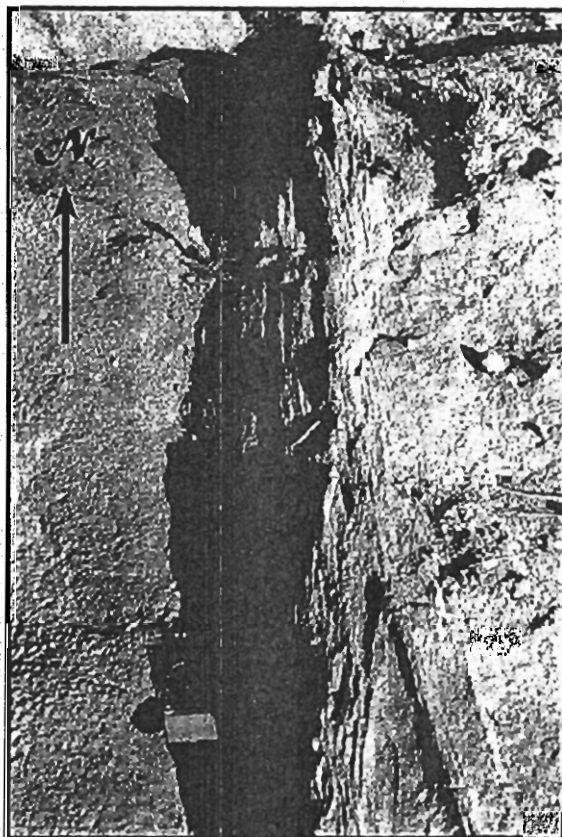
Fig. 3. 40. NS oriented DBSZ, relatively thick, massive and dense.
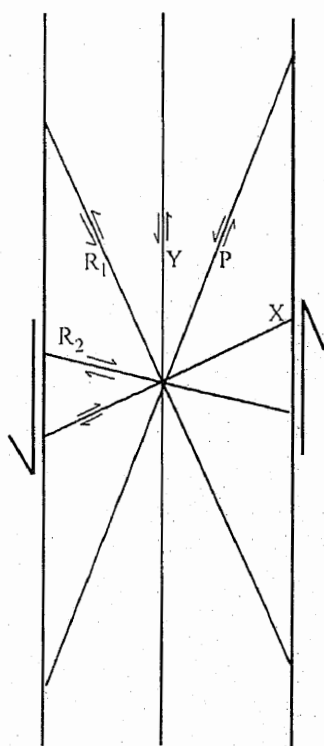
Fig. 3. 41. Idealized Riedel fracture geometry in sinistral shear zone
(Logan et al., 1979).
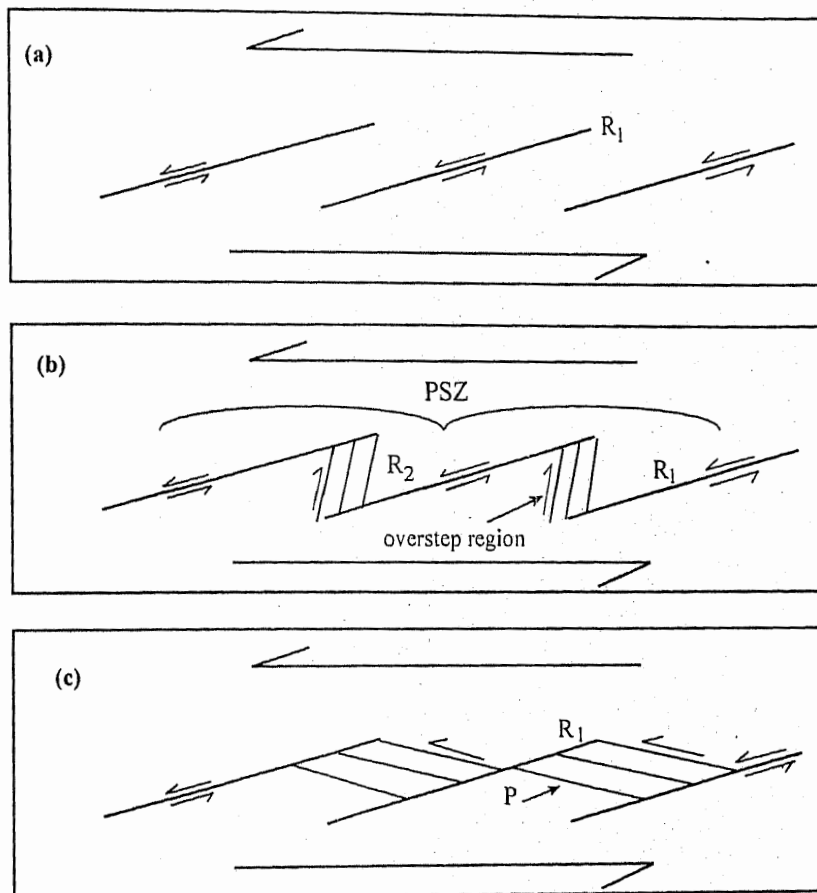
3. 42. The sequential development of R1,R2 and P Riedel shear zone (from Ahlgren, 2001).
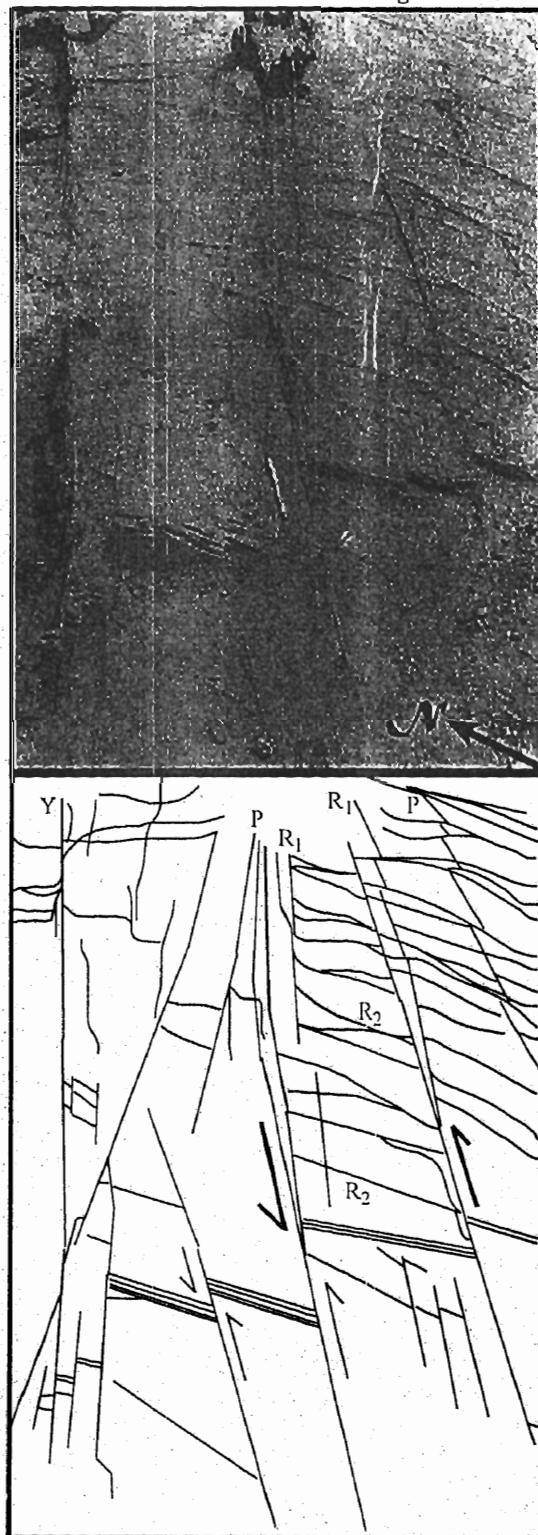
Fig. 3.43. N60°E tabular DBSZ with Riedel fracture sets.
Note that it sinisterly cuts the NS oriented shear zone.
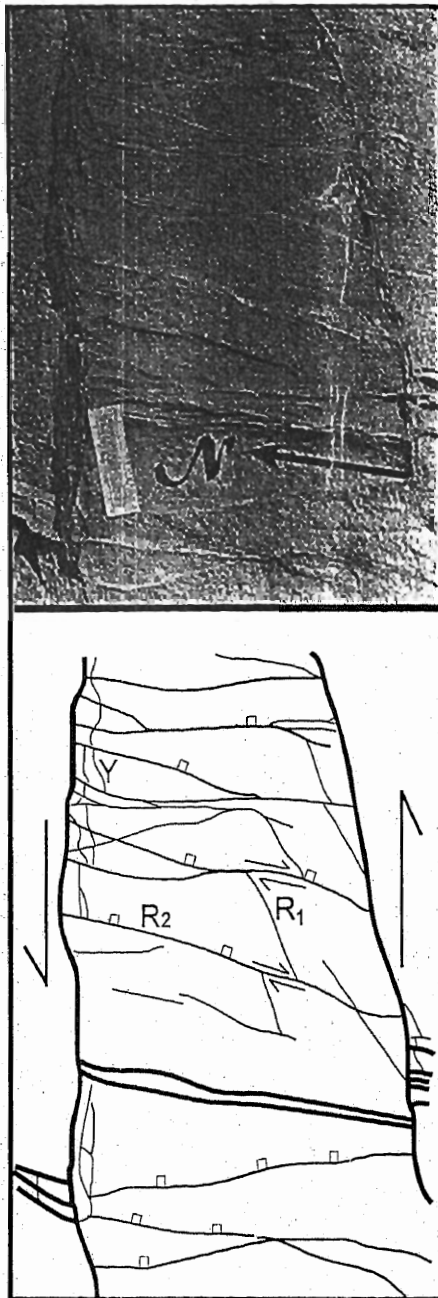
Fig. 3. 44. Tabular deformation band shear zone (N60°E) with distinct Riedel fractures. Note normal slip along R2 Riedel fracture set.
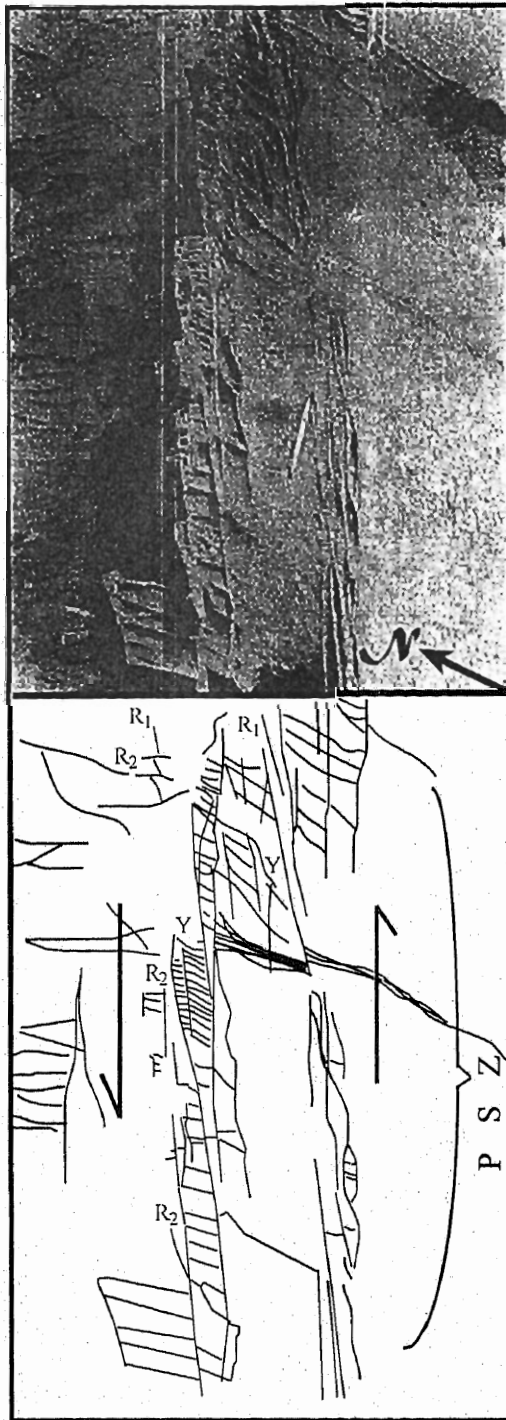
Fig. 3.45. The N50°E oriented deformation band shear zone cut sinisterly the NS oriented shear zone at an angle of about 50°. Note the Riedel R2 fracture pattern inside the shear zone.
PSZ: Principal Shear Zone
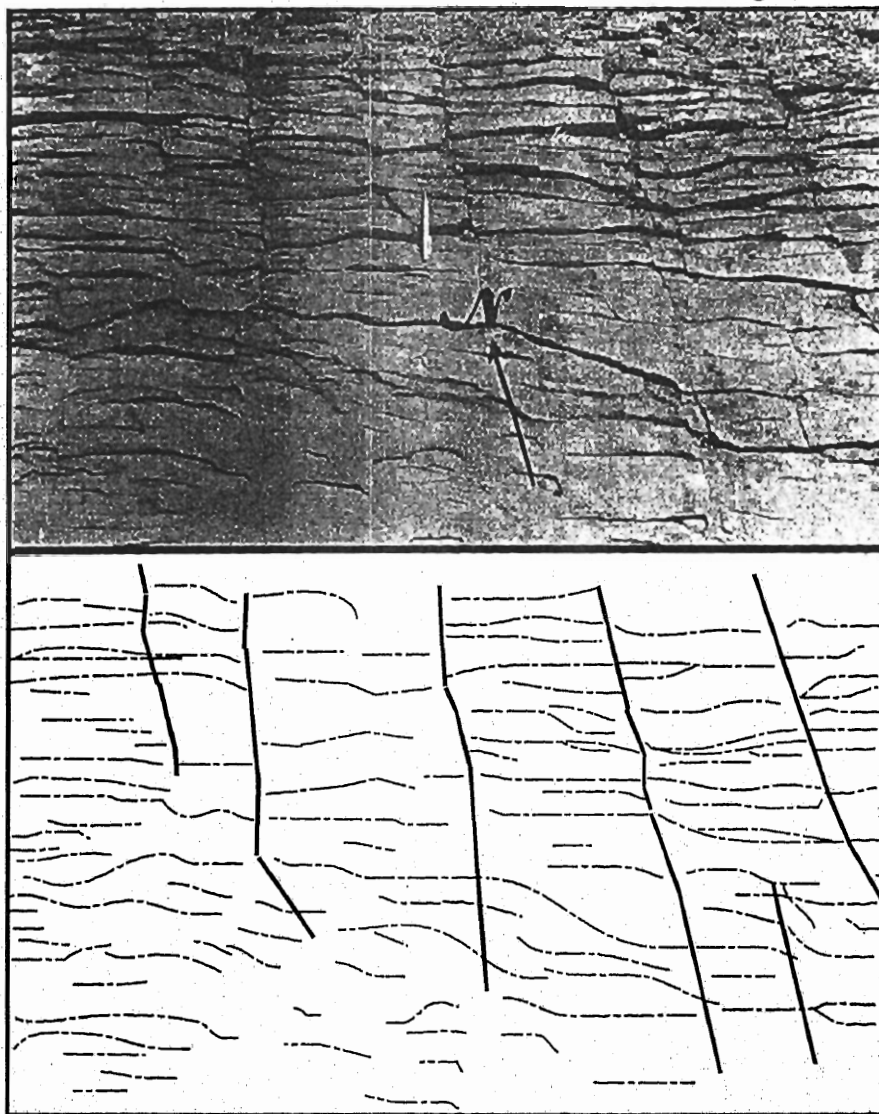
Fig. 3. 46. Orthogonal joints in the hard sandstone band showing east-west compression (thick line) and north-south extension (dash line) in the Mochi Mar area.
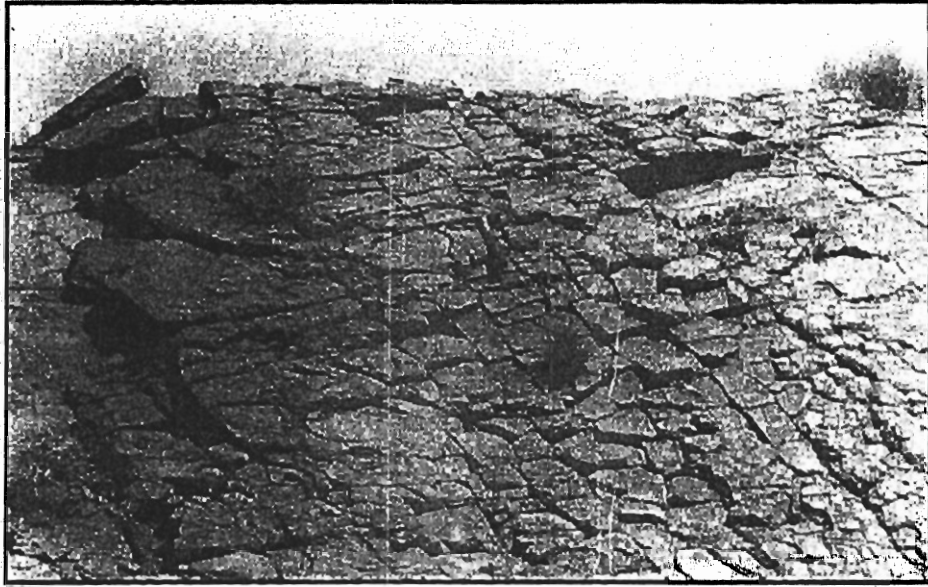
Fig. 3. 47. Tension joints indicating dilation in all four directions, observed at the western exposed flank of the SMM dome-shape anticlinal structure.
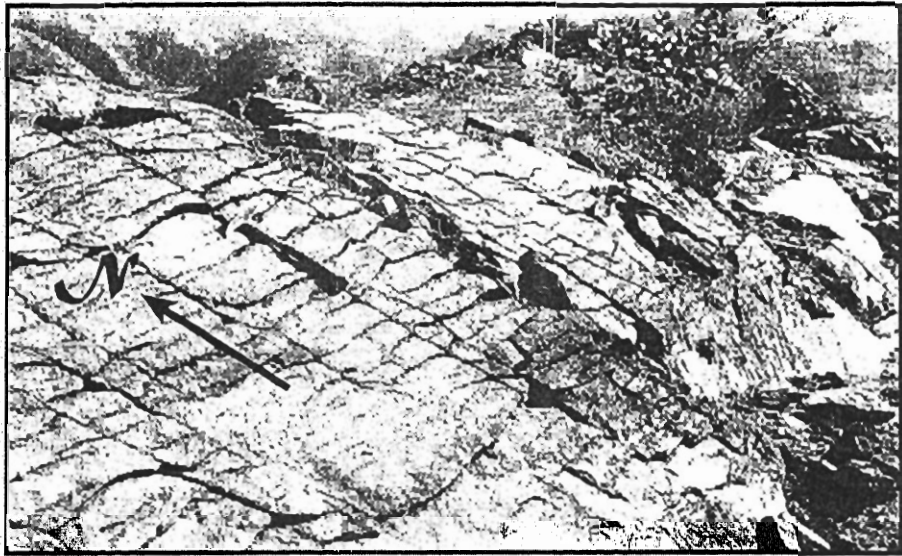
Fig. 3 .48. The axes of the minor folds is normal to the east-west oriented extensional joints.

Chapter 4

KINEMATIC & DYNAMIC ANALYSES

4.1. INTRODUCTION

Kinematic analysis takes off where descriptive analysis ends. The overall goal of kinematic analysis is to interpret the combination of translations, rotations, distortions, and dilations that altered the location, orientation, shape and size of a rock body (Davis and Reynolds, 1996). Evaluating changes in shape and size brought about by deformation is the focus of strain analysis.

Dynamic analysis interprets forces, stresses, and the mechanics that give rise to structures. The goal of dynamic analysis is to interpret the stresses that produce deformation; to describe the nature of forces from which the stresses are derived; and to evaluate the overall relationship among stress, strain and rock strength (Davis and Reynolds, 1996). Therefore, the aim of this chapter is to interpret the geological observations and field descriptions under stress and strain analyses.

4.2. FRACTURE PATTERNS WITHIN A FOLD

In environment of three-dimension strain, rocks tend to fracture in orthorhombic or diagonal patterns composed of three or more sets (Price, 1966; Price and Cosgrove,1990; Ramsay and Huber, 1987). There are few studies which are designed to establish the spatial relationship between minor fractures and major folds. Some of the most useful kinematic and dynamic models related with the major folding and development of minor fractures are proposed by Price (1966), Stearns (1964), Price and Cosgrove (1990) and Ramsay and Huber (1987). These models are here considered to understand the kinematic and dynamic functions regarding fracture analysis:

1. Price (1966) published a series of diagrams illustrating the typical interrelationships between minor fractures and cylindrical fold forms (Fig. 4.1).

The diagrams were purely based on field observations and from previous literature.

2. Stearns (1964) carried out the most comprehensive studies on macrofracture patterns on the Teton Anticline in northwestern Montana. His model shows nice geometrical distribution of tension and shear fractures around a domal anticline (Fig. 4.2).

3. Price and Cosgrove (1990) proposed a model for the geometric arrangement of dilational and shear fractures in folded strata and related it with flexural-slip model. According to their model, the dilational or extensional fractures usually cut the fold axes at 90° and are also perpendicular to the bedding and are usually vertical or steeply dipping features (Fig. 4.3a). These two sets of extensional fractures i.e., perpendicular and parallel to the fold axes did not develop at the same time.

The more commonly observed orientation of shear fractures relative to the limbs and axis of a fold are shown in the figure 4.3(b) and (c), where it will be seen that these shear fractures include normal, thrust, strike-slip and oblique-slip faults. Normal faults tend to be aligned parallel or perpendicular to the fold axis, while the thrusts may be well developed in the leading limb of an asymmetrical anticline. The oblique-slip faults developed on the limbs with little movement. Generally, the orientation and direction of slip of shear fractures is determined by the orientation of the bedding. Genetically, they are wrench faults and are called oblique-slip only because they are usually horizontal rather than a bedding plane slip.

4. The relationship of bedding, longitudinal, cross and oblique fractures/joints with reference to three mutually perpendicular orthogonal axes a, b and c to fold geometry is proposed by Ramsay and Huber (1987) (Fig. 4.4).

4.3. KINEMATIC AND DYNAMIC INTERPRETATIONS OF SHEAR AND DILATIONAL FRACTRUES

Stress produced proportional strain in their respective rocks. A kinematic model is proposed for bedding or layer-parallel shear fractures and longitudinal or fractures normal to the bedding planes inferred from flexural-slip model (Ramsay, 1967; Ramsay and Huber, 1987) and their timing history is depicted based on their geometrical relationship in the sandstones of the Siwalik Group of Surghar-Shinghar Range (Fig 4.5a & b; cross-section in pocket). Mutual cross-cutting relationship of these fractures confirms that the bedding or layer- parallel shear fractures are formed in the first deformation phase induced by flexural slip folding (Ramsay, 1967; Ramsay and Huber, 1987). The incompetent weak layers are characterized by clay ball scoured surfaces along bedding planes facilitate flexural-slip folding.

The longitudinal fractures might have initially formed as tensional fractures (Price, 1966; Ramsay and Huber, 1987), but due to changes in the stress direction (rotation of beds) experienced shear, displacing the bedding fractures. Since, both the bedding and longitudinal sets have opposite senses of shear, though with varying degree of angles, their consistent geometry throughout the range indicates systematic stress system related with regional folding of Surghar-Shinghar Anticline and associated Surghar Thrust on the eastern half of the anticlinal structure. Both the fracture sets accommodated east-west shortening.

The dilational or cross fractures exposed on the western limb of Surghar-Shinghar Anticline are perpendicular to the fold axis and, thus accommodated north-south extension. The geometrical orientation of the cross fracture sets in the Surghar-Shinghar Anticline is similar as illustrated in the above mentioned models. The relationship of diagonal or conjugate shear fractures in the western limb of Surghar-Shinghar Anticline is oblique-slip accommodated rotation of the beds.

It is interpreted that the development of bedding or layer-parallel shear fracture, longitudinal or fractures normal to the bedding planes, dilational and

conjugate shear fractures of the north-south oriented part of the Surghar-Shinghar Anticline are induced by regional flexural-slip folding, and associated stresses of Surghar Thrust (ST). This structural model for the development of fractures (Fig. 4.5a & b; cross-section in pocket) is accord with most of models proposed by Price (1966), Price and Cosgrove (1990) and Ramsay and Huber (1987). These fracture patterns in the Siwalik Group of Surghar-Shinghar Range indicate on-going neotectonics activities in the younger most lithological units of the range.

4.3.1. Significance of clay ball kinematics

4.3.1.1. Displaced clay balls

Most of the clay balls along the clay ball scoured sheared surfaces, which are moderately hard, are totally displaced along layer-parallel fractures. Their displacement clearly shows the reverse sense of movement and also the amount of shear. Some of the displaced clay balls form internal fabric in the form of Riedel fractures. Two sets i.e., synthetic R_1 and antithetic R_2 conjugate Riedel patterns have been recognized within the strained clay balls. Experimental deformation of a clay block induced by shearing the substrate of the clay is carried out by Twiss and Moores (1992). Two sets of fractures, R_1 and R_2 are formed at an angle of about 15° and 75°, respectively (Fig. 4.6). The R_1 Riedel fabric is parallel to the imposed shear, whereas R_2 fractures have opposite sense of shear. The geometrical pattern of R_1 and R_2 helps to resolve the sense of shear in most of the brittle shear zones (Mawer, 1992). Therefore, the clear-cut indication of reverse sense obtained from displaced clay balls is supported by the geometric pattern of R_1 and R_2 fabric within some of the clay balls, both suggesting the reverse sense of shear.

4.3.1.2. Rotated clay balls

Before going to the strain analysis of the rotated clay balls observed along the shear zones, the geometry of rotated porphyroclasts is important to discuss here, irrespective of their P/T conditions. As both clay balls and porphyroclasts behave plastically during deformation, i.e., their mechanism of deformation is same. Passchier and Simpson (1986) distinguished two different

types of tailed porphyroclasts, sigma (σ) and delta (δ) type in metamorphic shear zones (Fig. 4.7a & b). The σ-porphyroclasts show fine-grained tails attached to their leading and trailing edges, and the tails do not cross the line parallel to the foliation through the center of the grain, indicating the shear sense. The δ-type is derived from the σ-porphyroclasts by continued deformation and rotation in a sense consistent with the shear, and the tails do cross the center line. By applying this method to rotated clay balls to determine the sense of shear, most of the rotated clay balls with their leading and trailing tails or wings do not pass the center line, just like the σ-type porphyroclasts, indicating reverse movement (Fig 4.8a & b).

The kinematics of clay balls along bedding fractures in the Siwalik sandstones of the Surghar-Shinghar Range have developed under surface P/T conditions. Reverse sense of shear has been interpreted from asymmetric displaced and rotated clay-ball kinematic geometry. The geometry and kinematics of strained clay balls resemble closely with porphyroclasts in metamorphic rocks, despite considerable difference in the P/T conditions. Their deformation mechanism is same, both clay balls and porphyroclasts behave plastically during deformation. For instant, feldspar or quartz under high P/T conditions behave plastically to form asymmetric tails, whereas clay balls, at surface P/T conditions behave plastically to form asymmetric tails, as they are composed of very fine detritus. This is probably due to the inherited plastic nature of the clay balls.

Further justification of the reverse sense along these shear zones, where the rotated clay balls are observed, is obtained from the associated displaced clay balls.

4.4. STRAIN FIELD DIAGRAM (Ramsay, 1967)

The strain field diagram (Fig. 4.9) helps to understand the strain functions of different fractures and the ways in which the structures are combined in sets (Davis, 1984). The concept was first presented by Ramsay (1967).

The strain ellipse has been classified into three main types based on their principal extension, and these types fall into three main fields when plotted on a graph (Ramsay, 1967), i.e.,

Field 1 $\lambda_1 > \lambda_2 > 1$

Field 2 $\lambda_1 > 1 > \lambda_2$

Field 3 $1 > \lambda_1 > \lambda_2$

If the strain occurs in the plane of a competent and incompetent or ductile layer, different types of minor structures will develop in the layer according to the deformation field. If the strain ellipse falls in field 1, all directions within the layer will suffer extension and the structures that develop will be entirely of the boudinage type.

In field 2, strain ellipses have one principal extension and one principal contraction. This arrangement will produce folding in one direction and boudinge or cross-jointing perpendicular to the lines of the fold axes.

If the ellipse lies in field 3, all directions are contracted. The folds have little regularity and competent bands undergo a very complex crumpling.

By using stain field diagram, the bedding, longitudinal and cross or dilational fractures, in the study area, will occupy field 2 of Ramsay (1967) or field of compensation (Davis, 1984), where three kinematically coordinated sets simultaneously accommodated shortening and dilation.

4.5. STRESS & STRAIN ANALYSES OF JOINTS AND DBSZs

4.5.1. Joints

The general behavior and orientation of joints developed in the study area is as under:

- EW/WNW oriented extensional joints *(Je)*,
- NS/NNE oriented compressional joints *(Jc)*,
- North-south oriented minor folds *(fm)*, with fold axis parallel to the compressional joints set.

Both the joint sets (EW/WNW and NS/NNE) are initially formed as tensional joints during bending or folding of SMM dome-shape anticline as

93

observed in the northsouth oriented part. But, later, due to the tectonic stresses of Dara Tang Fault, the NS/NNE oriented joints *(Jc)* accommodated east-west compression with a component of minor folds and EW/WNW oriented joints *(Je)* accommodated north-south extension.

4.5.2. Deformation Band Shear Zones (DBSZs)

Descriptive analysis of deformation band shear zones (DBSZs) shows that both the sets (NS and N50°–60°E) cut across the bedding as well as the joint surfaces. Based on field evidences, two deformational phases have been suggested for the formation of joints and DBSZs:

1. formation of tensional joints, tension in all four directions, due to bending of layers during the fold formation,

2. second deformation phase is characterized by the development of compressional joints (NS/NNE) with a component of folding and extensional joints (EW/WNW) of the pre-existing tensional joints of first deformational phase. The second phase may be due to the stresses of the Dara Tang Fault, and contemporaneously the development of neotectonic conjugate strike-slip deformation band shear zones (NS and N50°–60°).

The intensity of these DBSZs is high close to the trace of the Surghar Thrust (ST). The ST is passing at the core of SMM dome-shape anticline in the form of high angle oblique-reverse Dara Tang Fault. Thus, this fault appears to be dynamically responsible for the shear fracture initiation and subsequent fracture propagation in the adjacent sandstone bodies or in other words the deformation bands are formed due to the imperfect transfer of the Dara Tang Fault in adjacent sandstone horizons. As the age of the upper levels of Dhok Pathan Formation is not more than 0.8 m.y., therefore, these strike-slip DBSZs in the Mochi-Mar and Qabul Khel areas reflect consequences of the neotectonics of the Dara Tang Fault (Surghar Thrust) in the form of incipient strike-slip splays.
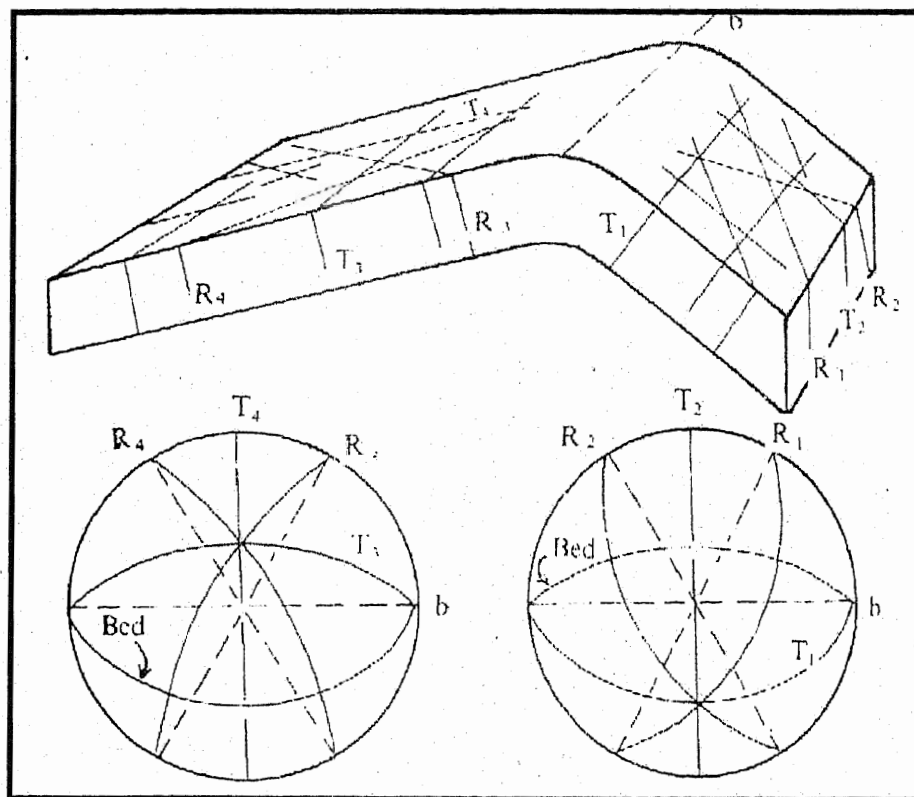
Fig. 4.1. Trends of fractures in a folded layer (Price, 1966).
T : Tension fractures.
R : Shear fractures
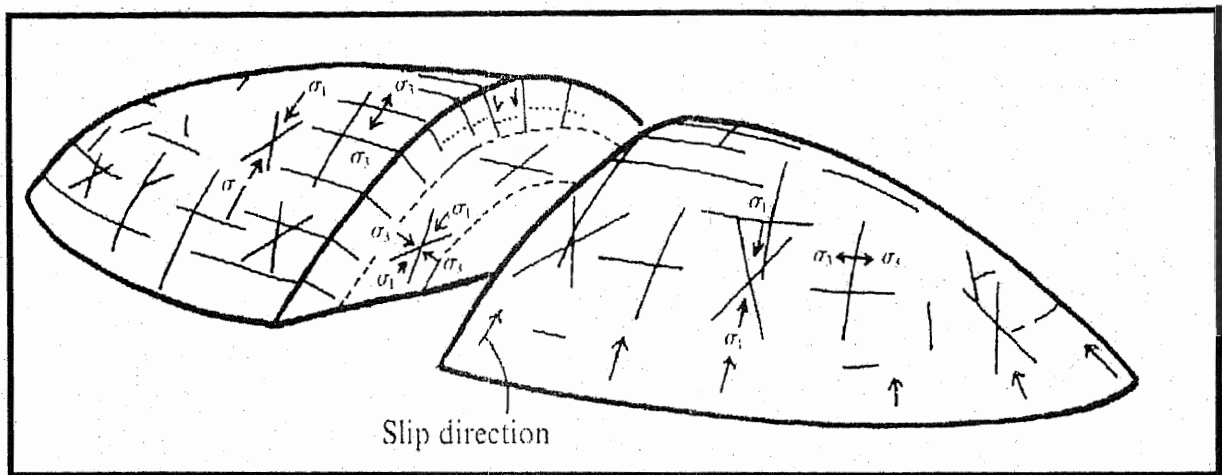
Fig. 4.2. Geometrical arrangement of fractures in a domal anticline (Stearns, 1964).
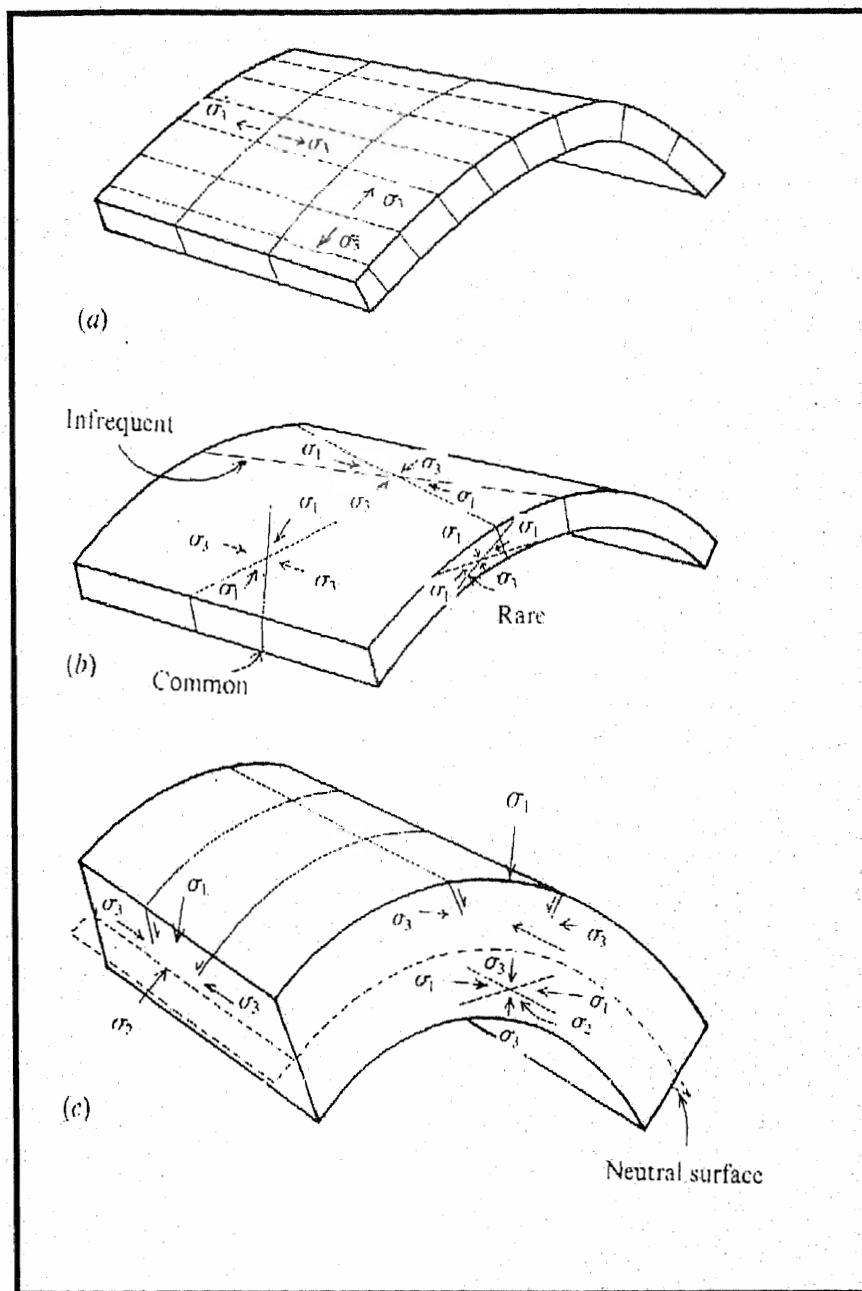
Fig. 4.3. (a) Typical relationship f dilational fractures to a fold.
(b) Typcial orientation of shear fractures in a thin
bedded layer, with associated stress system.
(c) Typcial oreintation of normal and thrust faults which
may develop in a thick, flexured unit (Price & Cosgrove, 1990)
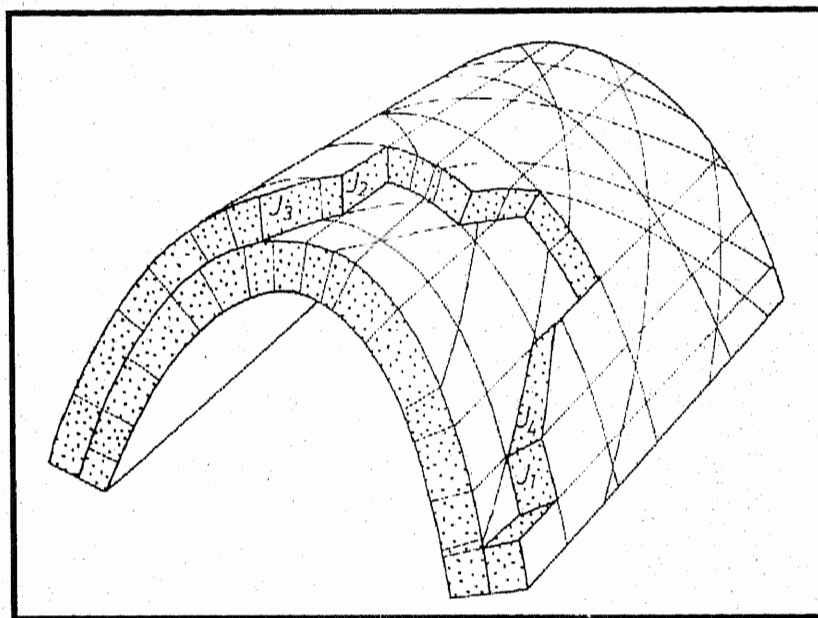
Fig. 4.4. Relationship of bedding, longitudinal, cross and oblique-slip fractures
/joints to fold geometry (Ramsay and Huber, 1987).

      J1 :   Cross Joints
      J2 :   Longitudinal Joints
      J3 & J4:   Diagonal Joints
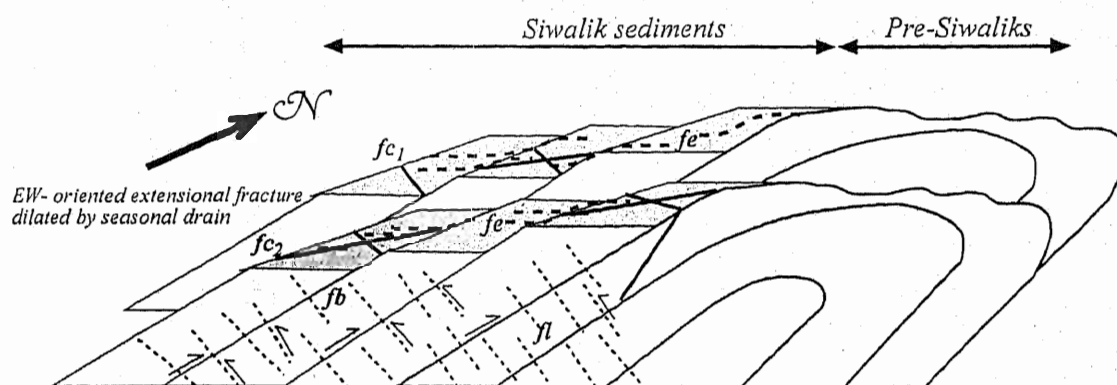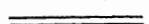
Fig. 4.5*a*. Kinematic relationship of bedding, longitudinal, extensional and conjugate shear fractrues related with the flexural-slip folding.

fb: bedding fractures
fl: longitudinal fractures
fe: extensional fractures
fc$_1$: conjugate shear fracture set 1
fc$_2$: conjugate shear fractrue set 2

Scale = 1:250,000
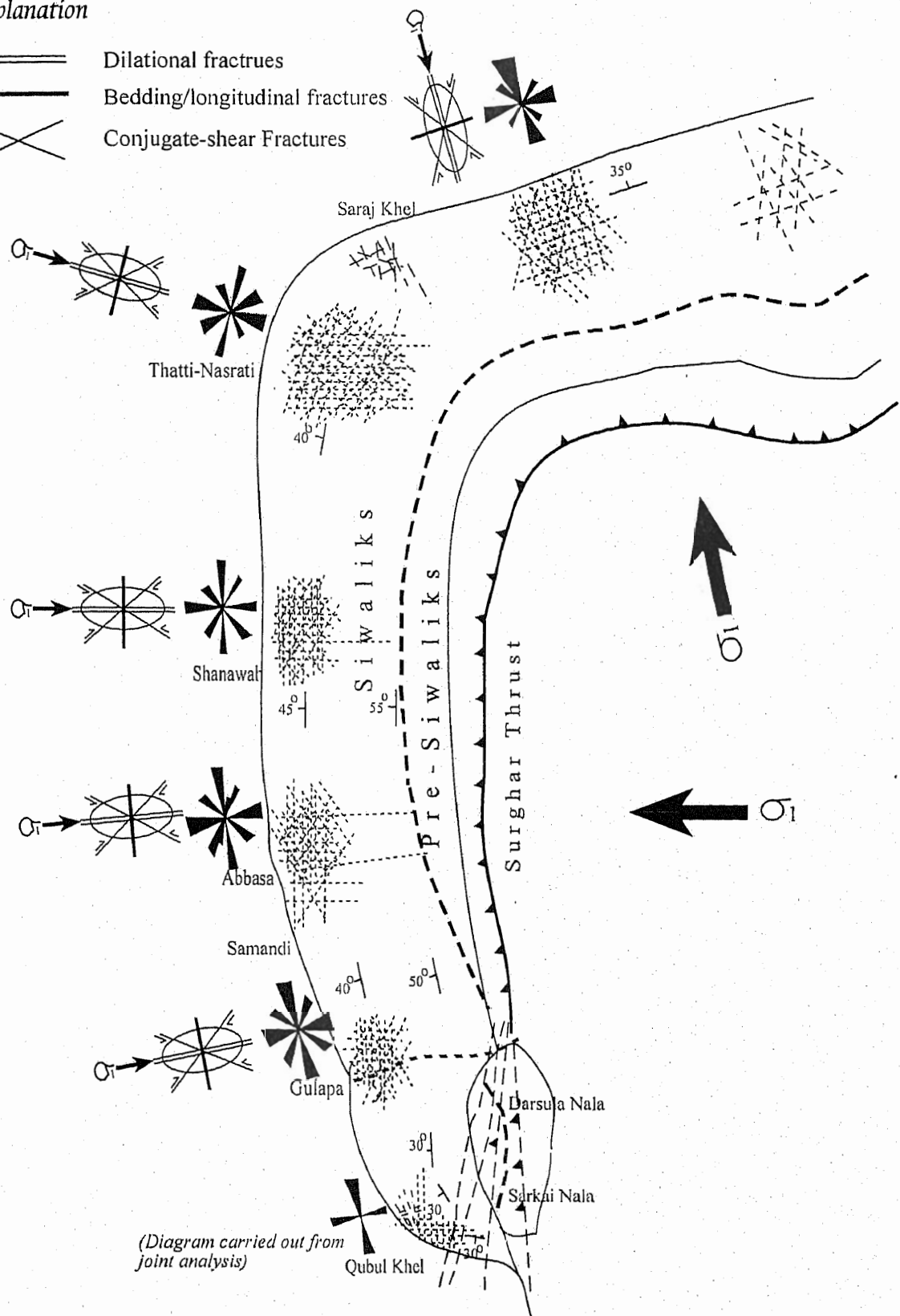
Fig. 4.5*b*. A preliminary structural map of fractures recorded in the Siwalik Group at different stations, illustrated by frequency and stress diagrams, Surghar-Shinghar Range, Trans-Indus Ranges.

100
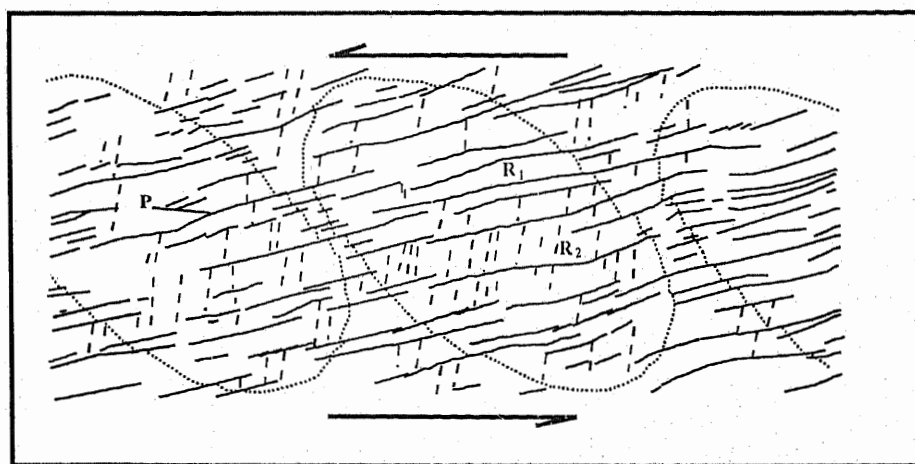
Fig. 4.6. Sinistral simple shear in a clay block model induced by shearing the substrate of the clay. Note the formation of R_1 and R_2 Riedel fractures (after Twiss and Moores, 1992).

σ- type
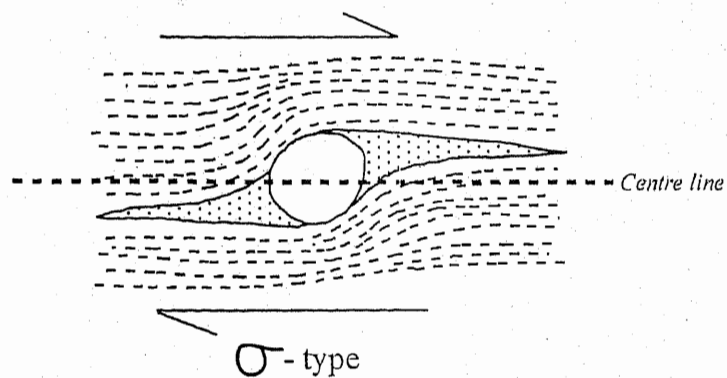
a: σ -type porphyroclast, showing sense of shearing. Note that the tails do not cross the line parallel to the foliation through the centre of the grain (Passchier and Simpson, 1986).

δ- type
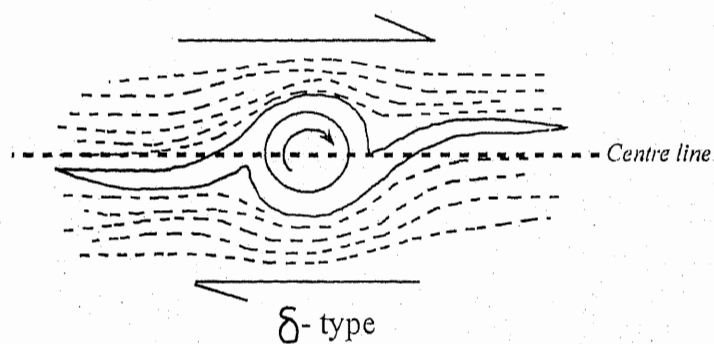
Fig. 4.7. b: δ-type porphyroclast, derived form the rotation of σ - type. Note the tails do cross the central line. (Passchier and Simpson, 1986).

(a)

(b)
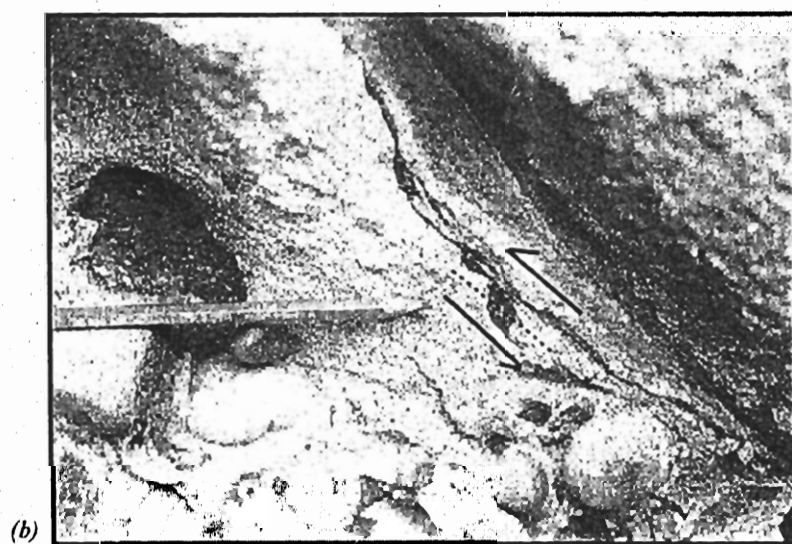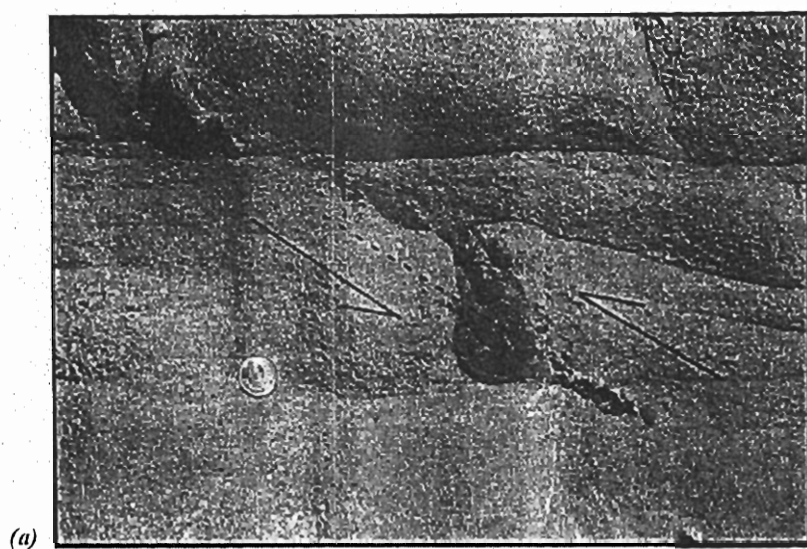
Fig. 4.8. The kinematic geometry of asymmetric tailed clay balls showing reverse-sense of movement. Note that the tails do not pass the center line.
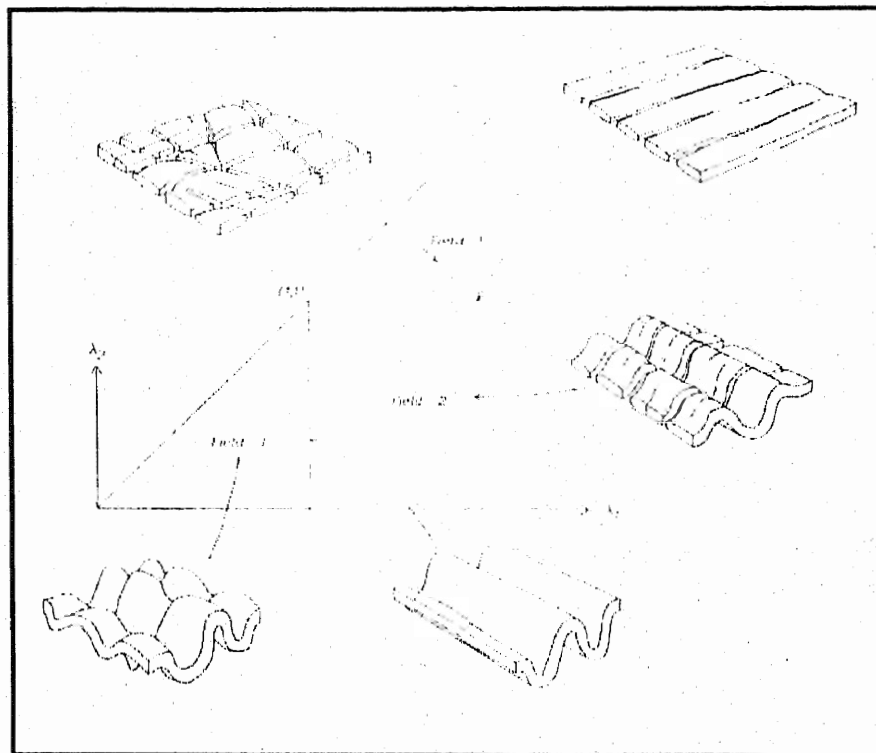
Fig. 4.9. Strain field diagram showing geological structures developed in three fields
of strain ellipse (Ramsay, 1967).

Chapter 5

DISCUSSION & CONCLUSION

Structural analysis of shear and dilational fractures in the Siwalik Group of Surghar-Shinghar Range constitute the main topic of the present study. These fracture sets are nicely developed in the western exposed flank of the Surghar-Shinghar Range. The geometrical behavior and orientation of these fractures, with the strike of Surghar-Shinghar Range, suggest that these could only be formed under systematic stress system. After detailed descriptive, kinematic and dynamic analyses, we can now discuss and draw conclusions for each of the fracture set.

5.1. BEDDING / LONITUDINAL FRACTURES

Bedding fractures, which are formed due to the flexural-slip folding (Ramsay and Huber, 1987) in the Siwalik Group of Surghar-Shinghar Range, are categorized as those that follow regional strike and dip of the range along the bedding planes. Mainly clay ball scoured surfaces provide incompetent weak planes for shearing. Reverse sense of shear has been interpreted from rotated and displaced clay ball kinematic geometry. The geometry of both rotated and displaced clay ball can be used as kinematic indicators to resolve the sense of movement along shear zones in other foreland terrains of the Himalayas or elsewhere. The understanding of these meso-kinematic structures can also help to explain the possible dynamics and kinematics of regional tectonics of the area.

Longitudinal fractures cut across the layer-parallel shear fractures and hence, bedding planes. These fractures may initially formed as tensional fractures, but, later, due to rotation of beds induced as shear fractures. Revere sense of shear has been interpreted for these fracture sets as they displaced the bedding fracture sets.

The bedding fractures play an important role in the uplifting of the western flank or outer flank of the Surghar-Shinghar Range. The thickness of

105

the Siwalik strata in the area is about 6km (Azizullah, 1995) and reverse faults have been noted along each and every clay ball scoured surfaces (frequent and prominent primary sedimentary features of Chinji, Nagri and Dhok Pathan formations). Thus, during flexural-slip regional folding of Surghar-Shinghar Anticline, reverse movement along the bedding planes/scoured surfaces on local scale facilitate regional uplifting of the western exposed flank of the Surghar-Shinghar Anticline.

5.2. EXTENSIONAL FRACTURES

The extensional component i.e., perpendicular to the fold axis of Surghar-Shinghar Anticline, is accommodated by roughly east-west oriented dilational fractures. These fractures are very pronounced geomorphic features of the range as stated in the descriptive analysis. Most of the streams in the Surghar-Shinghar Range have parallel, sub-parallel drainage flow pattern across the range from east to west. We interpreted that the extensional fractures in the Shinghar Range are further dilated by seasonal drain forming V-shape gorges in the Siwalik sediments. Thus, the extensional fractures in the Siwalik sediments facilitate drainage from east to west direction, controlling the geomorphic processes.

5.3. CONJUGATE SHEAR FRACTURES

Diagonal or conjugate shear fractures are nicely exposed at the outer limbs of Surghar-Shinghar Anticline. These fractures accommodate sinistral and dextral movements. The orientation of these fracture changes with the strike of range indicating systematic stress system.

Thus, fracture sets in Surghar-Shinghar Range form a distinct pattern of dilational and shear fractures indicating systematic stress system related with the flexural-slip folding of Surghar-Shinghar Anticline. As there is a change in the axis of the Surgher-Shinghar Anticline from Thatti-Nasrati, corresponding to the change in the orientation of fracture sets with the change in the regional strike of the beds.

Based on our field observations and interpretations we, therefore, suggest that the bedding, longitudinal, cross and diagonal shear fractures in Surghar-Shinghar Range are genetically and geometrically related with the flexural-slip folding of Surghar-Shinghar Anticline.

5.4. DEFORMATION BAND SHEAR ZONES (DBSZS) AND JOINTS

Structural analysis of two sets of joints with associated neotectonic deformation band shear fractures in the Dhok Pathan and Nagri formations reveals systematic joint pattern and development of deformation band shear zones (DBSZs). These joints are initially formed as tensional joints, however, set NS/NNE defines compressional geometry, whereas EW/WNW oriented joints form extensional geometry, both making an orthogonal relationship. The NS and N50°-60°E oriented DBSZs are conjugate strike-slip in character, which cut across the sedimentary bedding as well as the joint surfaces. The NS oriented DBSZs form thick bands, through going with dextral sense of shear, whereas the N50°-60°E oriented DBSZs are tabular and broad with distinct Riedel fractures. Both the sets form conjugate geometry at an angle of about 50°-60°.

Detailed structural analysis of the area shows that the orthogonal tensional joints are formed in the first deformation phase due to the bending of sedimentary layers, followed by second deformational episode, which is apparently related with the neotectonics of Dara Tang Fault. Consequently, the second deformational phase is well characterized by the development of conjugate strike-slip deformation band shear zones, which are formed due the imperfect transfer of the Dara Tang Fault to the adjacent sandstone horizons. The presence of both joints and deformation bands at the upper levels of the Dhok Pathan Formation (~0.8Ma; Khan, 1983), indicate on-going neotectonics in the area.

Appendix - I

Table-3.1. Circle-inventory method for evaluating fracture density in Gulapa area.

Table-3.1.1.

Location:	Gulapa, Shinghar Range
Toposheet No.:	38^p/$_2$
Formation:	Dhok Pathan Fm.
Radius of circle:	2m
Area:	12.56m^2

S. No.	Trend	Length (m)
1	N10°W	3.8
2	N11°W	3.3
3	N11°W	2.6
4	N12°W	2.6
5	N10°W	3.7
6	N11°W	2.6
7	N13°W	2.3
8	N14°W	2.2
9	N12°W	2.5
10	N13°W	0.5
11	N15°W	0.3
12	N71°W	1.6
	*C. L.	28

Fracture Density: 28/12.56 = 2.22m^{-1}

Cumulative length

Table-3.1.2.

Location:	Gulapa, Shinghar Range
Toposheet No.:	38^p/$_2$
Formation:	Nagri Fm.
Radius of circle:	2m
Area:	12.56m^2

S. No.	Trend	Length (m)
1	N16°W	3.1
2	N18°W	2.3
3	N19°W	2.5
4	N18°W	3.6
5	N18°W	2.3
6	N17°W	1.7
	C. L.	15.5

Fracture Density: 15.5/12.56 = 1.34m^{-1}

Table-3.1.3.

Location:	Gulapa, Shinghar Range
Toposheet No.:	38^p/$_2$
Formation:	Dhok Pathan Fm.
Radius of circle:	2m
Area:	12.56m^2

S. No.	Trend	Length (m)
1	N73°E	0.3
2	N74°E	0.2
3	N72°E	0.4
4	N74°E	0.2
5	N73°E	0.3
6	N74°E	0.1
7	N79°W	3.1

8	N76°W	2.3
9	N31°E	3.7
10	N32°E	3.0
11	N32°E	2.9
	C. L.	**16.5**

Fracture Density: $16.5/12.56 = 1.31m^{-1}$

Table-3.1.4.

Location: Gulapa, Shinghar Range
Toposheet No.: $38^{p}/_{2}$
Formation: Dhok Pathan Fm.
Radius of circle: 2m
Area: $12.56m^{2}$

S. No.	Trend	Length (m)
1	N74°E	0.2
2	N74°E	0.3
3	N76°E	0.2
4	N75°E	0.1
5	N76°E	0.3
6	N71°E	0.2
7	N79°E	0.1
8	N73°E	0.1
9	N72°E	0.1
10	N77°W	3.7
11	N76°W	3.6
12	N75°W	3.9
13	N39°E	3.6
14	N36°E	0.6
15	N37°E	0.3
16	N35°E	0.3
	C. L.	**17.6**

Fracture Density: $17.6/12.56 = 1.40m^{-1}$

Average fracture density in Gulapa area calculated from four inventory stations: 1.56m^{-1}.

Table-3.2.Circle-inventory method for evaluating fracture density in Samandi area.

Table-3.2.1.

Location: Samandi, Shinghar Range
Toposheet No.: $38^P/_1$
Formation: Dhok Pathan Fm.
Radius of circle: 2m
Area: $12.56m^2$

S. No.	Trend	Length (m)
1	N05°W	3.6
2	N06°W	3.2
3	N06°W	3.3
4	N07°W	2.2
5	N07°W	2.1
6	N06°W	1.4
7	N02°W	1.3
	C. L.	**17.1**

Fracture Density: $17.1/12.56 = 1.36m^{-1}$

Table-3.2.2.

Location: Samandi, Shinghar Range
Toposheet No.: $38^P/_1$
Formation: Nagri Fm.
Radius of circle: 2m
Area: $12.56m^2$

S. No.	Trend	Length (m)
1	N10°W	3.3
2	N11°W	3.4
3	N10°W	3.6
4	N10°W	1.2
5	N12°W	0.5
6	N13°W	0.5
7	N13°W	0.5
8	N12°W	0.6
9	N38°E	3.0
	C. L.	**16.6**

Fracture Density: $16.6/12.56 = 1.32m^{-1}$

Table-3.2.3.

Location: Samandi, Shinghar Range
Toposheet No.: $38^P/_1$
Formation: Dhok Pathan Fm.
Radius of circle: 2m
Area: $12.56m^2$

S. No.	Trend	Length (m)
1	N82°E	0.3
2	N80°E	0.5
3	N80°E	0.2
4	N79°E	0.3
5	N82°E	0.6
6	N80°E	0.2
7	N38°E	3.6
8	N39°E	2.9
	C. L.	**8.6**

Fracture Density: $8.6/12.56 = 0.68m^{-1}$

Table-3.2.4.

Location: Samandi, Shinghar Range
Toposheet No.: $38^p/_1$
Formation: Nagri Fm.
Radius of circle: 2m
Area: $12.56m^2$

S. No.	Trend	Length (m)
1	N39°E	3.6
2	N40°E	3.2
3	N38°E	3.3
4	N72°W	3.4
5	N74°W	1.2
6	N78°E	0.2
7	N76°E	0.1
8	N77°E	0.4
9	N79°E	0.1
10	N82°E	0.2
11	N80°E	0.1
	C. L.	**15.8**

Fracture Density: $15.8/12.56 = 1.25m^{-1}$

Average fracture density in Samandi area calculated from four inventory stations: 1.15 m^{-1}.

iv

Table-3.3.Circle-inventory method for evaluating fracture density in Abbasa area.

Table-3.3.1.

Location: Abbasa, Shinghar Range
Toposheet No.: $38^P/_1$
Formation: Dhok Pathan Fm.
Radius of circle: 2m
Area: $12.56m^2$

S. No.	Trend	Length (m)
1	NS	3.6
2	NS	3.7
3	N40°E	3.3
4	NS	2.5
5	NS	1.2
6	NS	0.2
7	NS	2.2
8	N60°W	2.3
9	N65°W	1.0
	C. L.	20

Fracture Density: $20/12.56 = 1.59m^{-1}$

Table-3.3.2.

Location: Abbasa, Shinghar Range
Toposheet No.: $38^P/_1$
Formation: Nagri Fm.
Radius of circle: 3m
Area: $28.26m^2$

S. No.	Trend	Length (m)
1	NS	3.1
2	NS	4.0
3	N4°E	3.2
4	NS	2.0
5	NS	0.8
6	N5°E	2.6
7	NS	0.3
	C. L.	16

Fracture Density: $16/12.56 = 1.27m^{-1}$

Table-3.3.3.

Location: Abbasa, Shinghar Range
Toposheet No.: $38^P/_1$
Formation: Dhok Pathan Fm.
Radius of circle: 2m
Area: $12.56m^2$

S. No.	Trend	Length (m)
1	EW	0.3
2	EW	0.4
3	EW	0.3
4	EW	0.2
5	EW	0.1
6	EW	0.1
7	EW	0.2
8	EW	0.7
9	EW	0.6
10	N48°E	2.1

11	N45°E	2.6
12	N62°W	3.6
	C. L.	**11.2**

Fracture Density: $11.2/12.56 = 0.89 m^{-1}$

Table-3.3.4.

Location:	Abbasa, Shinghar Range
Toposheet No.:	$38^P/_1$
Formation:	Dhok Pathan Fm.
Radius of circle:	2m
Area:	$12.56 m^2$

S. No.	Trend	Length (m)
1	N40°E	3.3
2	N42°E	3.8
3	N42°E	3.5
4	N45°E	2.2
4	N58°W	3.6
5	N56°W	2.3
6	EW	0.2
7	EW	0.3
8	EW	0.3
9	EW	0.1
10	EW	0.2
11	EW	0.3
12	EW	0.1
13	EW	0.2
14	EW	0.1
15	EW	0.1
	C. L.	**20.6**

Fracture Density: $20.6/12.56 = 1.64 m^{-1}$

Average fracture density in the Abbasa area calculated from four inventory stations: 1.34m⁻¹.

Table-3.4.Circle-inventory method for evaluating fracture density in Shanawah-Godi-Khel area.

Table-3.4.1.

Location: Shanawah-Godi Khel, Shinghar Range
Toposheet No.: $38^P/_1$
Formation: Dhok Pathan Fm.
Radius of circle: 2m
Area: $12.56m^2$

S. No.	Trend	Length (m)
1	NS	3.8
2	NS	3.8
3	NS	3.2
4	NS	3.3
5	NS	3.7
6	NS	1.2
7	NS	0.8
	C. L.	19.8

Fracture Density: $19.8/12.56 = 1.57m^{-1}$

Table-3.4.2.

Location: Shanawah-Godi Khel, Shinghar Range
Toposheet No.: $38^P/_1$
Formation: Nagri Fm.
Radius of circle: 2m
Area: $12.56m^2$

S. No.	Trend	Length (m)
1	NS	3.5
2	NS	3.3
3	NS	3.0
4	NS	0.2
5	NS	0.3
6	NS	0.6
7	NS	0.4
8	NS	0.4
9	NS	0.3
	C. L.	12

Fracture Density: $12/12.56 = 0.95m^{-1}$

Table-3.4.3.

Location: Shanawah-Godi Khel, Shinghar Range
Toposheet No.: $38^P/_1$
Formation: Dhok Pathan Fm.
Radius of circle: 2m
Area: $12.56m^2$

S. No.	Trend	Length (m)
1	EW	0.9
2	EW	0.3
3	EW	0.2
4	EW	0.2
5	EW	0.3
6	EW	0.1
7	EW	0.2
8	N40°W	2.0

9	N42°W	3.2
10	N43°W	2.6
	C. L.	**10**

Fracture Density: $10/12.56 = 0.79 \text{m}^{-1}$

Table-3.4.4.

Location:	Shanawah-Godi Khel, Shinghar Range
Toposheet No.:	$38^p/_1$
Formation:	Dhok Pathan Fm.
Radius of circle:	2m
Area:	12.56m^2

S. No.	Trend	Length (m)
1	N45°E	3.2
2	N50°E	3.6
3	N46°E	3.3
4	N57°W	3.4
5	N55°W	1.4
6	N55°W	2.8
7	EW	0.2
8	EW	0.1
9	EW	0.1
10	EW	0.2
11	EW	0.2
12	EW	0.3
13	EW	0.2
14	EW	0.1
	C. L.	**19.1**

Fracture Density: $19.1/12.56 = 1.52 \text{m}^{-1}$

Average fracture density in the Shanawah area calculated from four inventory stations: 1.20m⁻¹.

Table-3.5. Circle-inventory method for evaluating fracture density in Thatti-Nasrati area.

Table-3.5.1.

Location: Thatti-Nasrati-Nasrati, Shinghar Range
Toposheet No.:   38^P/$_1$
Formation: Dhok Pathan Fm.
Radius of circle: 2m
Area: 12.56m^2

S. No.	Trend	Length (m)
1	N14°E	3.1
2	N15°E	3.5
3	N16°E	2.9
4	N16°E	2.6
5	N15°E	2.8
6	N15°E	1.2
7	N15°E	1.8
	C. L.	17.9

Fracture Density: 17.9/12.56 = 1.58m^{-1}

Table-3.5.2.

Location: Thatti-Nasrati-Nasrati, Shinghar Range
Toposheet No.:   38^P/$_1$
Formation: Dhok Pathan Fm.
Radius of circle: 2m
Area: 12.56m^2

S. No.	Trend	Length (m)
1	N73°W	0.2
2	N73°W	0.2
3	N74°W	0.3
4	N72°W	0.1
5	N73°W	0.1
6	N74°W	0.3
7	N72°W	0.1
8	N40°W	3.6
9	N42°W	3.7
10	N71°E	3.0
11	N70°E	3.5
	C. L.	15.1

Fracture Density: 15.1/12.56 = 1.20m^{-1}

Table-3.5.3.

Location: Thatti-Nasrati-Nasrati, Shinghar Range
Toposheet No.:   38^P/$_1$
Formation: Dhok Pathan Fm.
Radius of circle: 2m
Area: 12.56m^2

S. No.	Trend	Length (m)
1	N56°W	3.8
2	N55°W	3.6
3	N58°W	3.6
4	N57°W	3.6
5	N54°W	1.5
6	N55°W	0.6
7	N74°E	3.3

8	N78°E	3.2
9	N77°E	3.0
10	N79°E	2.6
11	N74°E	2.2
12	N82°W	0.2
13	N81°W	0.3
14	N85°W	0.2
15	N87°W	0.1
	C. L.	**31.8**

Fracture Density: $31.8/12.56 = 2.53 \text{m}^{-1}$

Average fracture density in the Thatti-Nasrati area calculated from three inventory stations: 1.77m^{-1}.

Table-3.6.Circle-inventory method for evaluating fracture density in Seraj Khel area.

Table-3.6.1.

Location: Seraj Khel, Shinghar Range
Toposheet No.: $38^P/_1$
Formation: Nagri Fm.
Radius of circle: 2m
Area: 12.56m²

S. No.	Trend	Length (m)
1	N54°E	3.6
2	N53°E	3.1
3	N54°E	2.2
4	N52°E	2.6
5	N53°E	2.8
6	N55°E	2.3
7	N53°E	0.2
8	N55°E	0.3
9	N55°E	0.2
10	C. L.	17.3

Fracture Density: 17.3/12.56 = 1.37m⁻¹

Table-3.6.2.

Location: Seraj Khel, Shinghar Range
Toposheet No.: $38^P/_1$
Formation: Dhok Pathan Fm.
Radius of circle: 2m
Area: 28.26m²

S. No.	Trend	Length (m)
1	N21°W	0.2
2	N22°E	0.1
3	N21°W	0.3
4	N22°W	0.1
5	N20°W	0.2
6	N24°W	0.1
7	N23°W	0.3
8	N21°W	0.1
9	N24°E	3.5
10	N26°E	1.0
11	N27°E	0.6
12	N45°W	2.6
13	N46°W	1.3
	C. L.	10.4

Fracture Density: 10.4/12.56 = 0.82m⁻¹

Table-3.6.3.

Location: Seraj Khel, Shinghar Range
Toposheet No.: $38^P/_1$
Formation: Dhok Pathan Fm.
Radius of circle: 2m
Area: 12.56m²

S. No.	Trend	Length (m)
1	N54°W	3.9
2	N56°W	3.6
3	N56°W	3.5
	C. L.	11

Fracture Density: 11/12.56 = 0.87m⁻¹

Average fracture density in the Seraj Khel area calculated from three inventory stations: 0.73m⁻¹.

REFERENCES

Abid, I. A., Abbasi, I. A., Khan, M. A, and Shah, M. T. 1983. Petrology and geochemistry of Siwalik sandstone and its relationship to the Himalayan orogeny. Geol. Bull. Univ. Pesh. 16, 65-83.

Akhtar, M., 1983. Stratigraphy of the Surghar Range. Geol. Bull. Univ. Punj. 18, 32-45.

Ahlgren, S. G., 2001. The nucleation and evolution of Riedel shear zones as deformation bands in porous sandstone. Jr. of Struc. Geol., Vol. 23, 1203-1214.

Anderson, E. M., 1951. The dynamics of faulting and dyke formation with applications to Britain: Oliver and Boyed, Edinburgh, 206.

Allen, C. R., 1976. Report to the Pakistan Atomic Energy Commission on the geologic and seismic aspects of the proposed nuclear power plant at Chashma.

Angelier, J., 1994. Fault slip analysis and paleostress reconstruction. In: Continental Deformation, Hancok, P. L (ed.), Pergaman Press, Oxford, 53-100.

Antonellini, M., Aydin, A., Pollard, D. D., D'Onfro, P. 1994. Petrophysical study of faults in sandstone using petrographic image analysis and X-ray computerized tomography. Pure and Applied Geophysics 143, 181-201.

Aydin, A., 1978. Small faults formed as deformation bands in sandstone. Pure and Applied Geophysics. Vol., 116, 913-930.

Aydin, A. and Johnson, A, M., 1978. Development of faults as zones of deformation bands and as slip surfaces in sandstone. Pure and Applied Geophysics 116, 931-942.

Azizullah, 1995. Petrotectonic, petrology and genesis of uranium mineralization of the Siwalik Group of Thatti-Nasratti and Shava-Shanawah area. Unpublished Ph. D. thesis, Punjab Univ. Vol. 1 & II.

Auden, J. B., 1937. The structure of the Himalaya in Garwal. Geol. Survey India, Rec. 71, 407-433.

Badgley, P. C., 1965. Jointing and fracture analysis, In: Structural and tectonic principles. Harper & Row, John Weather Hill, Inc. 98.

Bajwa, M. S. and Shams, F. A., 1986. Petrology of lower Siwalik sandstone of Thatti area, Khushab District, Punjab, Pakistan. Geol. Bull. Univ. Punj. 21, 1-9.

Bajwa, M. S., 1987. Petrology of Siwalik sandstone of Rewat area Rawalpindi. District Punjab, Pakistan. Presented at 30th Sec. conf. Pak, Abs.

Bajwa, M. S., Shams, F. A. and Shiki, T., 1987. Geochemistry of garnet grains from Murree and Siwalik formations, Rawalpindi and Jhelum District, Punjab, Pakistan. Geol. Bull. Univ. Punj., 22, 1-10.

Ball, V. and Simpson, R. R., 1913. The coal fields of India. India Geol. Survey Rec., Vol., 41, 147.

Bartlett, W. L., Friedman, M., Logan, J. M., 1981. Experimental folding and faulting of rocks under confining pressure. Part IX. Wrench faults in limestone layes. Tectonophysics 79, 255-277.

Barton, C. C., 1933. Surface fracture system of south Texas. Am. Assoc. Pet. Geol. Bull., 17, 1194-1212.

Barton, N. R., 1973. Review of a new shear strength criterion for rock joints. Eng. Geol., 7, 287-332.

Bannert, D. 1986. Stress release in the Himalayan foreland areas of northern Pakistan as inferred from LandSat images. Fed. Inst. Geosci. And Natural Res., 56. Unpubl. Rep. BGR/HDIP; Hannover/Islamabad.

Bender, F. K.; Raza, H. R., 1995. Geology of Pakistan. Gebruder Borntraeger, 140.

Berthe, D., Choukroune, P. and Jegouzo, P. 1979. Orthogneiss, mylonite and non-coaxial deformation of granites: The example of the South Armorican shear zones. Jour. of Struct. Geol., Vol. 1, 31-42.

Bossart, P., Dietrich, D., Greco, A., Ottiger, R. and Ramsay, J. G., 1984. A new structural interpretation of the Hazara-Kashmir syntaxis (southern Himalaya), Pakistan. Kashmir, Jr. Geol., 2: 19-36.

Calkins, J. A., Offield, T. W., Abdullah, S. K. M. & Ali, S. T., 1975. Geology of the southern Himalaya in Hazara, Pakistan and adjacent areas. U. S. Geol. Survey Professional Paper, 716-C, C1-29.

Chester, F. M., Friedman, J. and Logan, J. M., 1985. Foliated cataclasites. Tectonophysics. Vol., 111, 139-146.

Chaudhry, R. S. 1970. Petrology of Siwalik formations of the north western Himalayas. Bull. India Geol. Association 3, No. 1 & 2, 19-25.

Chaudhry, M. N. & Ghazanfar, M., 1990. Position of the Main Central Thrust in the tectonic framework of the western Himalaya. Tectonophysics, 174, 321-329.

Cloos, H., 1922. Uber Ausbau and Anwendung der granittek-tonischen Methode:Preussischen Geologischen Landesanstalt, Vol. 89, 1-18.

Cobbold, P. R., Gapais, D., Means, W. D. and Treagus, S. H. (eds.), 1987. Shear criteria in rocks. Jour. of Struct. Geol. Vol. 9, 521-778.

Coward, M. P., 1985. A section through the Nanga Parbat syntaxis, Indus valley, Kohistan. Geol. Bull. Univ. Pesh. 18, 147-152.

Coward, M. P., Butler, R. W. H., 1985. Thrust tectonics and the deep structure of the Pakistan Himalaya. Geology, 13, 417-420.

Coward, M. P., Windley, B. F., Broughton, R. D., Luff, I. W., Petterson, M. g., Pudsey, C. J., Rex, D. C. and Khan, M. A., 1986. Collision tectonics in the NW Himalayas. In: Coward, M. P. & Ries, A. C. (eds). Collision Tectonics. Geol. Soc. Lond., Spec. Publ. 19, 203-129.

Danilchik, W. & Shah, S. M. I., 1987. Stratigraphy and coal resources of the Makarwal area, Trans-Indus Mountains, Mianwali District, Pakistan. U. S. Geol. Survey Professional. Paper 1341, 39.

Davis, G. H., 1984. Structural geology of rocks and regions. New York. Wiley. 325-352.

Davis, G. H., Bump, A. P., Garcia, P. E. and Ahlgren, S. G. 2000. Conjugate Riedel deformation band shear zones. Jour. of struc. Geol. Vol. 22, 169-190.

Davis, G. H. and Reynolds, S. J., 1996. Structural Geology of Rocks and Regions. John Wiley & Sons, Inc., 1-737.

Di Pietro, J. a., Pogue, K. R., Hussain, A. & Ahmad, I., 1996. Geology and tectonics of the Indus Syntaxis, northwest Himalaya, Pakista (in press, reference taken from Kazmi & Jan, Geology and Tectonics of Pakistan, 1997).

Duncan, R. A. & Pyle, D. G., 1988. Rapid extrusion of the Deccan flood basalt at the Cretaceous/Tertiary boundary. Nature, 333, 841-843.

Engelder, T., 1982. Is there a genetic relationship between selected joints and contemporary stress within lithosphere of North America? Tectonics, 1, 161-177.

Fineti, I., Giorgetti, F. and Poretti, G., 1979. The Pakistani segment of the DSS-profile Nanga Parbat – Karakul (1974-75). Boll. Geofis. Teorica ed Applicata, 21, 159-169.

Ganseer, A., 1964. Geology of the Himalayas. Wiley, New York, 289.

Gansser, A., 1980. The division between Himalaya and Karakoram. Geol. Bull. Univ. Pesh., 13, 9-22.

Gee, E. R., 1945. The age of the Saline series of the Punjab and Kohat. India Natl. Acad. Sci., Sec. B. Proc., 14(6). 269-310.

Gee, E. R., 1989. Overview of the geology and structure of the Salt Range, with observations on related areas of northern Pakistan. – In: MALINCONICO, L. L. & LILLIE, R. J. (eds.): Tectonics of the Western Himalayas; Geol. Soc. Amer. Spec. Paper 232, 95 – 112.

Greco, A., 1991. Stratigraphy, metamorphism and tectonics of the Hazara-Kashmir syntaxis area. Kashmir Jr. Geol., 8 & 9, 39-65.

Griggs, D. T. and Handin, J., 1960. Observations on fracture and a hypothesis of earthquakes. In Rock Deformation. Geol. Soc. Am. Mem., 79, eds. D. Griggs and J. Handin, 347-373.

Heim, A. & Gansser, A., 1939. Central Himalaya. Geological observations of the Swiss Expedition 1936. Denkschr, der Schweiz, Naturf. Gesell, 731, 243.

Hemphill, W. R. & Kidwai, A. H., 1973. Stratigraphy of the Bannu Basin and Dera Ismail Khan areas, Pakistan. U. S. Geol. Survey Prof. Paper 716-B, 36.

Hodgson, R. A., 1961. Classification of structures on joint surfaces. Am. Jour. Sci. 259, 493-502.

Jan, M. Q., 1980, Petrology of the obducted mafic metamor-phites from the southern part of the Kohistan island arc sequence. Geol. Bull. Univ. Pesh, 13, 95-107.

Johnson, B. D., Powell, C. M. A. & Veevers, J. J., 1976. Spreading history of the eastern Indian ocean, and Greater India's northward flight from Antarctica and Australia. Bull. Geol. Soc. Amer., 87, 1560-1566.

Jaume, S. T. & Lillie, R. J., 1988. Mechanics of the Salt Range-Potwar Plateau, Pakistan: A fold-and-thrust belt underlain by evaporites. Tectonics, Vol. 7, 57-71.

Kazmi, A. H., Lawrence, R. D., Anwar, J., Snee, L. W. & Hussain, S., 1986. Geology of the Indus suture zone in the Mingora-Shangla area of Swat, northern Pakistan. Geol. Bull. Univ. Pesh. 17, 127-143.

Kazmi, A. H., 1979. Preliminary seismotectonic map of Pakistan (1:2,000,000). Geol. Survey Pak., Quetta.

Kazmi, A. H., 1979. Active fault system systems in Pakistan. In: Farah. A. & DeJong, K. A. (eds.) Geodynamics of Pakistan. Geol. Survey Pak., Quetta, 285-294.

Kazmi, A. H. and Jan, M. Q., 1997. Geology and tectonics of Pakistan. Graphic Publishers. 1-500.

Kazmi, A. H. & Rana, R. A., 1982. Tectonic map of Pakistan. Geol. Survey Pak. Quetta. Scale: 1: 2,000,000.

Klootwijk, C. T., Gee, J. S., Peirce, J. W., Smith, G. W. and McFadden, P. L., 1992. An early India-Eurasia contact, Palaeomagnetic constraints from the Ninetyeast Ridge, ODP Leg, 121. Geology, 20, 395398.

Khan, F. K., 1991. A Geography of Pakistan: Environment, People and Economy. Oxford University Press.

Khan, M. A., Ahmed, R., Raza, H. A. and Kemal, A., 1986. Geology of petroleum in Kohat-Potwar depression, Pakistan, Bull. Amer. Assoc. Petrol. Geol., 70(4), 369-441.

Khan, M. J., 1983. Unpubish. Ph.D Thesis. Magnetostratigrapy of Neogene and Quaternary Siwalik Group sediments of the Trans-Indus Salt Range, northwestern Pakistan. 188p.

Khan, M. J., 1987. Sedimentation and tectonics of the Siwalik Group of the Trans-Indus Salt Range, Northern Pakistan. Geol. Bull. Univ. Pesh. Vol., 20., 129-141.

Khan, M. J. and Opdyke, N. D. 1987. Magnetic-polarity Stratigraphy of the Siwalik of the Siwalik Group of the Trans-Indus Salt Range, Northern Pakistan. Geol. Bull. Univ. Pesh. Vo., 20, 111-127.

Kravchenko, K. N., 1964. Soan formation-upper unit of Siwalik group in Potwar. Sci. & Industry, 2, 3: 230-233.

Le Fort, P., 1975. Himalaya: the collided range, Present knowledge of the continental Arc. Amer. Jr. Sci., 275A: 1-44.

Lewis, G. E., 1937. A new Siwalik correlation (India). Amer. Jr. Sci., 5,195,33: 191-204.

Lillie, R. J., Johnson, g. D., Yousaf, M. Zamin, A. S. H., & Yeats, R. S., 1987. Structural development within the Himalayan foreland fold-and-thrust belt of Pakistan. In: Beaumont & Tankard (eds.) sedimentary Basins and basin-forming Mechanisms. Can. Soc. Petro. Geol., Memoir 12, 379-392.

Lister G. S., and A. W. Snoke, 1984. S-C mylonites. Jour. of struc. Geol. Vol. 6, 617-638.

Macedo, J. and Marshak, S., 1999. Controls on the geometry of fold-thrust belt salients. GSA Bull., Vol., 111, No., 12, 1808-1822p.

Malinconico. L. L., 1989. Crustal thickness estimates for the western Himalaya. In Malinconico. L. L. & Lillie, R. J. (eds.) Tectonics of the western Himalayas. Geol. Soc. Amer., Spec. Paper, 232, 237-242.

Marshak, S. and Mitra, G., 1988. Analysis of fracture array geometry In: Basic methods of structural geology. Part-I, Elementary Techniques. 249-264.

Mawer, C. K. and J. C. White, 1987. Sense of displacement on the Cobequid-Chedabucto fault system, Nova Scotia, Canada: Canadian Jour. of Earth Sciences, Vol., 24, 217-223.

Mawer, C. K. 1992. Kinematic indicators in shear zones. International Basement Tectonics Association Publication No. 8, 67-81.

McClay, K. R. 1997. Structure geology for petroleum exploration. Course organized by: Premier Expl. Inc.

McDougall, J. W. and Khan, S. H., 1990. Strike-slip faulting in a foreland fold-thrust belt: the Kalabagh fault and western Salt Range, Pakistan. Tectonics, Vol. 9, No. 5, 1061-1075.

McDougall, J. W and Hussain, A., 1991. Fold and thrust propagation in the western Himalaya based on a balanced cross section of the Surghar Range and Kohat Plateau,

Pakistan. Bull. Amer. Assoc. Petrol. Geol., 75, 463-478.

McGill, G. E., and Stromquist, A. W., 1979. The grabens of Canyonlands National Park, Utah: geometry, mechanics, and kinematics: Jour of Geophysical Research, Vol. 4, 4547-4563.

McKenzie, D. P. and Sclater, J. G., 1976. The evolution of the Indian Ocean. In: Continental drift and continents ground. Readings form Sci. Amer. Freeman & Co., 139-148.

Moghal, M. Y., 1974a. Uranium in Siwalik sandstones, Sulaiman Range, Pakistan. In: Formation of Uranium ore Deposits. Proc. Symp. Athens, 383-403, IAEA Vienna.

Moghal, M. Y., 1974b. Exploration of uranium deposits in Dera Ghazi Khan District (Punjab), Pakistan. Geol. Survey, Pak., Geonews, 5, 72-78.

Moghal, M. Y., Baig, M. A. & Syed, S. A., 1997. Siwalik Group: A potential host for uranium mineralization. Thrid Geosas Workshop on Siwaliks of South Asia, March 1-5. Islamabad, Abtracts, 38p.

Morgenstern, N. R. and Tchalenko, J. S., 1967. Microscopic structures in kaolin subjected to direct shear. Geotechnique 17, 309-328.

Moore, D. E. and Byerlee, J., 1992. Relationships between sliding behavior and internal geometry of laboratory fault zones and some creeping and locked strike-slip faults of California. Tectonophysics, 211, 305-316.

Nakata, T., 1972. Geomorphic history and crustal movements of the foot hills of the Himalayas. Tohoku Univ. Sci. Rept., 7th Ser. 22, 39-177.

Nakata, T., 1989. Active faults of the Himalaya of India and Nepal. In: Malinconico, L. L. & Lilee, R. J. (eds). Tectonics of the Western Himalayas. Geol. Soc. Amer., Spec. Paper 232, 243-264.

Passchier, C., and C. Simpson. 1986. Porphyroclast system as kinematic indicators. Jour. of struc. Geol. Vol. 8, 831-843.

Parker, J. M., 1942. Regional systematic jointing in slightly deformed sedimentary rocks. Bull. Geol. Soc. Am., 53, 381-408.

Patriat, P. and Achache, J., 1984. India-Eurasia collision chronology and its implications for crustal shortening and driving mechanism of plates. Nature, 311, 615-621.

Pennock, E. S., Lillie, R. J., Zaman, S. H. & Mohammad, Y. 1989. Structural interpretation of seismic reflection data from eastern Salt Range and Potwar Plateau, Pakistan. Am. Assoc. Petr. Geol. Bull., 73, 7: 841-857.

Petit, J. P., 1987. Criteria for the sense of movement on fault surfaces in brittle rocks: Jour. of Struct. Geol. Vol. 9, 597-608.

Petterson, M. G. & Windley, B. F., 1985. Rb-Sr dating of the Kohistan arc batholith in the Trans-Himalaya of N. Pakistan and tectonic implications. Earth Planet Sci. Lett., 74, 54-75.

Pilgrim, G. E., 1913. The correlation of the Siwaliks with mammal horizons of Europe. Geol. Survey India, Rec. 43 (4), 264-326.

Pivnik, D. A. and Sercombe, W. J., 1993. Compressional and transpression-related deformation in the Kohat Plateau, NW Pakistan. In: Treloar, P. J. & Searle, M. P. (eds). Himalayan Tectonics. Geol. Soc. Lond., Spec. Publ. 74, 559-580.

Pivinik, D. A. & Wells., N. A., 1996. The transition from Tethys to the Himalaya as recorded in northwest Pakistan. Bull. Geol. Soc. Amer., 108, 1295-1313.

Powell, C. McA., 1979. A speculative tectonic history of Pakistan and surroundings: Some constraints from the Indian Ocean. In Farah, A. & DeJong, K. A. (eds). Geodynamics of Pakistan. Geol. Survey Pak., Quetta, 5-24.

Price, N. J., 1966. Fault and Joint development in brittle and semi-brittle rock. Pergamon. Oxford, 176.

Price, N. J. and Cosgrove, J. W., 1990. Analysis of geological structures. Cambridge University Press. 1-492.

Pudsey, C. J., 1986. The northern suture, Pakistan. Margin of a Cretaceous Island arc. Geol. Mag., 123, 405-423.

Ramsay, J. G., 1967. Folding and Fracturing of Rocks: McGraw Hill, New York, New York, USA.

Ramsay, J. G. and Huber, M. I., 1987. The techniques of modern structure geology. Vol. II, Folds and Fractures. Academic press, London, 309-665.

Rex, A. J., Searle, M. P., Tirrul, R., Crawford, M. B., Prior, D. J., Rex, D, C. & Barnicoat, A., 1988. The geochemical and tectonic evolution of the central Karakorum, North Pakistan. Phil. Trans. Roy. Soc. Lond., A.326, 229-225.

Riedel, W., 1929. Zur Mechanik geologischer Brucher-scheinungen: Zentralblatt fur Mineralogic, Geologie and Palaontologic, Vol. 1929B, 354-368.

Sanderson, D. J., 1979. The transition from upright to recumbent folding in the Variscan fold belt of southwest England: A model based on the kinematics of simple shear: Jour. of Struct. Geol., Vol., 1, 171-180.

Sarwer, G & DeJong, K. A., 1979. Arcs, oroclines, syntaxes- the curvatures of Mountain Belts in Pakistan. In: Farah, a. & Dejong, K. A. (eds.). Geodynamics of Pakistan. Geol. Survey Pakistan, Quetta, 341-350.

Searle, M. P., and Khan, M. A., 1996. Geologcial map of North Pakistan (1:650, 000).

Searle, M. P., 1991. Geology and tectonics of the Karakoram Mountains. J. Wiley & Sons, New York, 358.

Searle, M. P., 1988. Structural evolution and sequence of thrusting in the High Himalayan, Tibetan – Tethys and Indus suture zones of Zanskar and Ladakh, western Himalaya. Reply: Jr. Struc. Geol., 10, 130-131.

Seeber, L. and Armbruster, J., 1979. Seismicity of the Hazara arc in northern Pakistan: decollement versus basement faulting. In: Farah, A. & DeJong, K. A. (eds). Geodynamics of Pakistan. Geol. Surv. Pak., Quetta, 131-142.

Seeber, L. Quittmeyer, R. C. & Armbruster, J. G., 1980. Seismotectonics of Pakistan. A review of results from network data and implications for the Central Himalaya. Geol. Bull. Univ. Peshawar, 13, 151-168.

Secor, D. R. Jr., 1965. Role of fluid pressure in jointing. Am. Jr. Sci., 263, 633-646.
Shah, S. M. I. (eds), 1977. Stratigraphy of Pakistan. Geol. Survey Pak. Mem., 12, 138.

Sheldon, P., 1912. Some observations and experiments on joint planes. Jr. Geol., 20, 53-79.

Sibson, R. H., 1977. Fault rocks and fault mechanisms: Jour. of the Geol. Soci. of London, Vol. 133, 190-213.

Simpson, R. R., 1904. Report on the coal deposit of Isa-Khel, Mianwali, Punjab. India Geol. Survey Rec. 31, Pt. 1, 9-34.

Stearns D. W., 1964. Macrofracture patterns on Teton Anticline N. W. Montana (abstract) (Eos). Trans. A. G. U., 45, 107.

Tahirkheli, R. A. K and Jan, M. Q. (eds). 1979. Geology of Kohistan, Karakorum and Himalayas, northern Pakistan. Geol. Bull. Univ. Pesh. 11, 187.

Tahirkheli, R. A. K., 1989. Whether newly discovered Shontargali Thrust is an analogue of MCT in the North western Himalaya in Pakistan. Kashmir, Jr. Geol., 617, 23-28.

Tahirkheli, R. A. K., 1992. Shontargali Thrust: the Main Central Thrust (MCT) of Northwestern Himalaya in Pakistan. In: A. K. Sinha (ed.) Himalayan Orogen and Global Tectonics, 107-120.

Tehalenko, J. S. 1970. Similarities between shear zones of different magnitudes: Geol. Soc. of America Bulletin, Vol. 81, 1625-1640.

Treloar, P. J., Broughton, R. D., William, M. P., Coward, M. P. & Windley, B. F., 1989. Deformation, metamorphism and imbrication of the Indian Plate south of the Main Mantle Thrust, North Pakistan. Jr. Met. Geol., 7, 111-125.

Twiss, R. J. and Moores, E. M., 1992. Structural Geology. W. H. Freeman and Company.

Valdiya, K. S., 1980. Intra-crustal boundary thrust of the Himalaya. Tectonophysics, 55, 323-348.

Wadia, D. N., 1931. The syntaxis of the northwest Himalaya: its rocks, tectonics and orogeny. Geol. Survey India, Rec. 63, 1, 129-138.

Wang, Z., Chen, D., Mu. Ch., Hi. Lu. And Wang Zi., 1989. Report on basic geological studies, Qabul Khel, Siwalik of Pakistan. AEMC Internal Report.

Wang, Z., Tang, S., Chen, D., Wang, Zi. and Gong, B., 1995. Comprehensive evaluation of prospective uranium potential in Qabul Khel deposit, Bannu Distt. Pakistan. AEMC Internal Report.

Wheeler, R. L. and Dixon, J. M., 1980. Intensity of systematic joints: methods and applications. Geology, 8, 230-233.

White, S. H., P. G. Bretan, and E. H. Rutter 1986. Fault-zone reactivation: Kinematics and mechanisms: Philosophical Transactions of the Royal Soci. Of London, Vol., A317, 81-97.

Willis, B., and Willis, R., 1934. Geologic structures, 3rd ed., McGraw-Hill Book company, Inc., 544.

Wyne, A. B., 1878. Geology of the Salt Range in the Punjab: India Geol. Survey Mem., Vol., 14, 313p.

Wyne, A. B., 1880. On the Trans-Indus extension of the Punjab salt Range: India Geol. Survey Mem., Vol., 17, 95p.

Yeats, R. S., Khan, E. H. & Akhtar, M. (1984). Late Quaternary deformation of the Salt Range of Pakistan. Geol. Soc. Amer. Bull. 95: 958-966.

Yeats, R. S. & Lawrence, R. D., 1984. Tectonics of the Himalayan thrust belt in northern Pakistan. In: Haq, B. U. & Milliman, J. D. (eds). Marine Geology and Oceanography of Arabian sea and Coastal Pakistan. Van Nostrand Reinhold Co., New York, 177-200.

Zeitler, P. K., 1985. Cooling history of the NW Himalayas, Pakistan, Tectonics, 4, 127-151.